Multiuser TOA Estimation Techniques with Application to Radiolocation

BY

Zahid Ali

A Dissertation Presented to the

DEANSHIP OF GRADUATE STUDIES

KING FAHD UNIVERSITY OF PETROLEUM & MINERALS

DHAHRAN, SAUDI ARABIA

In Partial Fulfillment of the

Requirements for the Degree of

DOCTOR OF PHILOSOPHY

In

Electrical Engineering

June 2010

KING FAHD UNIVERSITY OF PETROLEUM AND MINERALS

DHAHRAN 31261, SAUDI ARABIA

DEANSHIP OF GRADUATE STUDIES

This thesis, written by **Zahid Ali** under the direction of his thesis advisor and approved by his thesis committee, has been presented to and accepted by the Dean of Graduate Studies, in partial fulfillment of the requirements for the degree of

DOCTOR OF PHILOSOPHY IN ELECTRICAL ENGINEERING.

THESIS COMMITTEE

Dr. Deriche, Mohamed (Chairman)

Dr. Landolsi, M.Adnan (Co – Chairman)

Dr. Sheikh, A.U.H. (Member)

Dr. Zerguine, Azzedine (Member)

Dr. Bokhari, Ashfaq (Member)

17 JAN 2011

Dr. Samir Abdul Jauwad
Department Chairman

Dr. Salam A. Zummo
Dean, Graduate Studies

23/1/11
Date

Dedication

I dedicate this humble effort to my wife
and my sons - Ahmad and Akram.
Their unconditional love, unselfishness
and generous understanding
kept me going throughout the course of this thesis

"Everywhere, we learn only from those whom we love."

Johann Wolfgang Von Goethe

Acknowledgements

All praise and glory is to Almighty Allah who gave me courage and patience to carry out this work, and peace and blessings of Allah be upon prophet Mohammed.

I would like to thank my thesis advisor, Dr. Mohamed Deriche, and co-advisor, Dr. Mohammed Adnan Landolsi, for having always believed in my work and for providing valuable insight and prompt feedback during all the stages of the research conducted in this thesis. Their consistent encouragement and suggestions helped me in forming the thesis structure and the content. I also owe my gratitude to other distinguished members of the thesis committee for their support and cooperation.

Acknowledgement is due to the King Fahd University of Petroleum and Minerals and Electrical Engineering department and its chairman, Dr. Samir H. Abdul-Jauwad for supporting this research. I would also like to acknowledge the research grant provided by King Abdul Aziz City of Science and Technology (KACST) in conducting this research.

Contents

List of Figures

List of Tables

LIST OF ABBREVIATIONS

2G	Second Generation
3G	Third Generation
AOA	Angle of Arrival
AML	Approximate Maximum Likelihood
AWGN	Additive White Gaussian Noise
BS	Base Station
CDF	Cumulative Distribution Function
CDMA	Code Division Multiple Access
CRLB	Cramer Rao Lower Bound
DLL	Delay Locked Loop
DDF	Divided Difference Filter
FIM	Fisher Information Matrix
EKF	Extended Kalman Filter
ESPRIT	Estimation of Signal Parameters via Rotational Invariance Techniques
FLOP	Floating Point Operations
GCC	Generalized Cross Correlation
GPS	Global Positioning System
GSM	Global Systems for Mobiles
ITS	Intelligent Transportation Systems
$\mathbf{J}$	Fisher Information Matrix
J	Cost Function
K	Number of Users
KF	Kalman Filter
LOP	Line Of Position
LOS	Line of Sight

LMS	Least Mean Squares
LS	Least Squares
M	Number of Paths
MAI	Multiple Access Interference
MAP	Maximum a Posteriori Probability
MF	Matched Filter
MLE	Maximum Likelihood Estimate
MS	Mobile Station
MSE	Mean Square Error
MUSIC	Multiple Signal Identification and Classification
NCDLL	Non Coherent Delay Locked Loop
NLOS	Non Line of Sight
$N_0/2$	Spectrum Density of White Noise Process
p.d.f.	Probability Distribution Function
PL	Path Loss
PN	Pseudo Noise
RF	Radio Frequency
RMS	Root Mean Square
RSS	Received Signal Strength
SIC	Successive Interference Cancellation
SNR	Signal to Noise Ratio
SPKF	Sigma Point Kalman Filter
TDL	Tau Dither Loop
TDOA	Time Difference of Arrival
TOA	Time of Arrival
UKF	Unscented Kalman Filter

VCC	Voltage Controlled Oscillator
WCDMA	Wideband Code Division Multiple Access

LIST OF SYMBOLS USED

$[\cdot]^T$	Matrix or vector transpose
$\lfloor \cdot \rfloor$	largest integer smaller than real number
$\lvert \cdot \rvert$	modulus of a scalar, elements of a vector
$\lVert \cdot \rVert$	Euclidean norm of a vector
$diag\{\cdot\}$	diag$\{\mathbf{X}_1, \cdots, \mathbf{X}_K\}$ denotes $K \times K$ block diagonal matrix whose kth block element is $\mathbf{X}_K$
α, β, κ	UKF sigma point scaling factors
β_i	ratio of average received power at BSi compared to BS1
$\delta_K(K-1)$	Kronecker delta ($\delta_K(K-l) = 1$ for $k = l$ and 0 otherwise)
δ	normalized delay error
$\epsilon(t)$	error signal
θ_k	phase angle for kth user
$\theta_{k,l}$	angle of arrival for the lth path of the kth user
γ_a^e	adjusted matched filter output for the early channel
γ_a^l	adjusted matched filter output for the late channel
μ	LMS step size
ξ	shadowing variable
$\mathbf{0}_M$	a zero matrix
$A_{k,l}$	information-bearing signal amplitude for the kth user's lth symbol
$a_k(t)$	spreading waveform used by the kth user
$\bar{a}_k(t)$	filtered spreading waveform used by the kth user
c	speed of light
$c_{k,i}(t)$	complex channel coefficients associated with the ith path of the kth user
$\mathbf{D}$	measured distance

$D_{\triangle}(\delta)$	S-curve characteristics
$d_{i,j}$	range measurement for the jth path of the ith base station
$\bar{d}_{k,m_k}(t)$	filtered mth symbol transmitted by the kth user
$d_{k,m_k}(t)$	mth symbol transmitted by the kth user
$\mathbf{F}$	state transition matrix
$\mathbf{F_c}$	state transition matrix for channel coefficients
$\mathbf{F}_k$	Jacobian matrix of $\mathbf{f}$ at current state estimate
$\mathbf{F}_{\boldsymbol{\tau}}$	state transition matrix for time delays
$E[\cdot]$	statistical expectation
$\mathbf{h}$	nonlinear observation function
h	interval length or divided difference step size for DDF
$\mathbf{J}$	Fisher information matrix
$\mathbf{I}_M$	the $M \times M$ identity matrix
K_{k+1}	Kalman gain at step $k+1$
ln	natural logarithm
$\hat{M}^e(i)$	estimated interference of the early channel
$\hat{M}^l(i)$	estimated interference of the late channel
n	path loss
$p(d)$	distance path loss
P_k	signal power for kth user
$\mathbf{P}_{k+1}^{-}$	predicted covariance estimate at $k+1$ step
$\mathbf{P}_{k+1}^{xy}$	predicted cross-correlation matrix between $\hat{\mathbf{x}}_{k+1}^{-}$ and $\hat{\mathbf{y}}_{k+1}^{-}$
$\mathbf{P}_{k+1}^{+}$	updated covariance estimate at step $k+1$
$\mathbf{P}_{k+1}^{vv}$	innovation covariance vector
$\mathbf{Q}_k$	covariance of process noise $\mathbf{w}_k$

$r(t)$	received signal
$\mathbf{R}_k$	covariance of measurement noise $\mathbf{v}_k$
R_i	true distance between the ith base station and the mobile station
$R^e_{kk}(i)$	early auto correlation of the kth user
$R^l_{kk}(i)$	late auto correlation of the kth user
$R^e_{km}(i)$	early cross-correlation of the kth and mth user
$R^l_{km}(i)$	late cross-correlation of the kth and mth user
$\hat{s}_k^{(s-1)}$	estimated signal in the $(s-l)st$ stage
S_r	transmitted signal power
S_t	received signal power
$\mathbf{S_v}$	Cholesky factor of $\mathbf{R}_k$
$\mathbf{S_w}$	Cholesky factor of $\mathbf{Q}_k$
$\mathbf{S_x}$	Cholesky factor of $\mathbf{P}_0$
$\mathbf{s}_{x,j}$	jth column of $\mathbf{S_x}$
$\mathbf{s}_{w,j}$	jth column of $\mathbf{S_w}$
T_b	symbol time
T_c	chip time
T_s	sampling time
$\tau_{i,j}$	delay for the lth path of the kth user
$\mathbf{v}_k$	measurement noise
$\mathbf{v}_{k+1}$	innovation at step $k+1$
$\mathbf{w}_k$	process noise
W_i	ith weighting coefficient for SPKF
$X \sim N(m, \sigma^2)$	means the random variable X has a Gaussian distribution with mean m and variance σ^2
X_i	ith sigma point for UKF

$\bar{\mathbf{x}}$	mean value of vector $\mathbf{x}$
x_m	x-coordinate for the mobile station
x_i	x-coordinate for the ith base station
$\hat{\mathbf{x}}_{k+1}^{-}$	predicted state estimate at $k+1$ step
$\hat{\mathbf{x}}_{k+1}^{+}$	updated state estimate at step $k+1$
y_m	y-coordinate for the mobile station
y_i	y-coordinate for the ith base station
$\hat{\mathbf{y}}_{k+1}^{-}$	observation propagation at step $k+1$
$Z_k^e(i)$	output of early matched filters
$Z_k^l(i)$	output of late matched filters

DISSERTATION ABSTRACT

Name: Zahid Ali

Title: Multiuser TOA Estimation Techniques with Application to Radiolocation

Degree: Doctor of Philosophy

Major Field: Telecommunications

Date of Degree: June 2010

Wireless location finding has emerged as an essential public safety feature of cellular systems. Apart from its mandatory implementation enforced by governments, wireless location also has many other potential applications in areas such as location sensitive billing, asset tracking, fraud protection, mobile yellow pages, fleet management, information services such as weather, traffic, navigation, directory assistance and the list continues to grow and so does the location based services (LBS) market.

We consider mobile location determination in code division multiple access (CDMA) cellular systems using the time of arrival method (TOA). Several location techniques utilizing terrestrial wireless network elements and radio signals have been proposed over the years. However, accurate positioning in a terrestrial wireless system is impeded by multipath propagation, multiple access interference (MAI), and non-line-of-sight (NLOS) propagation. Traditional location algorithms have derived location estimates assuming single user environment. However, this assumption is not correct as measurement bias will be introduced due to MAI. The objective of this thesis is

to develop new algorithms to estimate time delays in the presence of MAI with a particular emphasis on closely spaced paths in a multipath channel. First we present Kalman framework based filtering for parameter estimation in the presence of MAI. This approach is based on a deterministic sampling technique and yields a family of sigma-point Kalman filters (SPKF). Two main variants of SPKF, namely the unscented Kalman filter (UKF) and divided difference filter (DDF) have been considered. A comparison of these filters is made with linearized extended Kalman filter (EKF). We show that sigma point Kalman filters are robust and near-far resistant a multiuser environment and are simpler to implement. Also we present two new receiver structures. The first one is MAI cancellation based delay locked loop (DLL) employing successive interference cancellation (SIC). The other is an early late tracking loop employing LMS for the time update. The tracking analysis of the proposed algorithms has been carried out and simulation results of the proposed approach demonstrate that an accurate time delay can be achieved and hence accurate location estimation is possible in the presence of MAI.

Doctor of Philosophy of Science Degree
King Fahd University of Petroleum and Minerals
Dhahran, Saudi Arabia
June 2010

ملخص الاطروحة

الاسم: زاهد على

العنوان:

Multiuser TOA Estimation Techniques with Application to Radiolocation

الدرجة العلمية: دكتوراه فى الفلسفه

مجال التخصص: الاتصالات

تارخ الدرجه العلميه: يونيو 2010

لقد برز تحديد المواقع لاسلكيا كميزه اساسية للانظمة الخلويه. وبعيدا عن كون تنفيذه الزاميا من جانب الحكومات, فإن تحديد المواقع لاسلكيا له العديد من التطبيقات فى الكثير من المجالات ومنها الفوتره المبنية على الموقع, تتبع الاجهزه, الحماية من الاحتيال, الصفحات الصفراء المتنقله, ادارة الاسطول الى جانب العديد من خدمات المعلومات مثل حالة الطقس وحركة السير والنقل, ولازالت القائمه تزداد مع زيادة سوق الخدمات المبنيه على تحديد المواقع.

اننا نعتمد فى تحديد موقع الجوال فى نظام Code division multiple access (CDMA) فى الانظمة الخلوية على طريقة وقت الوصول (TOA). يوجد العديد من تقنيات تحديد المواقع والتى تستخدم اجزاء واشارات الراديو للشبكات اللاسلكية الارضيه والتى تم تقديمها على مر السنين, وكذلك فإن دقة تحديد المواقع باستخدام الشبكات اللاسلكيه الارضيه تتأثر بعديد من المعوقات مثل تعدد طرق الوصول multipath propagation, تداخل الاشاراتmultiple access interference , وعدم وضوح الرؤيه فى الاتصال None Line of Sight. والطرق المستخدمه فى تحديد المواقع تفترض فقط وجود مستخدم واحد فقط وهذا الافتراض ليس صحيحا لان القياس سوف يكود منحازا الى مستخدم على الاخر بسبب تداخل الاشارات. والهدف من هذه الاطروحة هو تطوير طريقة جديده لتقدير الوقت مع الاخد فى الاعتبار تداخل الاشارات, ويعتمد هذا الاسلوب على طريقه محدده لأخد

العينات وتحديدا unscented Kalman filter (UKF) و divided difference filter (DDF). وللمقارنة بين بينهما فاننا نستخدم linearized extended Kalman filter (EKF). وقد اثبتنا ان نقطة سيجما فى Kalman filters قويه ومقاومة سواء عن قرب او بعد فى بيئه متعددة المستخدمين وكذلك تتميز بسهولة التنفيذ. وكذلك فقد تقدمنا بهيكلين جديدين لجهاز الاستقبال , الاول مبنى على الغاء تداخل الاشارات فى الدائره المغلقه (DLL) عن طريق توظيف الغاء التداخل المتعاقب (SIC). والثانى حلقة تتبع المتقدم والمتاخر باستخدام LMS لتحديث الوقت. وقد قمنا بتحليل نتائج التتبع باستخدام الطريقة المقترحه وقم اظهرت نتائج المحاكاة ان الطريقه المقترحة قد وضحت ان الحساب الدقيق للتاخير فى الوقت يمكن تحقيقه وبذلك يمكن عمل تقدير للتتبع بدقه فى وجود تداخل للأشارات

درجة الدكتواره فى الفلسفه العلمية

جامعة الملك فهد للبترول والمعادن

الظهران , المملكة العربية السعودية

يونيو 2010

Chapter 1

Introduction

Over the past decade, considerable attention has been given to wireless cellular mobile positioning systems, and a plethora of new location-based applications have already been explored [1]. The recent advances in the wireless technologies and their deployment have changed the once voice-only service network to value added service network operating at very high data rates. One of the many of these services is the location finding and has been used in many applications such as emergency services and other commercial services like Intelligent Transportation System (ITS) [1-3]. Location based services (LBS) offer an increase in revenues generated for the carrier providers by providing location sensitive billing for the subscriber where a subscriber is offered a different rate according to whether the phone is used at home, in an office on the move. Mobile location guarantees access to emergency services, localized billing, radio resource management, mobile yellow pages, location based messages (commercials)

etc. [4].

The driving force behind the development of accurate wireless location techniques is the ever increasing revenue generated from location based services. It was estimated that the location based industry accounted for a revenue of about 40 billion in 2006 [5]. Numerous new and novel applications are being implemented to provide a range of new services to the subscribers.

The accuracy requirements for network-based and handset-based technologies have been outlined in [1]. In a hand-set based location system, the mobile station (MS) measures certain signal characteristics to locate itself. On the other hand, in network-based location the MS position is determined at the base stations (BSs). The two approaches have certain advantages and disadvantages which will be discussed in the next section. Both approaches are overlaid on the existing wireless communications infrastructure with no additional technology required such as in case of dead reckoning, proximity systems [6].

1.1 Problem Description and Solution

The objective of this research is to evaluate and enhance the performance of wireless location in CDMA networks by developing new solutions for the case of multiuser environment. MAI limits the accuracy of the parameters necessary for location estimation. In addition, near-far effect is also a major factor in the parameter estimation. It is necessary to investigate MAI effects on radiolocation. In the following, a brief

description of the problem and the proposed solution is presented.

1.1.1 Effects of Multiple Access Interference on Radiolocation

Users in CDMA share the same frequency band and are distinguished by different spreading codes. Since the codes are not orthogonal, interference arises among the active users. Due to non-orthogonality, the conventional correlator receiver suffers from the near-far problem [1]. This implies that the cross correlation between the spreading sequence of the user of interest and the signal from a strong interferer can be larger than the correlation with the signal from the desired user. Detection is rendered unreliable. The classical approach to deal with this problem is power control, whereby all users transmit powers are controlled so that the powers received from all users are equal.

At least three base stations (BS) are required to form location estimate, the transmitted signal from mobile station (MS) needs to be detected and time delays tracked at these BSs. In CDMA, DLL is used to fine track the signals at the BS. Power control may be applied in the home BS to mitigate near-far effect, but it is a problem at other non home BSs involved in location estimation since MS is not power controlled at these BSs. So the ability to detect and track the time delays with high accuracy translates into inaccuracies in the estimation process.

MAI not only reduces the tracking performance of the DLL but it also makes it

difficult for non-home BSs to detect the desired user signal with power control in place [5,6]. Many of the proposed radiolocation algorithms take into account a single user environment and ignore MAI in the analysis.

In this work we focus on the multiuser radiolocation using time of arrival measurements in CDMA cellular network. Since MAI affects the time delay measurements, we address the problem in two different ways:

- **Recursive filtering approach:** We approach the problem from a system identification point of view where an adaptive filter is used to approximate the output of the channel to estimate the channel coefficients and time delays. In this context, we have first considered linearized EKF. Efficient and accurate approximate non-linear filters have recently been proposed as alternatives to the EKF for recursive nonlinear estimation of the states. First, as sampling-based nonlinear filters, the sigma point Kalman filters, the unscented Kalman filter and the divided difference filter are investigated. These filters have been used to estimate the multiuser parameter in a multipath environment taking a state space approach. A comparison of these approaches has been made with the EKF.

- **Classical Approach:** A delay tracker based on the classical time delay estimation technique in CDMA is proposed. The algorithm takes a successive interference cancellation (SIC) approach to detect the strongest users and successively cancels their effect from the received signal. A second approach based on an early late tracking loop employing LMS for the time update is also discussed.

Finally, a number of simulations are conducted to compare the performance of these algorithms under a multiuser radiolocation framework.

1.2 Research Objectives

In a wireless environment, multipath propagation, shadowing, line-of-sight (LOS), hearability, and MAI present challenges for an accurate mobile location in cellular networks. Various algorithms have been proposed to address the aforementioned problems. Each location method has its advantages and limitations, with no single solution yet to meet all the requirements for location services. Therefore new schemes for mobile positioning are still being investigated. At the same time various methods have been proposed to mitigate effects of different factors influencing the robust location estimation.

The propagation environment introduces, among other things, interference. It results from users sharing the same bandwidth in CDMA systems. As CDMA systems are interference limited, MAI will limit not only the accuracy of parameter estimation, but also whether estimation can be obtained at all in the presence of near-far effect.

The MAI will affect the ability of a conventional receiver at other BSs to accurately estimate the mobile station (MS) delay which is the key to accurate time based radiolocation techniques. The mobile location accuracy is greatly affected by LOS blockage, multipath propagation and MAI. Most of the research related to the location estimation has been carried out by investigating the effects of one or both of

the first two factors mentioned above. However, the effects of MAI on the location estimation when the arriving paths are closely spaced has generally not been explored by the researchers. This constitutes a basis for conducting research to analyze MAI on mobile location and propose techniques to mitigate its effects.

The objective of this research is to develop solutions for accurate mobile location in multiuser CDMA cellular network. The location accuracy is likely to be affected in a multiuser scenario as is the case in practical situation [1]. The foregoing argument necessitates the development of new algorithms and techniques that provide reliable and accurate location estimation in a multiuser scenario.

In particular ,the objectives of this research are

- To propose new TOA estimation techniques that may be subsequently used for wireless location in cellular systems to provide location estimates that are reliable and reduce the ambiguity in the subscriber location in CDMA cellular environment.
- To develop solutions for MAI impairment found in such location systems that are robust and are able to minimize the MAI effects on location estimation in a multiuser CDMA cellular environment.
- To provide an overall performance analysis of the proposed location solutions to the subscriber location problem in CDMA cellular systems.

To accomplish these objectives, we have proposed two new approaches. The first approach is based on sigma point Kalman filters and the second approach is based on a modified DLL and early late tracking loop integrated with successive interference

cancellation.

1.3 Outline of the thesis

The thesis has been organized as follows. A background of related research and techniques on radiolocation is provided in Chapter 2 along with applications and overview of location systems, major challenges in location estimation, and parameter estimation algorithms. Chapter 3 presents the fundamentals of CDMA for location estimation with focus on DLL. Then, we investigate the effects of MAI on DLL. In chapter 4, we present our proposed schemes based on recursive filters using a state space approach. Chapter 5 presents interference cancellation based DLL. Multiuser radiolocation estimation based on approximate maximum likelihood (AML) is presented in chapter 6 with location estimates derived for the proposed approaches in different scenarios. Finally chapter 7 presents a summary of the dissertation contributions with a brief discussion on the directions for future research and conclusion.

Chapter 2

Wireless Location Systems

2.1 Background

Wireless location estimation refers to the problem of estimating the position information of a mobile subscriber in a cellular environment. Such positioning information is usually provided in terms of geographic coordinates of the mobile subscriber with respect to a geographic reference point. Wireless location is also called mobile positioning, radiolocation, and geolocation. It has emerged as an essential part of cellular systems with a number of potential applications in many diverse areas. In this chapter, we present an overview of the main applications of wireless location techniques with discussion on the locations systems types, technology constraints, challenges and radiolocation data fusion methods.

2.2 Applications of Wireless Location Systems

The availability of the MS location information can be useful for different location-related services. In general, these applications can be categorized into three groups: security services, business services, and network management [2,4].

1. Security services:

   - Surveillance, roadside assistance, stolen vehicle recovery

2. Business services:

   - Fleet management, tracking (packages, cars, people, busses etc.), location based advertisement, mobile yellow pages

   - Intelligent Transportation Systems such as highway traffic management, traveler information system, navigation system

3. Network management services:

   - Location based billing system, radio resource management, mobility management, handover assistance

Other location dependent information services include:

- Location of hotels and restaurants, vehicle repair/maintenance services, parking space information

In addition to the value added services, location technology can be used to provide entertainment related services as well. Location based games such as GPS assisted Glofun Raygun, Blisterent Swordfish, Blisterent Torpedo Bay, NewtGames Mogi are some of the location technology based games available to the consumer.

Position finding has become one of the most important features of the mobile communications systems. It can play a very crucial part in case of dealing emergency situations requiring immediate response. This includes emergency alert services, roadside assistance and safety alarms for social workers, watchmen and alone-working people like forestry workers. Location based charging allows a subscriber to be charged different rates depending on the subscriber's location or geographic zone, or changes in location or zone [8]. Fleet and asset management services allow the tracking of location and status of certain service persons such as a supervisor of a delivery service may determine the location and status of employees, parents may locate where their children are, animal tracking, and tracking of assets.

Intelligent transportation system (ITS) uses mobiles in cars to be anonymously sampled to determine average velocity of vehicles and detect and report congestion using average flow rates, vehicle occupancy etc. [1-3]. Location based information services allow subscribers to access information based on their location. The service includes city sighting, location dependent content broadcast, mobile yellow pages, finding friends, driving directions and navigation. Another important use of accurate location estimates is to optimize the internal network. The information about the location of the mobile stations may be used not only to provide a subscriber service, but also may be used for network internal operations such as location assisted handover [9-10]. This internal use of the information may lead to higher traffic capacity and improved call completions. Many routing algorithms for ad hoc networks have also

been developed that use location dependent information of the mobile hosts for route discovery [11–13].

2.3 Overview of Location Systems

For locating wireless terminals in cellular and wireless communication networks, the different practical technologies can be arranged into three main categories:

- Terrestrial radio-based or Cellular based systems

- Satellite based systems, and

- Database oriented systems

Although there are other location technologies including dead reckoning and proximity systems [1, 6], these are not under active consideration for implementation by wireless carriers or standard bodies due to coarse positioning. We will discuss in what follows the different technologies listed above.

Terrestrial radio-based Systems

A terrestrial based location system is overlaid on the existing cellular communication systems with (or without) some minor modifications. The location system takes advantage of existing transceivers, communication bandwidth, two way messaging, and well established infrastructure. Unfortunately, it also inherits the disadvantages of underlying communication systems i.e. near-far effects, non-line-of-sight (NLOS) propagation paths, and timing estimation accuracy.

Terrestrial based location involves the measurement of radio signals between the MS and a set of fixed BSs to estimate certain parameters that are dependent on the MS position. These parameters include Received Signal Strength (RSS), Angle of Arrival (AOA), Time of Arrival (TOA) and Time Difference of Arrival (TDOA) of the transmitted signal.

Satellite-based systems

These systems, such as the Global Positioning System (GPS), are based on similar radio signal measurement principles discussed for terrestrial radio-based system, the difference being that the MS handset has to be enabled with a special receiver for the satellite signals to self locate itself. A GPS receiver requires receiving signals from at least four satellites in order to obtain the longitude, latitude, and altitude of its position. For indoor environment or some urban area, the GPS system fails due to the absence of the clear link to the satellites. Hybrid technology that incorporates terrestrial and satellite based locations is also gaining popularity leading to techniques such as Assisted GPS [8].

Database-oriented Systems

The major part of such systems is a pre-constructed database, which contains the mapping information of the received features and exact physical location of the transmitters. The signal features consists of a collection of attributes, such as the prop-

agation delay, the signal phase, the signal amplitude, the direction of signal arrival, and the multipath profiles. Once a set of features measurements is obtained, the system searches through the database for the closest match using the pattern matching techniques. This approach circumvents the need for a direct communication path; however, it demands constant database updates to adopt to the changes of seasons, weather conditions, and reconfiguration of city buildings [14].

2.4 Comparison of Existing Location Systems

For network-based systems, the main advantage is that it does not require any modifications or specialized equipment in the MS handset, thus a range of handsets in the existing cellular networks can be accommodated. Moreover, such systems do not require the use of GPS components, thus avoiding any political issue that may arise due to their use. The main disadvantage of network-based wireless location is its relatively lower accuracy, when compared to GPS-based location methods.

On the other hand, GPS receivers usually have a relatively high degree of accuracy, which can reach less than 10 meters with differential GPS server-aided systems Moreover, GPS satellite signals are available all over the globe, hence, can be used to provide global location information. However, some of the disadvantages include increased cost, size, and battery consumption of GPS enabled mobile handsets. In order for this technology to be operational, we require to replace hundreds of millions of legacy handsets already in use with new GPS-aided handsets. Similarly, wireless

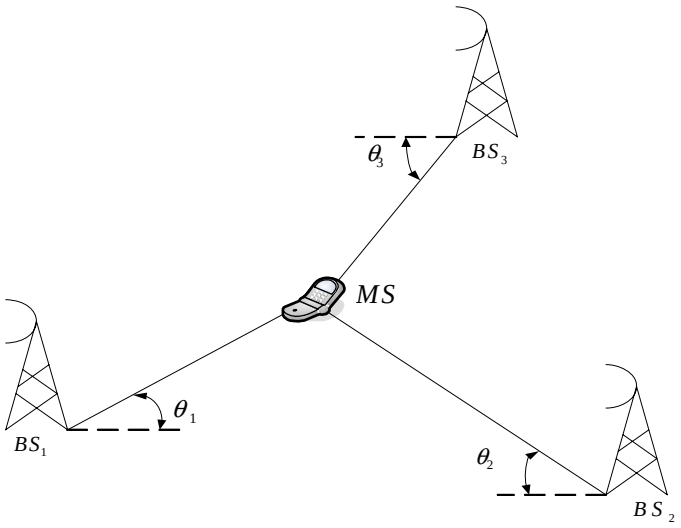

Figure 2.1: MS position location using AOA measurements

base station need to be equipped with GPS aiding servers that increases overall cost of GPS-aided location systems. Other disadvantages include degraded accuracy of GPS measurements in indoor and urban environments , where one or more satellites are obstructed by buildings.

Before completing our discussion on location systems, we will discuss in what follows different techniques used in location systems.

One of the most popular techniques is Angle of Arrival (AOA) estimation, or Direction finding technique [2,15]. It involves the use of antenna arrays to determine the direction from which a signal was received at one or more receivers. These antenna arrays are located at the base stations. Given the knowledge of the BS, the AOA defines lines of positions (LOP) whose intersection provides an estimate of the position for the MS in 2-dimensional space as shown in Figure (2.1)

Location systems based on ranging make distance measurements (i.e., ranges) between the MS and BS. Common methods for measuring ranges include TOA estimation and signal strength estimation. When TOA is estimated, the distance from the MS to the communicating BS traversed by a radio wave can be obtained by multiplying the TOA by the speed of light. As shown in Figure (2.2), the range measurements define LOPs that are circular and centered at the BSs. Two range measurements provide an ambiguity for the MS while three measurements determine a unique position. Similarly, range-differencing determines the difference in distances between the MS and two BSs, and these can be measured directly from estimated TDOA measurements, or formed by differencing two range measurements. The position of the MS is determined based on trilateration. In this case, the range-difference measurements define LOPs that are hyperbolas with foci at each BS. As illustrated in Figure (2.3), the intersection of LOPs from three BSs provides an estimate of the MS's location in two dimensions. A few terrestrial hybrid location techniques can be employed that utilize a combination of time and angle measurements [16–18]. These hybrid methods are very useful when there is an insufficient number of measurements of one type or if the measurements are erroneous.

Besides these well known methods, there are other terrestrial based techniques that can be used to determine the MS location. One simple method is to use the cell ID of the caller to find the approximate location of the MS [8]. In this case, the best approximation to the MS position is given by the location of the serving BS. Obviously,

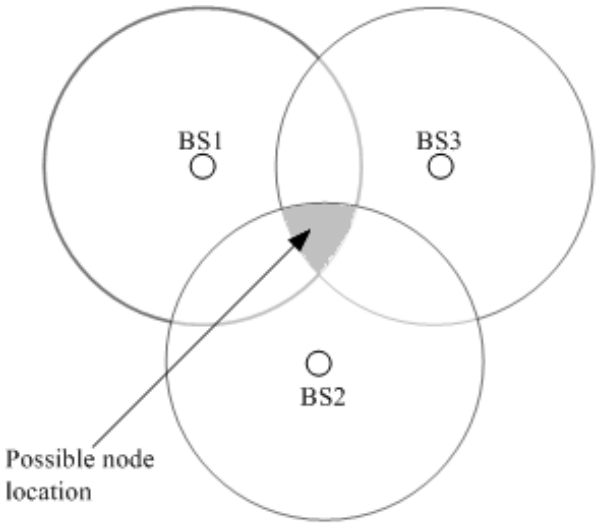

Figure 2.2: MS position location using TOA measurements

the accuracy of this method depends on the cell size. This can be used as default when other accurate methods fail or cannot be implemented. Another technology called Wireless Location Signatures [19] is based on measuring signal strengths at the user's handset that are then relayed to the serving BS for position determination. The signal measurements are correlated to a central database of signal strength maps and the most likely position of the user is given by the best match. Another database correlation method for mobile localization in multipath scenarios was proposed in [20].

2.5 Location Technology Constraints

The choice of the right location technology for a particular application depends on several factors. As is the case with any commercial application, the primary re-

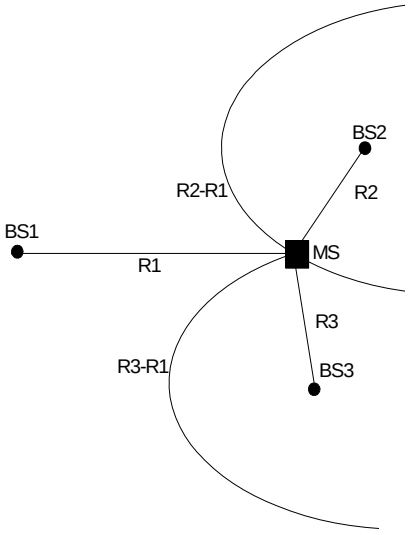

Figure 2.3: MS position location using TDOA measurements

quirement is low cost of development, implementation, maintenance and upgrade. A signal strength based method employing database matching techniques may only require new software installation and processing at the network and handset side, while arrival time-based technology may require relatively more expensive hardware and software modifications to the network infrastructure. Other applications such as location-based advertising may provide some freedom to wireless carriers to maximize revenue by adopting less expensive although less accurate technology. Nevertheless, the higher the accuracy, the better the service and hence, high accuracy is the most desired performance indicator of any wireless location technology. Another desired feature of any location technology is that it must be flexible enough to work with different network air interfaces. As wireless operators shift from 2G to 3G technol-

ogy, the location technology should be compliant and minimize the need for expensive hardware and software updates or reinstallation. Handset-based positioning utilizing embedded GPS receivers may be the favored technology for 3G phones and provide the best accuracy but requires subscribers to purchase new handsets and cannot be applied to existing or legacy handsets. Ideally, the location solution should allow carriers to locate existing users using the existing network without expensive modifications and be adaptable to complement satellite handset-based techniques. Finally, the quality of the signal parameter estimates used for radiolocation depends on the type of environment (indoor/outdoor, rural, suburban, urban, mountainous/hilly) and can be a significant factor affecting the accuracy. The optimum location technology should provide consistent results in all environments such that users can be located throughout the service area and even while roaming.

2.6 Challenges in Location Estimation

Error can be introduced to the location process in a variety of ways. The radiolocation system accuracy is dependent upon how well it can mitigate these impairments. One of the sources of error for radio location estimation is the TOA/AOA/TDOA measurement error. This error comes either from the limitations on the equipment or estimator precision. There are three other sources of error that affect location accuracy: multipath propagation, NLOS propagation and MAI for CDMA systems. Also near-far effect contributes to the errors [21]. Steps must be taken to mitigate these

impairments to improve the location accuracy. We will discuss in what follows briefly the effects these factors in estimation of signal parameters and radiolocation.

2.6.1 Multipath Propagation

In wireless communications, multipath phenomenon is a result of radio signals reaching the receiver from two or more paths. These multiple copies of the same received signal are phase shifted by following different paths and hence interfere at the receiver either constructively or destructively giving rise to fading[1, 22-23]. This may affect the accuracy with which we can measure AOAs, TOAs and TDOAs [1].

Many multipath mitigation techniques have been investigated to estimate AOA corresponding to the true AOA. The accuracy of the MS location estimates are affected if the AOA algorithm uses estimates that correspond to the multipath AOAs (not the true AOA). Similarly time-based location estimates obtained using correlation techniques are also affected by measurements taken in the presence of multipath [1,23]. In conventional receivers, If the one arriving multipath ray has more power than the other arriving rays, then the delay estimates will be biased towards the strong multipath ray making them far from the true delay estimates. Hence the accuracy of the location estimate will be lowered. Location algorithms relying on delay estimates to locate the MS, an error will be introduced in the location estimate due to multipath. The effect of multipath on code acquisition (for TOA estimation) is discussed in [24,25], and on DLL in [26] where the multipath component is seen to bias the tracking of

the DLL. Many different methods have been proposed to provide better resolution for estimating TOA in multipath scenario such as subspace techniques [27-32] and adaptive techniques [33-37]. Maximum likelihood (ML) based delay estimates in the presence of multipath have been discussed in [38,39]. Similarly multipath resistant conventional DLL methods have been described in [40-41] and those based on the EKF in [42].

2.6.2 Multiple Access Interference

In CDMA systems, different users utilize the same channel by multiplying their data with different codes to separate them from each other. Those codes are not fully orthogonal to each other. Thus, different users induce some error into the desired user data. This error is called MAI and depends on how orthogonal the users' codes are to each other. The effect of MAI on the TOA estimation is discussed in [4]. It is shown in this paper that the performance of the DLL is drastically degraded as we increase the number users, and it becomes worse if the other users have higher received power than the desired user. This is also known as near-far problem. We will further elaborate MAI in the chapter 3.

2.6.3 NLOS Propagation

Non-line-of-sight (NLOS) is used to describe radio transmission along a path that is partially obstructed by some physical object between the transmitter and the receiver.

Location algorithms require the presence of a direct, or LOS, path between the MS and the BS to increase the estimation accuracy. However in most of the cases, the signal propagating from the MS to the BS and vice versa are obstructed by many objects such as buildings, trees, hills, mountains etc. Hence the signal arriving at the BS from the MS may take a path which is usually longer one than the true path and also arrives from a different direction than the direct path resulting in NLOS error. For algorithms based on time-based techniques, the extra propagation time because of the NLOS path adds positively to the measured time and hence results in an added error to the true distance between the MS and BS [43]. It has been reported that the NLOS error in GSM can average between 500-700 meters [44]. For angle of arrival based algorithms NLOS may make the angle from which the signal arrives at the BS different from the true direction of the MS. The measured angle will correspond to reflections from obstruction around the MS. This directly results in poor location accuracy.

2.7 Overview of Estimation Techniques

Location estimation of the MS involves performing the following two steps:

- the first step is to estimate the MS signal parameters such as such as signal strength, TOAs, TDOAs, AOAs estimates either at the MS handset or the BS.

- the second step involves the use of any of the radiolocation data fusion methods discussed previously on the estimated parameters [45-47].

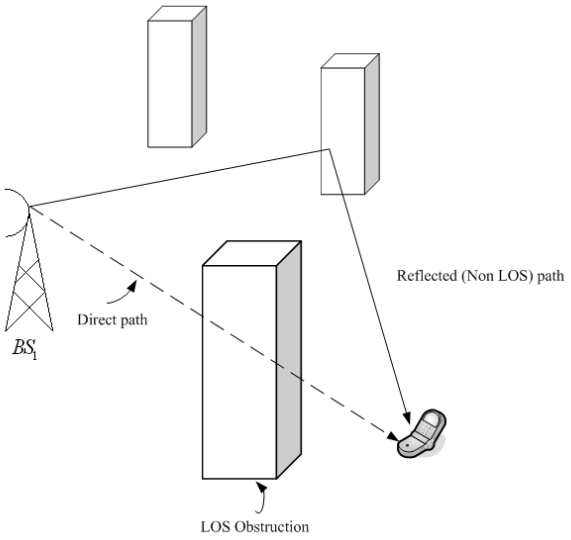

Figure 2.4: Multipath scenario

Parameter estimation has been and continues to be a widely researched field of study. In this section, we will discuss some of the popular approaches for the estimation of signal angle, range and range difference parameters.

2.7.1 TOA Estimation

The distance between an MS and a BS is calculated by multiplying the measured TOA , τ, of the radio signal by the velocity of light in free space, c. In CDMA delay estimation usually consists of two parts: code acquisition and code tracking [1]. In code acquisition an initial synchronization of the received spreading code with the receiver's local spreading code is achieved. Whereas code tracking attempts to maintain synchronization after initial acquisition. Both of these approaches can be

used for the location. Many techniques have been used to obtain coarse acquisition. These include,among others, sliding correlator, matched filter, serial search, parallel search, Fourier-based, subspace based code acquisition [1]. Similarly methods have been proposed for fine acquisition such as the delay-lock loop (DLL) and Kalman filtering based code tracking.

Other signal processing approaches for TOA estimation include ML based method [23], iterative successive cancellation technique based on a correlation or subspace based techniques to estimate TOAs in a multipath scenario [48]. One of the requirements for the TOA method is an precise time synchronization of all involved fixed measuring units usually the BSs and MS clocks. If there is a drift in the MS clock, then it is directly reflected into an error in the location estimate of the TOA method [2].

2.7.2 TDOA/Range Difference Estimation

Accurate TDOA estimation requires the use of some delay estimation techniques that is resistant to noise and interference and has the ability to resolve multipath signal components. Many approaches have been proposed to estimate TDOA with varying degrees of accuracy and robustness. These include the Generalized Cross-Correlation (GCC) and Cyclic Cross-Correlation (CCC) methods [49].These methods estimate the TDOA as the value that maximizes the cross-correlation between signals received at a pair of BSs. The advantage of combining two or more TDOA measurements results

in a MS location estimate that avoids MS clock synchronization errors [1].

2.7.3 AOA Estimation

The direction of arrival of the MS signal can be calculated by measuring the phase difference between the antenna array elements or by measuring the power spectral density across the antenna array in what is known as beamforming. These antenna arrays are located at the BSs. Thus, AOA estimation techniques are usually used for network-based solutions. Two popular techniques are the so called maximum likelihood method (MLM) based on the work of Capon [50] using frequency wave number analysis, and maximum entropy method (MEM) based on the work of Burg[51].

A ML-based estimator proposed for the AOA measurements is based on iterative Alternative Projection (AP) which transforms the multivariate nonlinear maximization problem into a sequence simpler one-dimensional maximization problems [52]. Perhaps, the most important high resolution methods are based on the subspace techniques proposed by Schmidt [53] with the Multiple SIgnal Classification (MUSIC) algorithm for AOA. MUSIC is based on separating a signal subspace from a noise subspace and the parameters can be achieved using the orthogonality of the signal and noise subspace. Many different variants of the MUSIC algorithm exist such as Root-MUSIC [54] and recursive unitary MUSIC algorithm (RUMA). Another subspace-based AOA estimation techniques include the Estimation of Signal Parameters by Rotational Invariance Techniques (ESPRIT) algorithm [55] and its variants.

The idea of ESPRIT is to divide the array in two equivalent subarrays separated by a known displacement D. The DOA estimates are then angles of arrival with respect to the direction of D [56].

One advantage of AOA estimation is that it requires less number of BS than that of TOA and TDOA methods. Another advantage of AOA location methods is that they do not need any MS-BS clock synchronization. However, the disadvantage of AOA method is the requirement of added antenna array at each BS. Deploying these antenna arrays in all existing BSs is costly for wireless service providers. AOA techniques require modifications at the network side without requiring any modification to the handset. Moreover antenna orientation need to be very precise for slight array misalignment would make AOA's measurements inaccurate. The accuracy of the AOA technique is dependent on the beamwidth of the antenna array.

2.7.4 Signal Strength Estimation

Estimates of the range between a MS and BS can also be derived from measured signal strength measurements at either the MS or BS. Based on empirical models describing signal attenuation with distance [57, 58], the range between the MS and BS can be estimated by measuring the received signal power and calculating the path loss assuming transmit power is known.

The advantages of this method is that there is no need to modify the handset as well as the cellular network and most modern radio modules already provide a

received signal strength indicator (RSSI). On the other hand, the disadvantage is that this method is not very reliable because of the high variability of the received signal strength measurements as the signal level attenuates significantly in a multipath, with variations in the RSS can be 30-40 dB over distance of the order of an half wavelength. The power control mechanisms employed in cellular systems also imposes another difficulty in estimating the location via RSS measurements. Therefore, it is considered as the least reliable technique.

2.7.5 Joint Parameter Estimation

Joint parameter estimation techniques estimating more than one type of parameter simultaneously have recently been developed. With reference to the location estimation, joint estimation of angle of arrival and time of arrival (AOA/TOA) techniques have also been proposed. Most of these joint AOA/TOA estimation approaches are based on ML techniques, signal subspace techniques such as MUSIC or ESPRIT and Kalman filter based techniques, estimating a single user's multipath components at a receiver. The ML based joint AOA/TOA in a static channel is an iterative scheme transforming a multidimensional ML criterion into two sets of one dimensional problems [47]. The methods in [42,73] use EKF for joint channel and delay tracking. The algorithm in [1] uses the UKF to estimate and track the channel coefficients and delays in a time-varying CDMA system. Joint estimation based on particle filters and expectation-maximization (EM) algorithm have also been proposed. These joint

algorithms need both AOA and TOA measurements to locate the MS.

2.8 Data Fusion Methods

Data fusion for wireless location refers to the process of combining the parameter estimates obtained from multiple base stations. The purpose is to produce a fused result hat gives reliable estimate of the MS position. This is normally done at a central location. Various data fusion methods have been proposed for radiolocation and the most widely used are: signal strength measurement, time-of-arrival (TOA), time-difference-of-arrival (TDOA) and angle-of-arrival (AOA).

2.8.1 Signal Strength Measurements

This method is based on the strength of the received signal which is delayed and attenuated version of the transmitted signal. The received signal power is a random variable as it passes through a fading channel. An estimate of the received signal power is obtained by averaging the received signal over an observation window. The relationship between the transmitted signal power and the received power as described by the path loss model provides an estimate of the distance between the transmitter and the receiver. Knowing the transmitted signal power S_t , the received signal power S_r is obtained by the following relationship [9,22],

$$S_r = S_t a(d, n) \tag{2.1}$$

where $a(d, n) = \frac{1}{d^{\mu}}$with $a(d, n)$ is the path loss function, d is the distance between the transmitter and receiver and n is the path loss exponent.

By knowing S_t, S_r and n, the distance between the transmitter and the receiver can be calculated as

$$\mathbf{d} = \left(\frac{S_t}{S_r}\right)^{\frac{1}{n}} \tag{2.2}$$

2.8.2 Angle of Arrival Algorithm

Figure (2.1) shows the intersection of bearings for different BS's. In the case of two bearings the solution is trivial. But when we consider three or more bearings with additive noise, the bearings may not all intersect at the same point. Taking into the account the coordinates of the MS (x_m, y_m) and the ith BS (x_i, y_i),we calculate the true angle of arrival, θ_i, as [2],

$$\theta_i = \arctan \frac{x_i - x_m}{y_i - y_m} \tag{2.3}$$

However the measured AOA, θ_i, are affected by the measurement noise. In [2,4], AOA measurements involving N BS has been treated as a system of linear equations

given by

$$\mathbf{A}_a\mathbf{x} = \mathbf{b}_a \tag{2.4}$$

where

$\mathbf{A}_a = [\alpha_1 \ \cdots \ \alpha_N]^T$

$\mathbf{b}_a = [\alpha_1^t x_1 \ \cdots \ \alpha_N x_N]^T$

$\alpha_i = [\sin\theta_i \ \ -\cos\theta_i]^T$

$\mathbf{x} = [x_m \ y_m]^T$

The least squares solution for the estimated MS position is calculated as

$$\hat{\mathbf{x}} = (\mathbf{A}_a^T\mathbf{A}_a)^{-1}\mathbf{A}_a^T\mathbf{b}_a \tag{2.5}$$

2.8.3 Range-based Algorithms

In range based algorithms, the MS is located at the intersection of a number of circles, of which the BSs are the centers and the measured MS-BS distances are the radii of the circles. Hence the MS-BS range is a function of the MS coordinates,(x_m, y_m), and the *ith* BS coordinates, (x_i, y_i). The distance between MS and BSi is calculated by

$R_i = \|x - x_i\|$

$= \sqrt{(x_m - x_i)^2 + (y_m - y_i)^2}$

However the measured ranges l_i are different from the true ranges by an error term, γ_{ri}, and is written as

$l_i = R_i + \gamma_{r_i}$

where γ_{r_i} is assumed to be a random variable normally distributed with zero mean and a small known variance.

Time of Arrival Algorithm

In TOA data fusion approach, the measurements are the absolute signal transmission times between MS and BSs that represent the MS-BS distances. For the purpose of radiolocation,at least three TOA measurements are required to distinctively estimate the 2-D position of an MS if the entire system is assumed to completely time-synchronized. In this method the distance between MS and BS, can be calculated by:

$r_i = (t_i - t^0)c$

where t^0 represents the actual time when the MS starts transmission and t_i represents the time of arrival of the MS signal at ith BS. Referring to Figure (2.5), we have chosen BS_1 to arbitrarily located at $(0, 0)$ with BS_2 and BS_3 located at (x_2, y_2) and (x_3, y_3) respectively. The measured distances (r_1, r_2, r_3) from three BS are used to estimate the MS coordinates (x_m, y_m) by solving the following set of equations [2],

$$r_1^2 = x_m^2 + y_m^2 \tag{2.6}$$

$$r_2^2 = (x_2 - x_m)^2 + (y_2 - y_m)^2 \tag{2.7}$$

$$r_3^2 = (x_3 - x_m)^2 + (y_3 - y_m)^2 \tag{2.8}$$

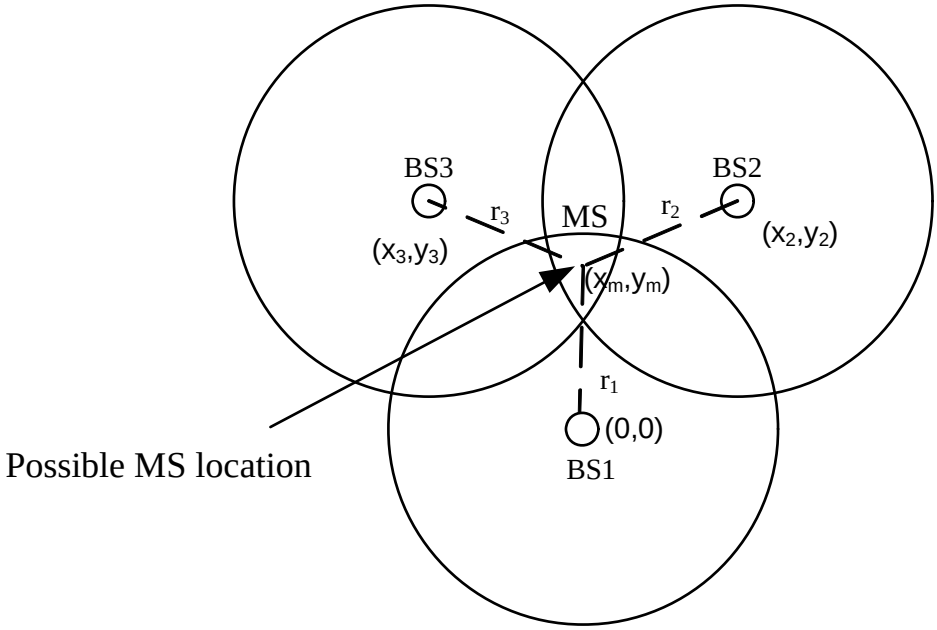

Figure 2.5: MS position location using TOA measurements

subtracting (2.6) from (2.7), we get

$$r_2^2 - r_1^2 = x_2^2 - 2x_2x_m + y_2^2 - 2y_2y_m \tag{2.9}$$

and subtracting (2.6) from (2.8), we get

$$r_3^2 - r_1^2 = x_3^2 - 2x_3x_m + y_3^2 - 2y_3y_m \tag{2.10}$$

after rearranging the terms in the above two equations namely (2.9) and (2.10), we can get the following matrix

$$\begin{bmatrix} x_2 & y_2 \\ x_3 & y_3 \end{bmatrix} \begin{bmatrix} x_m \\ y_m \end{bmatrix} = \frac{1}{2} \begin{bmatrix} K_2^2 - r_2^2 + r_1^2 \\ K_3^2 - r_3^2 + r_1^2 \end{bmatrix} \tag{2.11}$$

where

$$K_i^2 = x_i^2 + y_i^2$$

eq. (2.11) can also be written as

$$\mathbf{Hx} = \mathbf{b} \tag{2.12}$$

where

$$\mathbf{H} = \begin{bmatrix} x_2 & y_2 \\ x_3 & y_3 \end{bmatrix}, \mathbf{x} = \begin{bmatrix} x_m \\ y_m \end{bmatrix}, \mathbf{b} = \frac{1}{2} \begin{bmatrix} K_2^2 - r_2^2 + r_1^2 \\ K_3^2 - r_3^2 + r_1^2 \end{bmatrix}$$

The least square solution of (2.12) is given by [2],

$$\hat{\mathbf{x}} = (\mathbf{H}^T\mathbf{H})^{-1}\mathbf{H}^T\mathbf{b} \tag{2.13}$$

Hence the estimated mobile location using the TOA data fusion method is given by $\hat{\mathbf{x}}$ in the above equation.

Time Difference of Arrival Algorithm

Figure (2.3) shows the intersection of range difference hyperbolae for different pairs of BS's on which the MS is located. The range difference between the ith and the jth BS can be expressed as [49],

$$R_{ij} = \|x - x_i\| - \|x - x_j\|$$

$$= \sqrt{(x_m - x_i)^2 + (y_m - y_i)^2} - \sqrt{(x_m - x_j)^2 + (y_m - y_j)^2} \tag{2.14}$$

where

$R_{ij} = R_i - dR_j$

Again the measured range difference, l_{ij} , includes the additive measurement noise, $\gamma_{d_{ij}}$, which is an independent Gaussian random variable with zero mean and variance σ_d^2.

Given two BSs are needed to generate one hyperbolic line, we require a minimum of three BSs to locate the MS in two dimensions. However there may be an ambiguity in the computed location which may be resolved by using another range difference measurement. A two-step LS estimator for location has been proposed [60] and found to be near optimum in terms of meeting the Cramer-Rao lower bound (CRLB). When the number of participating BSs is more than the minimum necessary, this algorithm has been widely accepted as the best possible solution to locate a MS by trilateration.

It tries to solve the following optimization problem [61]

$$\hat{\mathbf{x}} = \arg\min \sum_{i,j \in S, i \neq j} (R_{ij} - |\|\mathbf{x} - \mathbf{X}_i\| - \|\mathbf{x} - \mathbf{X}_j\||)^2 \tag{2.15}$$

where $\mathbf{x}$ is MS location, R_{ij} is the range difference measurement of the MS to the ith and jth BSs, S is the set of all BSs, and $\mathbf{X}_i$ and $\mathbf{X}_j$ are coordinates of BS_i and BS_j.

Chapter Summary

In this chapter, a brief introduction to radiolocation and various radiolocation algorithms has been presented. Also we discussed different factors that affect radiolocation. Then we looked into the signal parameters that have been used for the purpose of radiolocation. In the next chapter we consider CDMA fundamentals related to the radiolocation with particular emphasis on MAI and its effects on code tracking loop.

Chapter 3

An Overview of CDMA

The proposed research on radiolocation is to be done in the cellular systems, it is pertinent to study the fundamentals of CDMA briefly with reference to time estimation techniques.

3.1 Introduction

Spread spectrum communication is a scheme that transmits a signal with a much larger bandwidth than that of the original data signal. The purpose of the bandwidth expansion is to protect the transmitting signal against interference, such as multipath interference and interference from other systems. At the transmitting side, the data sequence is multiplied by a pseudo-random noise (PN) sequence (spreading code), which has a higher rate than that of the data sequence. This process is called spreading, since the resulting signal bandwidth is spread out. Let T be the data period

and T_c be the PN code chip period. Then, the bandwidth expansion factor due to spreading is $N = T/T_c$ which is known as processing gain.

At the receiving side, the received signal is despreaded by the multiplication of the same PN code. However, the phase of the PN code generated at the receiver must be synchronized with the receiving signal in order to extract the data properly. This is known as code acquisition and tracking problem. It is essential for determining the TOA estimates. The basic principle of spread spectrum ranging technique is based on the correlation of spreading codes. In DS-CDMA systems the time delay is estimated by correlating the incoming spreading code with the local spreading code. It is accomplished by using code acquisition, followed by code tracking. Code acquisition is a coarse timing synchronization technique that may involve sliding correlator or matched filter. Code tracking is to provide a fine timing synchronization. One of the most popular tracking algorithms is the delay-locked loop.

3.2 Code Acquisition

code acquisition is also called coarse acquisition, which means that the local PN generator at the receiver must be aligned within one chip (or a fraction of one chip) of the received spreaded signal. This is accomplished by different techniques including search algorithms such as parallel search or serial search algorithms. Each of the algorithms has its own advantages and disadvantages [65].

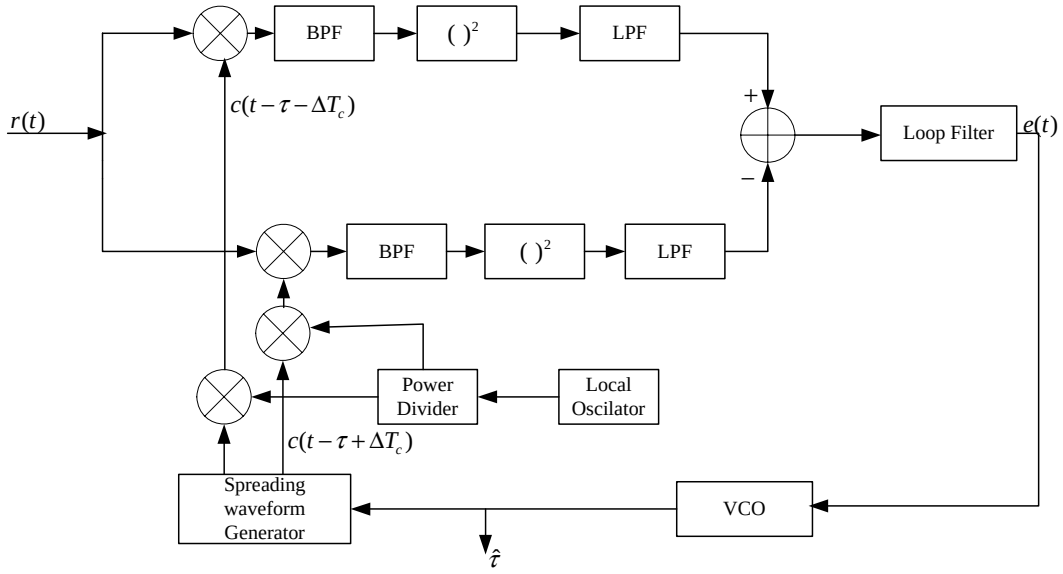

Figure 3.1: Non coherent DLL

3.3 Code Tracking

Once coarse acquisition has been achieved, the next stage is code tracking. The delay-lock loop (DLL) is a technique for allowing fine synchronization of the incoming code and the local code. As a result, more accurate arrival time estimates can be obtained from the DLL. TOA estimation is carried out by tracking the received PN sequence. This is accomplished by using a DLL. A conventional DLL is shown in Figure (3.1).

The early and late waveforms are separated from each other by a period equal to $2\Delta T_c$, where Δ is the early late discriminator offset and T_c is the chip duration. The voltage controlled clock (VCC) source adjusts the phase of the locally generated PN code. The changes in level of $e(t)$ dictate if the phase of the locally generated PN code has to be advanced or retarded. The error signal $\varepsilon(t)$ is expressed as [65]

$$\varepsilon(\delta) = \frac{P}{2}\left[R_c^2(\delta - \frac{\triangle}{2})T_c - R_c^2(\delta + \frac{\triangle}{2})T_c\right] \tag{3.1}$$

where P is the received power, R_c is the auto correlation of the sequence and δ is the delay error normalized with respect to chip duration T_c, give by

$$\delta = \frac{t_d - \hat{t}_d}{T_c} \tag{3.2}$$

$\epsilon(\delta)$ is often written as

$$\varepsilon(\delta) = \frac{P}{2}D_{\triangle}(\delta) \tag{3.3}$$

where

$$D_{\Delta}(\delta) = R_c^2\left[\left(\delta - \frac{\Delta}{2}\right)T_c\right] - R_c^2\left[\left(\delta + \frac{\Delta}{2}\right)T_c\right] \tag{3.4}$$

$D_{\Delta}(\delta)$ is S-curve characteristics of the tracking loop. The S-curve for rectangular pulse with $\frac{\delta}{\triangle} = 2$ is shown in Figure (3.3)

3.4 Multiple Access Interference

In a CDMA cellular system, users share the same frequency band at the same time, but each of them is distinguished among others by using different spreading codes.

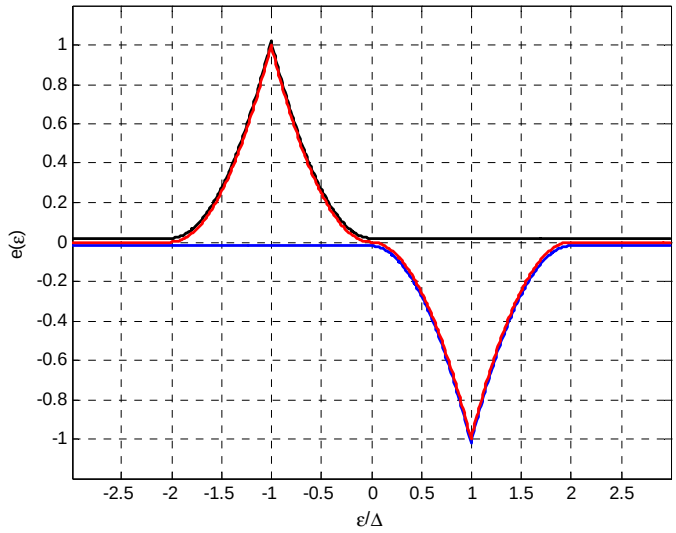

Figure 3.2: Discriminator curve for DLL

Signal received at the receiver is basically composed of signals from all the users and background noise. The desired user's signal is separated from others and despreaded by multiplying the received signal with the associated spreading code. As a result, other users signals, which do not match the associated spreading code contribute to MAI. So the signals transmitted by all of these users on the reverse link interfere with one another resulting in near-far effect; a phenomenon in which the signals from different MSs are received with unequal power at a BS making it difficult to recover the weaker users. With forward link transmissions, the interference comes from other BSs.

3.4.1 Effects of MAI

Multiple access interference within a coverage area can be broadly classified as:

• **Intracellular interference:** Intracell interference experienced at a BS is caused by other users in the same cell. This is due to the non orthogonality in the users PN sequences.

For example, consider cell C_i. At BS_i while processing the signals from users are power controlled while signals from the other n_i - 1 users would act as interferes.

• **Intercellular interference:** Intercell interference experienced at a particular BS, is caused by the users in other cells. These users are power controlled by another BS. Users within a cell are all power controlled by the same BS and hence the received power at the controlling BS, from the users it power controls, is same and is equal to the nominal power. For example, for cell C_i, the received power due to all the n_i users of cell C_i at BS_i would be the same and be equal to nominal power P. Same is the case the users in other cells. But, the received powers of n_i users, power controlled by BS_i , at BS_j would not be the same. The power received at BS_j from user, power controlled by BS_i, at the edge of cell i, would be comparable to the power received from home user, even though it is not power controlled by BS_j. Thus, it will act as an interferer at BS_j. Similar will be the case with all the users of other cells. Such an interference is called intercellular interference.

One solution that has been proposed in literature is to use power control. With power control, an attempt is made to receive each user's signal with equal power at

the BS. Even with power control, the near-far effect is the main factor in accurate parameter estimation. The interference will affect the ability of a conventional receiver at other BSs to accurately estimate the TOA or TDOA information. This can be illustrated by the Figure (3.4), where the target MS is being served by BS1 [1]

In order to estimate its position, the other two nearby base stations BS2 and BS3 are also used in addition to the home BS1. If the power control is to be applied, then the signal from all the MS present in the home BS will arrive at the BS1 with approximately same power. The same applies to the MSs in BS2 and BS3. In order to make a location estimate, BS2 and BS3 must also detect the signal being transmitted by the target MS. But the signal from the target MS undergoes severe MAI from the MSs present in BS2 and BS3. The very reason being the target MS is not power controlled by those BSs.

3.5 Multiuser Radiolocation

Importance of the Problem

The mobile location accuracy is greatly affected by LOS blockage, multipath propagation and MAI. The performance evaluation of the radiolocation algorithms, presented in the previous section as well as those discussed in [1,66, 67] and references therein, and others, has been done assuming a single user in the system. For location in a CDMA cellular system, the near-far effect remains a factor even when power control

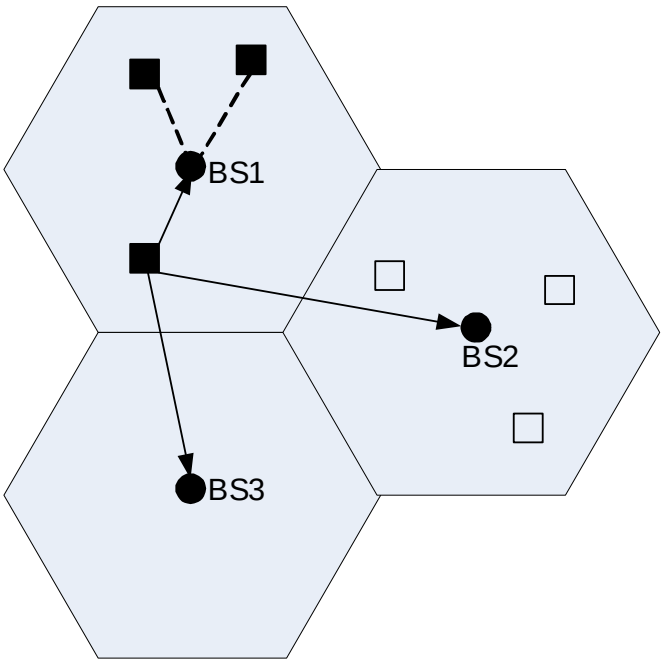

Figure 3.3: CDMA multiuser interference scenario

schemes are used since the interference will affect the ability of a conventional receiver at other BSs to estimate the TOA. The interference from other users has a drastic effect on the accuracy to which time delay estimates can be made [68,69]. Not only is the tracking performance reduced, but it becomes difficult for nearby BSs, other than the serving BS, to detect the desired user's signal even with perfect power control [70]. In CDMA, the conventional means of obtaining TOA estimates is through coarse or fine propagation delay acquisition. It has been shown that MAI greatly affects the coarse code acquisition of spread spectrum signals [71,72]. Likewise, the effects of MAI on code tracking techniques,such as the conventional DLL, have been shown to be quite drastic [5].

When other users are considered, the multiple-access interference will interfere with the tracking ability of conventional delay trackers, such as DLL [69]. In conventional DLL, used to provide TOA estimate for location, the accuracy of the computed location estimate will be directly affected. Delay estimation in CDMA receivers has been carried out traditionally using DLL. The DLL has optimal performance for single user, single path systems [2], but their performance deteriorate significantly in multipath environments, especially for closely-spaced paths scenarios. The following impairments affect the performance of the conventional DLL.

- It is demonstrated that when near-far effect exists and MAI is not accurately modeled as white Gaussian random process, it will bring considerable influence on the code tracking loop - not only promoting the rms tracking jitter but also introducing the steady state tracking error. When the powers of some of the interfering users are dominant, the reliable tracking, that is the exact time delay estimation, isn't achieved. When MAI is dominant, the rms tracking jitter, that is the variance of tracking error increases, and system performance degrades [6]. When a single user is received with significantly more power than the desired user, even in a two-user scenario, the effects are worse than when there are many users with equal received strength [5].

- When the successive paths are spaced at less than one chip distance (closely-spaced path), traditional DLL is not able to estimate closely spaced path delays with good accuracy [73].

These expositions serve as a justification for the need to develop methods that

are either near-far resistant or mitigate the effects of MAI on code tracking. With this background, we will first focus on signal processing techniques based on nonlinear filters where delay estimation is treated as a parameter estimation problem. We will look into nonlinear filtering approaches based on Kalman framework such as

- Extended Kalman filter based estimation
- Unscented filter based parameter estimation
- Divided difference filter based estimation

Secondly, we will look into two novel receivers based on DLL and early late algorithm combined with interference cancellation. These techniques have been presented in the subsequent chapters.

Chapter Summary

In this chapter we discussed how the performance of the code tracking loop is degraded by the multiuser interference which in turn is going to effect the accuracy of estimation. The next chapter presents multiuser parameter estimation using recursive filters. Comparison among these filters will be provided to show that the nonlinear filtering approaches estimate the time delay accurately even in the presence of MAI.

Chapter 4

Multiuser Time of Arrival Estimation using Kalman Filters

The Kalman filter is a data processing algorithm that evaluates the most recent state based on the information available at a certain point. In contrast, nonrecursive estimators, such as maximum likelihood requires the whole series of information when updating the parameter estimates, and the estimation process is updated iteratively, rather than sequentially. This sequential nature of the Kalman filter approach give rise to high computational speed. Compared to approaches such as maximum likelihood with nonlinear constraints, the Kalman filter approach is easier to implement as it reduces the amount of implementation complexity in specifying the nonlinear relationship explicitly.

In this chapter we will provide a description of the joint parameter estimation

problem of the multipath delays and channel coefficients. Due to nonlinear nature of time delay estimation, a nonlinear filtering approach will be adopted. The nonlinear filtering problem consists of estimating the states of a nonlinear dynamic system. In a broad sense, the optimal nonlinear filtering is described by the recursive Bayesian approach. However, in nonlinear systems the optimal exact solution to the recursive Bayesian filtering problem is intractable since it requires multi-dimensional integrals. Therefore, approximate nonlinear filters have been proposed. The most widely used approximate nonlinear filters are based on Kalman filter framework. The work presented in this chapter involves the investigation of nonlinear filtering algorithms that are based on Kalman filter framework. We will also introduce three different algorithmic forms of estimation and show how the shortcomings of EKF are addressed by more robust and simpler SPKF estimation approaches.

4.1 Signal Model

We consider a typical asynchronous CDMA system model where K users transmit over an M-path fading channel. The received baseband signal sampled at $t = lT_s$ is given by

$$r(l) = \sum_{k=1}^{K} \sum_{i=1}^{M} c_{k,i}(l) d_{k,m_k(l)} a_k(lT_s - m_k(l)T_b - \tau_{k,i}(l)) + n(l) \tag{4.1}$$

where $c_{k,i}(l)$ represents the complex channel coefficients associated with the ith path

of the kth user, $d_{k,m_k(l)}$ is the mth symbol transmitted by the kth user, $m_k(l) = \lfloor (lT_s - \tau_{k,i}(l))/T_b \rfloor$, T_b is the symbol interval, $a_k(l)$ is the spreading waveform used by the kth user, $\tau_{k,i}(l)$ is the time delay associated with the ith path of the kth user, and $n(l)$ represents additive white Gaussian noise (AWGN) assumed to have a zero mean and variance $\sigma^2 = E[|n(l)|^2] = N_0/T_s$ where T_s is the sampling time.

In order to use a Kalman filtering approach, we adopt a state-space model representation where the unknown channel parameters (path delays and gains) to be estimated are given by the following $2KM \times 1$ vector [1],

$$\mathbf{x} = [\mathbf{c}\,;\boldsymbol{\tau}] \tag{4.2}$$

with

$\mathbf{c} = [c_{11}, c_{12}, ..., c_{1M}, c_{21}, ..., c_{2M}, ..., c_{K1}, ..., c_{KM}]^T$

and

$\boldsymbol{\tau} = [\tau_{11}, \tau_{12}, ..., \tau_{1M}, \tau_{21}, ..., \tau_{2M}, ..., \tau_{K1}, ..., \tau_{KM}]^T$

The hidden system state x_k evolves over time as an indirect or partially observed first order Markov process. Therefore the complex-valued channel amplitudes and real-valued time delays of the K users are assumed to obey a Gauss-Markov dynamic channel model [1], i.e.

$$c(l+1) = \mathbf{F}_c c(l) + \mathbf{v}_c(l) \tag{4.3}$$

$$\tau(l+1) = \mathbf{F}_\tau \tau(l) + \mathbf{v}_\tau(l) \tag{4.4}$$

where $\mathbf{F_c}$ and $\mathbf{F_\tau}$ are $KM \times KM$ state transition matrices for the amplitudes and time delays respectively, $\mathbf{v}_c(l)$ and $\mathbf{v}_\tau(l)$ are $KM \times 1$ mutually independent Gaussian random vectors with zero mean and covariance given by

$$\mathrm{E}\{\ v_c(i)v_c^T(j)\} = \delta_{ij}\mathbf{Q}_c,$$

$$\mathrm{E}\{\ v_\tau(i)v_\tau^T(j)\} = \delta_{ij}\mathbf{Q}_\tau,$$

$$\mathrm{E}\{\ v_c(i)v_\tau^T(j)\} = 0\ \forall\, i,j$$

with $\mathbf{Q_c} = \boldsymbol{\sigma_c^2}\mathbf{I}$ and $\mathbf{Q_\tau} = \boldsymbol{\sigma_\tau^2}\mathbf{I}$ are the covariance matrices of the process noise $\mathbf{v_c}$ and $\mathbf{v_\tau}$ respectively and δ_{ij} is the two-dimensional Kronecker delta function equal to 1 for $i = j$ and 0 otherwise. The state model can be written as

$$\mathbf{x}(l+1) = \mathbf{F}\mathbf{x}(l) + \mathbf{v}(l) \tag{4.5}$$

where $\mathbf{F} = \begin{bmatrix} \mathbf{F}_c & 0 \\ 0 & \mathbf{F}_\tau \end{bmatrix}$ is $2KM \times 2KM$ state transition matrix,$\mathbf{v}(l)$ is $2KM \times 1$ process noise vector with zero mean and covariance matrix $\mathbf{Q} = \begin{bmatrix} \mathbf{Q}_c & 0 \\ 0 & \mathbf{Q}_\tau \end{bmatrix}$.The scalar measurement model follows from the received signal of (4.99) by

$$z(l) = h(\mathbf{x}(l)) + n(l) \tag{4.6}$$

The scalar measurement $z(l)$ is a non-linear function of the state $\mathbf{x}(l)$. Given the state-space and measurement models, we may find the optimal estimate of $\mathbf{x}(l)$ denoted as $\hat{\mathbf{x}}(l|l) = E\{\mathbf{x}(l)|z(l)\}$, with the estimation error covariance

$$\mathrm{P} = \mathrm{E}\left\{\left[\mathbf{x}(l) - \hat{\mathbf{x}}(l|l)\right]\left[\mathbf{x}(l) - \hat{\mathbf{x}}(l|l)\right]^T |z(l)\right\} \tag{4.7}$$

where $z(l)$ denotes the set of received samples up to time l, $\{z(l), z(l-1), \ldots, z(0)\}$.

4.2 Cramer-Rao Lower Bound (CRLB)

The CRLB is a lower bound on the covariance matrix of any unbiased estimator. The derivation of the Cramer-Rao bound is based on computing the gradient of the log-likelihood function with respect to the unknown parameter vector $\mathbf{x}$.

Let $\hat{\mathbf{x}}$ be an unbiased estimator of a vector of deterministic unknown parameters $\mathbf{x}$; hence $E[\hat{\mathbf{x}}] = \mathbf{x}$. Then the estimator's covariance matrix satisfies [1],

$$J^{-1} \leq E\{(\hat{\mathbf{x}} - \mathbf{x})(\hat{\mathbf{x}} - \mathbf{x})^T\} \tag{4.8}$$

where J is the Fisher information matrix given by

$$J = \left\{\left[\frac{\partial}{\partial \mathbf{x}} \ln \Lambda(z^l)\right]\left[\frac{\partial}{\partial \mathbf{x}} \ln \Lambda(z^l)\right]^T\right\} \tag{4.9}$$

and $\Lambda(z^l)$ is the likelihood function of the received data vector z^l with respect to $\mathbf{x}$.

The observed data of the received samples is $z^l = [z(1) \dots z(l)]^T$ for $l = 1, 2, \dots, L$. We can write [1],

$$\mathbf{z}(l) = \mathbf{c}^T(l)\mathbf{B}(l)\mathbf{a}(l) + \mathbf{n}(l) \tag{4.10}$$

where

$$\mathbf{c}(l) = \begin{bmatrix} c_{11}(l) \\ . \\ . \\ c_{KM}(l) \end{bmatrix}, \mathbf{B}(l) = \begin{bmatrix} d_{11}(l) & & \\ & . & \\ & & . \\ & & d_{KM}(l) \end{bmatrix}$$

and

$$\mathbf{a}(l) = \begin{bmatrix} \bar{a}_1 \left(lT_s - m_l(l) T_b - \tau_{11}(l) \right) \\ . \\ . \\ \bar{a}_K \left(lT_s - m_l(l) T_b - \tau_{KM}(l) \right) \end{bmatrix}$$

The likelihood function of $z(l)$ given $\mathbf{x}$ is

$$\ln \Lambda(z^l) = \frac{1}{(2\pi\sigma_n^2)^{L/2}} \exp \left\{ \frac{1}{2\sigma_n^2} \sum_{l=1}^{L} \left| z(l) - \mathbf{c}^T(l)\mathbf{B}(l)\mathbf{a}(l) \right|^2 \right\} \tag{4.11}$$

from which the log-likelihood function density follows

$$\ln \Lambda(z^l) = const - \frac{1}{2\sigma_n^2} \sum_{l=1}^{L} \left| z(l) - \mathbf{c}^T(l)\mathbf{B}(l)\mathbf{a}(l) \right|^2 \tag{4.12}$$

The Fisher information matrix $\mathbf{J}$ is given by

$$\mathbf{J} = \begin{bmatrix} \mathbf{J_{cc}} & \mathbf{J_{c\tau}} \\ \mathbf{J_{c\tau}^T} & \mathbf{J_{\tau\tau}} \end{bmatrix} \tag{4.13}$$

where the matrices $\mathbf{J_{cc}}$,$\mathbf{J_{c\tau}}$, $\mathbf{J_{\tau\tau}}$ are defined as [1],

$$\mathbf{J_{cc}} = \frac{1}{\sigma_n^2} \sum_{l=1}^{L} \mathbf{B}(l)\bar{\mathbf{a}}(l)\bar{\mathbf{a}}^T(l)\mathbf{B}(l) \tag{4.14}$$

$$\mathbf{J}_{\mathbf{c}\tau} = \frac{1}{\sigma_n^2} \sum_{l=1}^{L} \mathbf{B}(l)\mathbf{C}(l)\bar{\mathbf{a}}(l)\bar{\mathbf{a}}_d^T(l)\mathbf{C}(l)\mathbf{B}(l) \tag{4.15}$$

$$\mathbf{J}_{\tau\tau} = \frac{1}{\sigma_n^2} \sum_{l=1}^{L} \mathbf{B}(l)\bar{\mathbf{a}}_d(l)\bar{\mathbf{a}}_d^T(l)\mathbf{B}(l)\mathbf{C}(l) \tag{4.16}$$

where $\bar{\mathbf{a}}_d(l) = {}^{\partial\bar{\mathbf{a}}(l)}/_{\partial_{\tau k}}$ and $\mathbf{C}(l) = diag[c(l)]$. So the CRLBs of the channel coefficients and the delays are

$$\text{CRLB}(\mathbf{c}) = [\mathbf{J_{cc}} - \mathbf{J_{c\tau}}\mathbf{J}_{\tau\tau}^{-1}\mathbf{J}_{c\tau}^T]^{-1} \tag{4.17}$$

$$\text{CRLB}(\boldsymbol{\tau}) = [\mathbf{J_{\tau\tau}} - \mathbf{J}_{c\tau}^T\mathbf{J}_{cc}^{-1}\mathbf{J_{c\tau}}]^{-1} \tag{4.18}$$

The CRLBs of the amplitudes and delays for each user is given by the appropriate

diagonal elements of each CRLB formula.

Various filtering techniques, which will be presented in the sections to follow, are based on Kalman filter framework for the purpose of estimating the parameters of the system. We begin with the Kalman filter (KF), which is unquestionably the most popular choice, along with its own variation, the Extended Kalman Filter (EKF) for nonlinear systems. In 1960, Kalman showed that if the uncertainty associated with a measurement is given in terms of its covariance, accurate estimates can be derived from multiple noisy measurements using the proposed mathematical framework. However, most of the real world dynamics are essentially nonlinear in nature, a nonlinear version of the KF was developed. We then present the unscented Kalman filter (UKF), which was introduced by Julier and Uhlmann in 1994. The UKF is based on the fact that approximating Gaussian distribution is easier than to approximate an arbitrary non-linear function, and the UKF promises more accurate estimates with a lower expected error covariance than the EKF. It linearizes to higher order than the standard EKF. Finally, we present two variants of the Divided-Difference filter (DDF1 and DDF2), which is very similar to an UKF, but the covariance approximation of the DDF2 filter is slightly more accurate.

4.3 Extended Kalman Filter

The most well known application of the Kalman filter framework to nonlinear inference problems is the EKF. It linearizes the system and observation equations about the current state estimate with the assumption that the apriori distribution is Gaussian, and uses the Kalman filter framework for obtaining the estimates for the state and covariance of these estimates. The current state estimate is chosen as the best estimate, that is, the approximation of the conditional mean.

Consider the following nonlinear system

$$\mathbf{x}_{k+1} = \mathbf{f}(\mathbf{x}_k, \mathbf{w}_k, k) \tag{4.19}$$

$$\mathbf{y}_k = \mathbf{h}(\mathbf{x}_k, \mathbf{v}_k, k) \tag{4.20}$$

where $\mathbf{w}_k$ is the $q \times 1$ additive and independent process noise that is drives the dynamic system model through the nonlinear state transition function $\mathbf{f}$,and $\mathbf{v}_k$ is the $s \times 1$ additive and independent observation or measurement noise corrupting the observation of the state through the nonlinear observation function $\mathbf{h}$. The noise vectors are assumed to be zero-mean Gaussian processes and covariance

$$E[\mathbf{w}_k \mathbf{w}_j^T] = \delta_{kj}\mathbf{Q}_k, \qquad E[\mathbf{v}_k \mathbf{v}_j^T] = \delta_{kj}\mathbf{R}_k, \qquad E[\mathbf{v}_k \mathbf{w}_j^T] = 0, \qquad \forall\ k, j \tag{4.21}$$

For system model with initial state and covariance values, the EKF propagates the first two moments of the distribution of $\mathbf{x}_k$ recursively. Given imperfect measurements, the EKF updates the estimates of the state vector and the covariance.

The EKF first linearizes the system around the current state estimate $\hat{\mathbf{x}}_k$ using a first-order truncation of the multidimensional Taylor series expansion. The predicted state estimate and covariance are approximated by [74],

$$\hat{\mathbf{x}}_{k+1}^{-} = \mathbf{f}(\hat{\mathbf{x}}_k,k) \tag{4.22}$$

$$\mathbf{P}_{k+1}^{-} = \mathbf{F}_k\mathbf{P}_k\mathbf{F}_k^T + \mathbf{Q}_k \tag{4.23}$$

where $\mathbf{F}_k$ is the Jacobian matrix of $\mathbf{f}$ evaluated around the current state estimate $\hat{\mathbf{x}}_k$. The observation propagation is calculated as

$$\hat{\mathbf{y}}_{k+1}^{-} = \mathbf{h}(\hat{\mathbf{x}}_{k+1}^{-}, k+1) \tag{4.24}$$

$$\mathbf{P}_{k+1}^{vv} = \mathbf{H}_{k+1}\mathbf{P}_{k+1}^{-}\mathbf{H}_{k+1}^T + \mathbf{R}_{k+1} \tag{4.25}$$

$$\mathbf{P}_{k+1}^{xy} = \mathbf{P}_{k+1}^{-}\mathbf{H}_{k+1}^T \tag{4.26}$$

where $\mathbf{P}_{k+1}^{xy}$ is the predicted cross-correlation matrix between $\hat{\mathbf{x}}_{k+1}^{-}$ and $\hat{\mathbf{y}}_{k+1}^{-}$. The update equations are written as

$$\hat{\mathbf{x}}_{k+1}^{+} = \hat{\mathbf{x}}_{k+1}^{-} + K_{k+1}\mathbf{v}_{k+1} \tag{4.27}$$

$$\mathbf{P}_{k+1}^{+} = \mathbf{P}_{k+1}^{-} - K_{k+1}\mathbf{P}_{k+1}^{vv}K_{k+1}^{T} \tag{4.28}$$

where $\mathbf{v}_{k+1}$ is the innovative vector given by

$$\mathbf{v}_{k+1} = \mathbf{y} - \hat{\mathbf{y}}_{k+1}^{-} \tag{4.29}$$

The covariance of the innovation vector is given by

$$\mathbf{P}_{k+1}^{vv} = \mathbf{P}_{k+1}^{yy} + \mathbf{R}_{k+1} \tag{4.30}$$

where $\mathbf{P}_{k+1}^{yy}$ is the output covariance. The Kalman gain K_{k+1} is computed by

$$K_{k+1} = \mathbf{P}_{k+1}^{xy}(\mathbf{P}_{k+1}^{vv})^{-1} \tag{4.31}$$

EKF can be represented by the block diagram as shown in Figure (4.1) and table 4.1 lists the algorithmic steps.

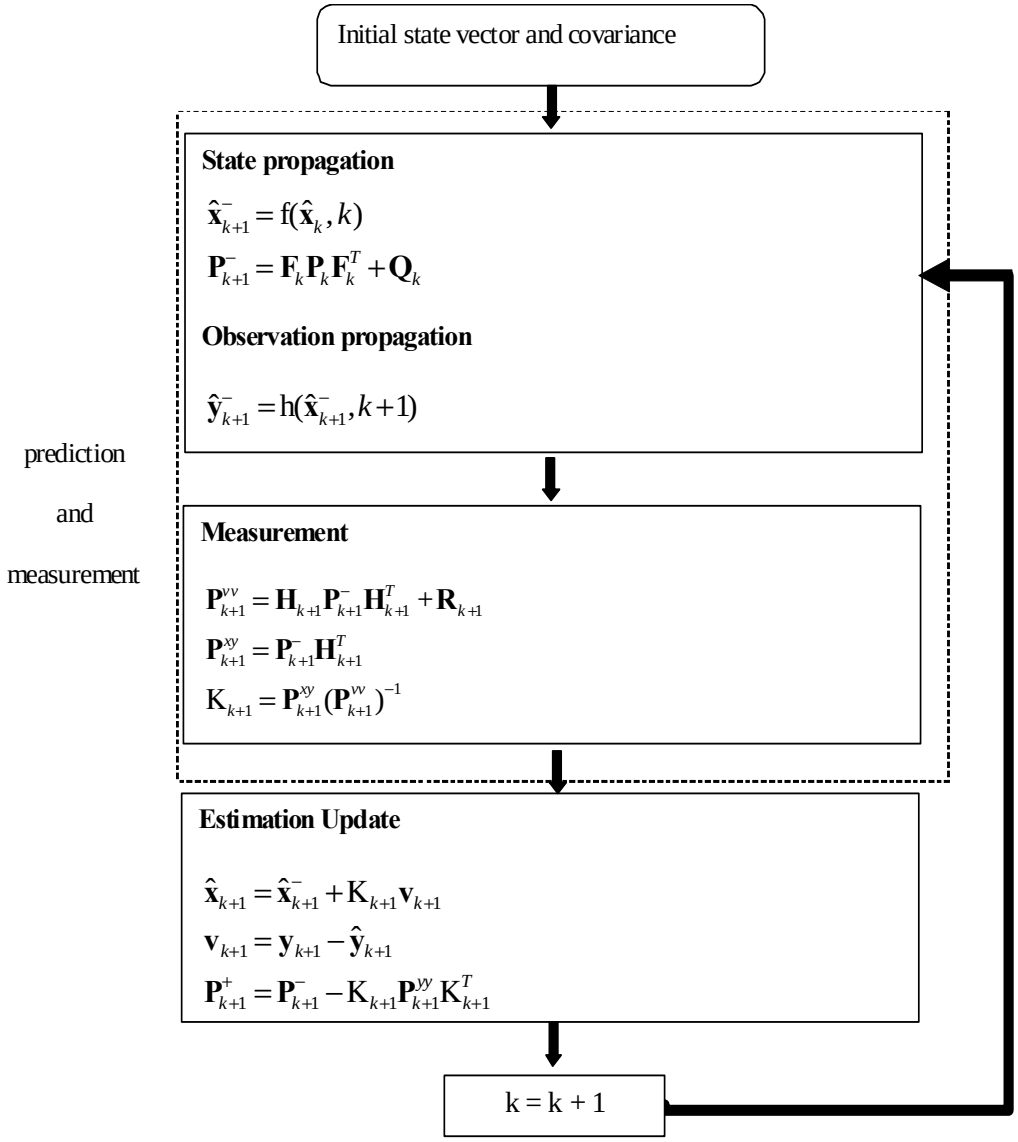

Figure 4.1: Extended Kalman filter algorithm

Step I Initialization:

$$\hat{\mathbf{x}}_0 = E[x0]$$
$$\mathbf{P}_0 = E[(\mathbf{x}_0 - \mathbf{x}_0)(\mathbf{x}_0 - \mathbf{x}_0)T]$$

Step II Propagation

State propagation:

$$\hat{\mathbf{x}}^-_{k+1} = \mathbf{f}(\hat{\mathbf{x}}_k, k)$$
$$\mathbf{P}^-_{k+1} = \mathbf{F}_k \mathbf{P}_k \mathbf{F}^T_k + \mathbf{Q}_k$$

Step III Observation propagation:

$$\hat{\mathbf{y}}^-_{k+1} = \mathbf{h}(\mathbf{x}^-_{k+1}, k+1)$$
$$\mathbf{P}^{vv}_{k+1} = \mathbf{H}_{k+1} \mathbf{P}^-_{k+1} \mathbf{H}^T_{k+1} + \mathbf{R}_{k+1}$$
$$\mathbf{P}^{xy}_{k+1} = \mathbf{P}^-_{k+1} \mathbf{H}^T_{k+1}$$

Step IV Update:

$$\mathbf{v}_{k+1} = \mathbf{y} - \hat{\mathbf{y}}^-_{k+1}$$
$$\mathbf{K}_{k+1} = \mathbf{P}^{xy}_{k+1} (\mathbf{P}^{vv}_{k+1})^{-1}$$
$$\mathbf{P}^+_{k+1} = \mathbf{P}^-_{k+1} - \mathbf{K}_{k+1} \mathbf{P}^{vv}_{k+1} \mathbf{K}^T_{k+1}$$
$$\hat{\mathbf{x}}^+_{k+1} = \hat{\mathbf{x}}^-_{k+1} + \mathbf{K}_{k+1} \mathbf{v}_{k+1}$$

Table 4.1: EKF algorithm

4.4 The Extended Kalman Filter and its Limitation

Even though the EKF is one of the most widely used approximate solution for non-linear estimation and filtering, it has some limitations as those discussed in [74-78]. Here we briefly describe them.

The EKF first linearizes the system around the current state estimate using a first-order truncation of the multidimensional Taylor series expansion. However, these approximations are valid if all the higher order derivatives of the non-linear function are effectively zero over the 'uncertainty region' of $\mathbf{x}$. Stated in other words it requires the zeroth and first order terms to dominate the rest of the terms, over the region of the state-space defined by the prior distribution of $\mathbf{x}$. It is important to note here, that although this probabilistic spread of $\mathbf{x}$ (or equivalently that of $\delta_{\mathbf{x}}$ around $\bar{\mathbf{x}}$), as captured by the covariance $\mathbf{P}_{\mathbf{x}}$, plays an important role in the validity of the EKFs "first order linearization" during the linearization process. The linearization method employed by the EKF fails to take into account the inherent uncertainty in the prior random variable. This has large implications for the accuracy and consistency of the resulting EKF algorithm. These approximations often introduce large errors in the EKF calculated posterior mean and covariance of the transformed Gaussian random variable (GRV), which may lead to suboptimal performance and sometimes divergence of the filter.

It is quite evident when the models are highly non-linear and the local linearity assumption breaks down, i.e., the effects of the higher order terms of the Taylor series expansion become significant, the EKF often introduce large errors in the calculated posterior mean and covariance of the transformed random variable, which may lead to suboptimal performance and sometimes divergence of the filter.

And also linearization can be applied only if the Jacobian matrix exists. However, this is not always the case. Some systems contain discontinuities,others have singularities. Calculating Jacobian matrices can be very difficult.

In the next section we will discuss an alternative approach which also linearizes the nonlinear function based on Sterling interpolation formula but avoids the calculation of Jacobians. It uses functional evaluation instead.

4.5 Divided Difference Filter

In this section, we present the DDF proposed by Norgaard [78], as an efficient extension of the Kalman Filter for nonlinear systems. The DDF belongs to the sampling-based polynomial filters. The DDF is described as a sigma point Kalman filter (SPKF) where the filter linearizes the nonlinear dynamic and measurement functions by using an interpolation formula through systematically chosen sigma points. The linearization is based on polynomial approximations of the nonlinear transformations that are obtained by Stirling's interpolation formula, rather than the derivative-based Taylor series approximation. Conceptually, the implementation principle resembles that of

the EKF, with significantly simpler implementation as it is not necessary to formulate the Jacobian matrices of partial derivatives of the nonlinear dynamic and measurement equations. Thus, the new nonlinear state filter, DDF, can also replace the EKF and its higher-order estimators in practical real-time applications that require accurate estimation, but less computational cost. The other advantage of DDF is its ability to estimate the state even if there are singular points present where the derivatives are undefined.

A description of the formulation based on the Stirling polynomial expansion has been provided in Appendix I.

4.5.1 First-Order Divided Difference Filter (DDF1)

We start with the nonlinear system as described for the EKF case. It is assumed that the noise vectors are uncorrelated white Gaussian processes with expected means and covariances [78-80]

$$\begin{aligned} E\{\mathbf{w}_k\} &= \bar{\mathbf{w}}\,, \;\; E\left\{[\mathbf{w}_k - \bar{\mathbf{w}}_k][\mathbf{w}_j - \bar{\mathbf{w}}_k]^T\right\} = \mathbf{Q}_k \\ E\{\mathbf{v}_k\} &= \bar{\mathbf{v}}\,, \;\; E\left\{[\mathbf{v}_k - \bar{\mathbf{v}}_k][\mathbf{v}_j - \bar{\mathbf{v}}_k]^T\right\} = \mathbf{R}_k \end{aligned} \tag{4.32}$$

Let the square Cholesky factorizations

$\mathbf{P}_0 = \mathbf{S_x}\mathbf{S_x}^T, \mathbf{Q} = \mathbf{S_w}\mathbf{S_w}^T, \mathbf{R}{=}\mathbf{S_v}\mathbf{S_v}^T$

The predicted state vector is

$$\hat{\mathbf{x}}_{k+1}^{-} = \mathbf{f}(\hat{\mathbf{x}}_k, \bar{\mathbf{w}}, k) \tag{4.33}$$

The predicted state covariance is determined by the symmetric matrix product

$$\mathbf{P}_{k+1}^{-} = \mathbf{S}_x^{-}(k+1)(\mathbf{S}_x^{-}(k+1))^T \tag{4.34}$$

where

$$\mathbf{S}_x^{-}(k+1) = \left[\mathbf{S}_{x\hat{x}}^{(1)}(k+1) \;\; \mathbf{S}_{xw}^{(1)}(k+1)\right] \tag{4.35}$$

with

$$\begin{aligned} \mathbf{S}_{x\hat{x}}^{(1)}(k+1) &= \tfrac{1}{2h}\left\{\mathbf{f}_i(\hat{\mathbf{x}}_k + h\mathbf{s}_{x,j}, \bar{\mathbf{w}}_k) - \mathbf{f}_i(\hat{\mathbf{x}}_k - h\mathbf{s}_{x,j}, \bar{\mathbf{w}}_k)\right\} \\ \mathbf{S}_{xw}^{(1)}(k+1) &= \tfrac{1}{2h}\left\{\mathbf{f}_i(\hat{\mathbf{x}}_k, \bar{\mathbf{w}}_k + h\mathbf{s}_{w,j}) - \mathbf{f}_i(\hat{\mathbf{x}}_k, \bar{\mathbf{w}}_k - h\mathbf{s}_{w,j})\right\} \end{aligned} \tag{4.36}$$

where $\mathbf{s}_{x,j}$ is the column of $\mathbf{S}_\mathbf{x}$ and $\mathbf{s}_{w,j}$ is the column of $\mathbf{S}_\mathbf{w}$ and h is the interval length or divided difference step size. The Cholesky factorization of $\mathbf{P}_{k+1}^{-}$ is given by

$\mathbf{P}_{k+1}^{-} = \mathbf{S}_x^{-}\mathbf{S}_x^{-T}$

The predicted observation vector and its predicted covariance is given by

$$\hat{\mathbf{y}}_{k+1}^{-} = +(\hat{\mathbf{x}}_{k+1}^{-}, \bar{\mathbf{v}}_{k+1}, k+1) \tag{4.37}$$

$$\mathbf{P}_{k+1}^{vv} = \mathbf{S}_v(k+1)\mathbf{S}_v^T(k+1) \tag{4.38}$$

where

$$\mathbf{S}_v(k+1) = \left[\mathbf{S}^{(1)}_{y\hat{x}}(k+1)\ \ \mathbf{S}^{(1)}_{yv}(k+1)\right] \tag{4.39}$$

$$\mathbf{S}^{(1)}_{y\hat{x}}(k+1) = \frac{1}{2h}\left\{\mathbf{h}_i(\hat{\mathbf{x}}_{k+1} + h\mathbf{s}^-_{x,j}, \bar{\mathbf{v}}_{k+1}) - \mathbf{h}_i(\hat{\mathbf{x}}^-_{k+1} - h\mathbf{s}^-_{x,j}, \bar{\mathbf{v}}_{k+1})\right\} \tag{4.40}$$

$$\mathbf{S}^{(1)}_{yv}(k+1) = \frac{1}{2h}\left\{\mathbf{h}_i(\hat{\mathbf{x}}_{k+1}, \bar{\mathbf{v}}_{k+1} + h\mathbf{s}_{v,y}) - \mathbf{h}_i(\hat{\mathbf{x}}_{k+1}, \bar{\mathbf{v}}_{k+1} - h\mathbf{s}_{v,y})\right\} \tag{4.41}$$

where $\mathbf{s}^-_{x,j}$ is the column of $\mathbf{S}^-_{\mathbf{x}}$ and $\mathbf{s}_{v,j}$ is the the column of $\mathbf{S}_{\mathbf{v}}$. The cross correlation is calculated by using

$$\mathbf{P}^{xy}_{k+1} = \mathbf{S}^-_x(k+1)\left(\mathbf{S}^{(1)}_{y\hat{x}}(k+1)\right)^T \tag{4.42}$$

The Kalman gain is obtained using

$$K_{k+1} = \mathbf{P}^{xy}_{k+1}\left(\mathbf{P}^{vv}_{k+1}\right)^{-1} \tag{4.43}$$

Now update the state estimate and error covariance

$$\hat{\mathbf{x}}_{_{k+1}} = \hat{\mathbf{x}}^{-}_{_{k+1}} + K_{k+1}\left(\mathbf{y}_{k+1} - \hat{\mathbf{y}}_{k+1}\right) \tag{4.44}$$

$$\mathbf{P}^{+}_{k+1} = \mathbf{P}^{-}_{k+1} - K_{k+1}\mathbf{P}^{vv}_{k+1}K^{T}_{k+1} \tag{4.45}$$

where $\mathbf{P}^{vv}_{k+1}$ is the innovation covariance given by

$$\mathbf{P}^{vv}_{k+1} = \mathbf{P}^{yy}_{k+1} + \mathbf{R}_{k+1}$$

and

$$\mathbf{P}^{yy}_{k+1} = \mathbf{S}^{(1)}_{y\hat{x}}(k+1)\left(\mathbf{S}^{(1)}_{y\hat{x}}(k+1)\right)^{T}$$

The DDF1 algorithm is shown in block diagram in Figure (4.2) below and described in the table 4.3.

4.5.2 Second-Order Divided Difference Filter (DDF2)

The second-order DDF2 is obtained by using the calculation of the mean and covariance in the second-order polynomial approximation section [80].

Earlier we defined the first order terms as [78-80],

$$\mathbf{S}^{(1)}_{x\hat{x}}(k+1) = \frac{1}{2h}\left\{\mathbf{f}_i(\hat{\mathbf{x}}_k + h\mathbf{s}_{x,j}, \bar{\mathbf{w}}_k) - \mathbf{f}_i(\hat{\mathbf{x}}_k - h\mathbf{s}_{x,j}, \bar{\mathbf{w}}_k)\right\} \tag{4.46}$$

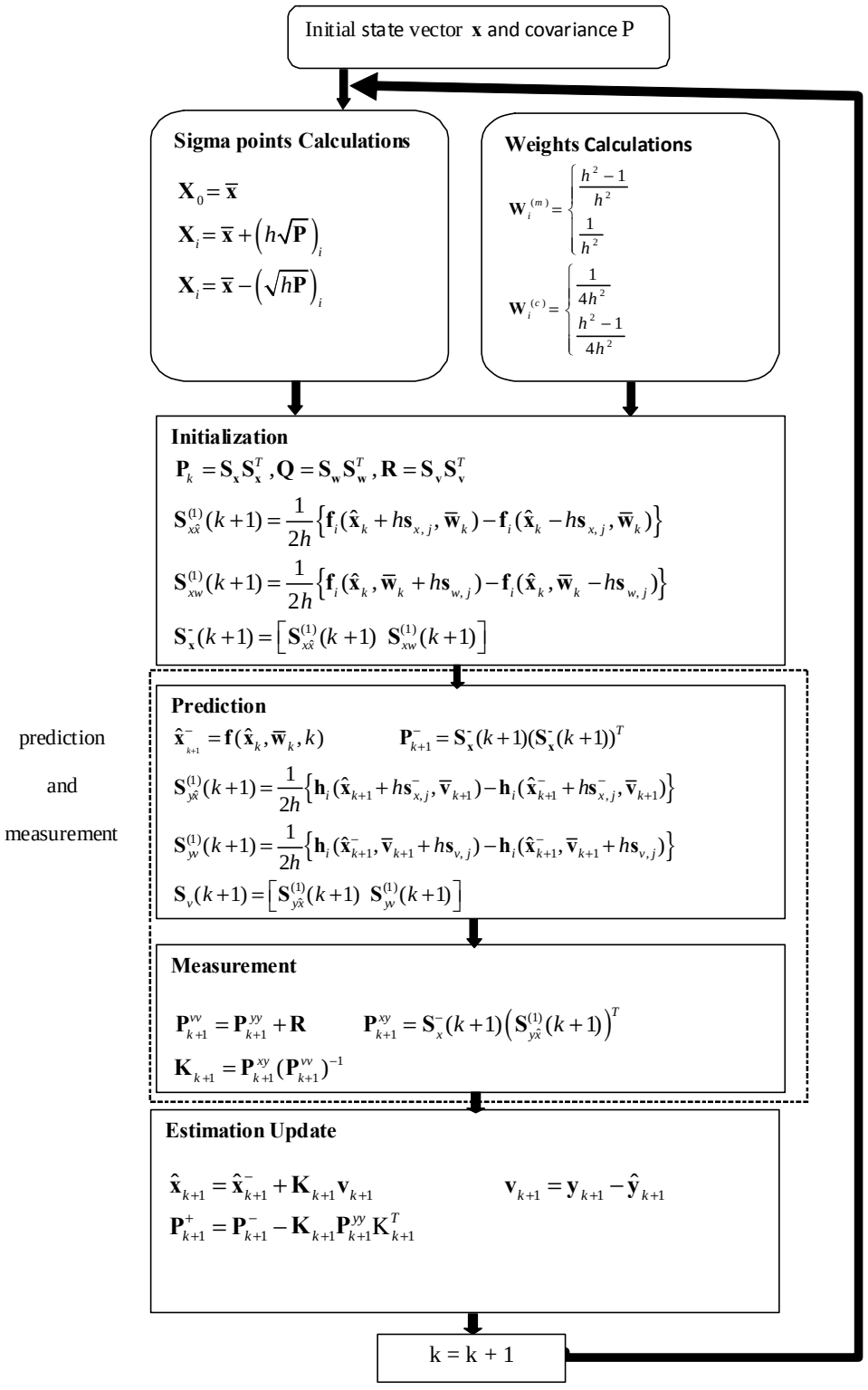

Figure 4.2: Divided difference filter I algorithm

Step I: Initialization:
$\hat{\mathbf{x}}_k = \mathbf{E}[\mathbf{x}_k]$,
$\mathbf{P}_k = E[(\mathbf{x}_k - \hat{\mathbf{x}}_k)(\mathbf{x}_k - \hat{\mathbf{x}}_k)^T]$

Step II: Square Cholesky factorizations:
$\mathbf{P}_k = \mathbf{S}_{\mathbf{x}}\mathbf{S}_{\mathbf{x}}^T, \quad \mathbf{Q} = \mathbf{S}_{\mathbf{w}}\mathbf{S}_{\mathbf{w}}^T, \quad \mathbf{R}=\mathbf{S}_v\mathbf{S}_v^T$
$\mathbf{S}_{x\hat{x}}^{(1)}(k+1) = \frac{1}{2h}\left\{\mathbf{f}_i(\hat{\mathbf{x}}_k + h\mathbf{s}_{x,j}, \bar{\mathbf{w}}_k) - \mathbf{f}_i(\hat{\mathbf{x}}_k - h\mathbf{s}_{x,j}, \bar{\mathbf{w}}_k)\right\}$
$\mathbf{S}_{xw}^{(1)}(k+1) = \frac{1}{2h}\left\{\mathbf{f}_i(\hat{\mathbf{x}}_k, \bar{\mathbf{w}}_k + h\mathbf{s}_{w,j}) - \mathbf{f}_i(\hat{\mathbf{x}}_k, \bar{\mathbf{w}}_k - h\mathbf{s}_{w,j})\right\}$
$\mathbf{S}_x^-(k+1) = \left[\mathbf{S}_{x\hat{x}}^{(1)}(k+1) \;\; \mathbf{S}_{xw}^{(1)}(k+1)\right]$

Step III*: State and covariance Propagation:*
$\hat{\mathbf{x}}_{k+1}^- = \mathbf{f}(\hat{\mathbf{x}}_k, \bar{\mathbf{w}}_k, k)$
$\mathbf{P}_{k+1}^- = \mathbf{S}_x^-(k+1)(\mathbf{S}_x^-(k+1))^T$
$\mathbf{S}_{y\hat{x}}^{(1)}(k+1) = \frac{1}{2h}\left\{\mathbf{h}_i(\hat{\mathbf{x}}_{k+1} + h\mathbf{s}_{x,j}^-, \bar{\mathbf{v}}_{k+1}) - \mathbf{h}_i(\hat{\mathbf{x}}_{k+1}^- - h\mathbf{s}_{x,j}^-, \bar{\mathbf{v}}_{k+1})\right\}$
$\mathbf{S}_{yv}^{(1)}(k+1) = \frac{1}{2h}\left\{\mathbf{h}_i(\hat{\mathbf{x}}_{k+1}, \bar{\mathbf{v}}_{k+1} + h\mathbf{s}_{v,y}) - \mathbf{h}_i(\hat{\mathbf{x}}_{k+1}, \bar{\mathbf{v}}_{k+1} - h\mathbf{s}_{v,y})\right\}$
$\mathbf{S}_v(k+1) = \left[\mathbf{S}_{y\hat{x}}^{(1)}(k+1) \;\; \mathbf{S}_{yv}^{(1)}(k+1)\right]$

Step IV: *Observation and Innovation Covariance Propagation:*
$\hat{\mathbf{y}}_{k+1}^- = h(\hat{\mathbf{x}}_{k+1}^-, \bar{\mathbf{v}}_{k+1}, k+1)$
$\mathbf{P}_{k+1}^{vv} = \mathbf{S}_v(k+1)\mathbf{S}_v^T(k+1)$

$\mathbf{P}_{k+1}^{xy} = \mathbf{S}_x^-(k+1)\left(\mathbf{S}_{y\hat{x}}^{(1)}(k+1)\right)^T$
$\mathbf{P}_{k+1}^{xy} = \mathbf{S}_x^-(k+1)\left(\mathbf{S}_{y\hat{x}}^{(1)}(k+1)\right)^T$

Step V: *Update*
$K_{k+1} = \mathbf{P}_{k+1}^{xy}\left(\mathbf{P}_{k+1}^{vv}\right)^{-1}$
$\hat{\mathbf{x}}_{k+1} = \hat{\mathbf{x}}_{k+1}^- + K_{k+1}\left(\mathbf{y}_{k+1} - \hat{\mathbf{y}}_{k+1}\right)$
$\mathbf{P}_{k+1}^+ = \mathbf{P}_{k+1}^- - K_{k+1}\mathbf{P}_{k+1}^{vv}K_{k+1}^T$

Table 4.2: DDF1 algorithm

$$\mathbf{S}_{xw}^{(1)}(k+1) = \frac{1}{2h}\left\{\mathbf{f}_i(\hat{\mathbf{x}}_k, \bar{\mathbf{w}}_k + h\mathbf{s}_{w,j}) - \mathbf{f}_i(\hat{\mathbf{x}}_k, \bar{\mathbf{w}}_k - h\mathbf{s}_{w,j})\right\} \tag{4.47}$$

The second order terms are defined as

$$\mathbf{S}_{x\hat{x}}^{(2)}(k+1) = \frac{\sqrt{\gamma-1}}{2\gamma}\left\{\mathbf{f}_i(\hat{\mathbf{x}}_k + h\mathbf{s}_{x,j}, \bar{\mathbf{w}}_k) - \mathbf{f}_i(\hat{\mathbf{x}}_k - h\mathbf{s}_{x,j}, \bar{\mathbf{w}}_k) - 2\mathbf{f}_i(\hat{\mathbf{x}}_k, \bar{\mathbf{w}}_k)\right\} \tag{4.48}$$

$$\mathbf{S}_{xw}^{(2)}(k+1) = \frac{\sqrt{\gamma-1}}{2\gamma}\left\{\mathbf{f}_i(\hat{\mathbf{x}}_k, \bar{\mathbf{w}}_k + h\mathbf{s}_{w,j}) + \mathbf{f}_i(\hat{\mathbf{x}}_k, \bar{\mathbf{w}}_k - h\mathbf{s}_{w,j}) - 2\mathbf{f}_i(\hat{\mathbf{x}}_k, \bar{\mathbf{w}}_k)\right\} \tag{4.49}$$

where $\gamma = h^2$, $\mathbf{s}_{x,j}$ is the column of $\mathbf{S}_\mathbf{x}$ and $\mathbf{s}_{w,j}$ is the jth column of $\mathbf{S}_\mathbf{w}$. If we take $n = n_x - n_w$, We define the predicted state as

$$\begin{aligned}\hat{\mathbf{x}}_{k+1}^{-} &= \frac{\gamma-(n_x+n_w)}{\gamma}\mathbf{f}(\hat{\mathbf{x}}_k, \bar{\mathbf{w}}_k) + \frac{1}{2\gamma}\sum_{p=1}^{n_x}\{\mathbf{f}(\hat{\mathbf{x}}_k + h\mathbf{s}_{x,p}, \bar{\mathbf{w}}_k) + \mathbf{f}(\hat{\mathbf{x}}_k - h\mathbf{s}_{x,p}, \bar{\mathbf{w}}_k)\} \\ &\quad + \frac{1}{2\gamma}\sum_{p=1}^{n_w}\{\mathbf{f}(\hat{\mathbf{x}}_k, \bar{\mathbf{w}}_k + h\mathbf{s}_{w,p}) + \mathbf{f}(\hat{\mathbf{x}}_k, \bar{\mathbf{w}}_k - h\mathbf{s}_{w,p})\}\end{aligned} \tag{4.50}$$

where n_x is the state vector dimension and n_w is the process noise vector dimension. The predicted covariance is given by

$$\mathbf{S}_{\mathbf{x}}^{-}(k+1) = \begin{bmatrix} \mathbf{S}_{x\hat{x}}^{(1)}(k+1) & \mathbf{S}_{xw}^{(1)}(k+1) & \mathbf{S}_{x\hat{x}}^{(2)}(k+1) & \mathbf{S}_{xw}^{(2)}(k+1) \end{bmatrix} \tag{4.51}$$

The predicted covariance

$$\mathbf{P}_{k+1}^{-} = \mathbf{S}_{\mathbf{x}}^{-}(k+1)(\mathbf{S}_{\mathbf{x}}^{-}(k+1))^{T} \tag{4.52}$$

The predicted observation vector and its predicted covariance is given by

$$\begin{aligned} \hat{\mathbf{y}}_{k+1}^{-} &= \frac{\gamma-(n_x+n_v)}{\gamma}\mathbf{h}(\hat{\mathbf{x}}_{k+1},\bar{\mathbf{v}}_{k+1}) + \frac{1}{2\gamma}\sum_{p=1}^{n_x}\{\mathbf{h}(\hat{\mathbf{x}}_{k+1}^{-}+h\mathbf{s}_{x,p}^{-},\bar{\mathbf{v}}_{k+1}) + \mathbf{h}(\hat{\mathbf{x}}_{k+1}^{-}-h\mathbf{s}_{x,p}^{-},\bar{\mathbf{v}}_{k+1})\} \\ &+\frac{1}{2\gamma}\sum_{p=1}^{n_w}\left\{\mathbf{h}(\hat{\mathbf{x}}_{k+1}^{-},\bar{\mathbf{v}}_{k+1}+h\mathbf{s}_{v,p}) + \mathbf{h}(\hat{\mathbf{x}}_{k+1}^{-},\bar{\mathbf{v}}_{k+1}-h\mathbf{s}_{v,p})\right\} \end{aligned} \tag{4.53}$$

where n_v is the state vector dimension, $\mathbf{s}_{x,p}^{-}$ is the column of $\mathbf{S}_{\mathbf{x}}^{-}$ and $\mathbf{s}_{v,p}$ is the pth column of $\mathbf{S}_{\mathbf{v}}$. Now the innovation covariance is given by

$$\mathbf{P}_{k+1}^{vv} = \mathbf{S}_{v}(k+1)\mathbf{S}_{v}^{T}(k+1) \tag{4.54}$$

here the $\mathbf{S}_v(k+1)$ is given as

$$\mathbf{S}_v(k+1) = \begin{bmatrix} \mathbf{S}_{x\hat{x}}^{(1)}(k+1) & \mathbf{S}_{xw}^{(1)}(k+1) & \mathbf{S}_{x\hat{x}}^{(2)}(k+1) & \mathbf{S}_{xw}^{(2)}(k+1) \end{bmatrix} \tag{4.55}$$

$$\mathbf{S}_{y\hat{x}}^{(2)}(k+1) = \frac{\sqrt{\gamma-1}}{2\gamma}\{\mathbf{h}_i(\hat{\mathbf{x}}_{k+1}^- + h\mathbf{s}_{x,j}^-, \bar{\mathbf{v}}_{k+1}) + \mathbf{h}_i(\hat{\mathbf{x}}_{k+1}^- - h\mathbf{s}_{x,j}^-, \bar{\mathbf{v}}_{k+1}) + 2\mathbf{h}_i(\hat{\mathbf{x}}_{k+1}^-, \bar{\mathbf{v}}_{k+1})\} \tag{4.56}$$

$$\mathbf{S}_{yv}^{(2)}(k+1) = \frac{\sqrt{\gamma-1}}{2\gamma}\{\mathbf{h}_i(\hat{\mathbf{x}}_{k+1,}^-, \bar{\mathbf{v}}_{k+1} + h\mathbf{s}_{x,j}^-) + \mathbf{h}_i(\hat{\mathbf{x}}_{k+1}^-, \bar{\mathbf{v}}_{k+1} - h\mathbf{s}_{x,j}^-) + 2\mathbf{h}_i(\hat{\mathbf{x}}_{k+1}^-, \bar{\mathbf{v}}_{k+1})\} \tag{4.57}$$

The cross correlation is calculated by using

$$\mathbf{P}_{k+1}^{xy} = \mathbf{S}_x^-(k+1)\left(\mathbf{S}_{y\hat{x}}^{(1)}(k+1)\right)^T \tag{4.58}$$

The Kalman gain is obtained using

$$K_{k+1} = \mathbf{P}_{k+1}^{xy}\left(\mathbf{P}_{k+1}^{vv}\right)^{-1} \tag{4.59}$$

Now update the state estimate and error covariance

$$\hat{\mathbf{x}}_{_{k+1}} = \hat{\mathbf{x}}_{_{k+1}}^- + K_{k+1}\left(\mathbf{y}_{k+1} - \hat{\mathbf{y}}_{k+1}\right) \tag{4.60}$$

$$\mathbf{P}_{k+1}^{+} = \mathbf{P}_{k+1}^{-} - K_{k+1}\mathbf{P}_{k+1}^{vv}K_{k+1}^{T} \tag{4.61}$$

The DDF2 block diagram is shown in Figure (4.3) and described in the table 4.4.

Sigma Points for the Divided Difference Filters

It can be seen from the above algorithms that the 2n sigma points for the DDF are

$$\begin{aligned} \mathbf{X}_0 &= \bar{\mathbf{x}} \qquad\qquad i = 0 \\ \mathbf{X}_i &= \bar{\mathbf{x}} + (h\sqrt{\mathbf{P}}) \quad i = 1, ..., n \\ \mathbf{X}_i &= \bar{\mathbf{x}} - (h\sqrt{\mathbf{P}}) \quad i = 1, ..., 2n \end{aligned} \tag{4.62}$$

and the corresponding weighting coefficients are

$$\begin{aligned} W_0^{(m)} &= \tfrac{h^2-1}{h^2} \qquad i = 0 \\ W_i^{(m)} &= \tfrac{1}{h^2} \quad i = 1, ..., 2n \\ W_i^{(c_1)} &= \tfrac{1}{4h^2} \quad i = 1, ..., 2n \\ W_i^{(c_2)} &= \tfrac{h^2-1}{4h^2} \quad i = 1, ..., 2n \end{aligned} \tag{4.63}$$

These sigma-points are propagated through the true nonlinear function. We see that the implementation principle of the DDF algorithm is quite similar to that of the EKF. However, it does not require to formulate the Jacobian matrix of partial derivatives of the nonlinear dynamic and measurement equations. Thus, DDF algorithms,

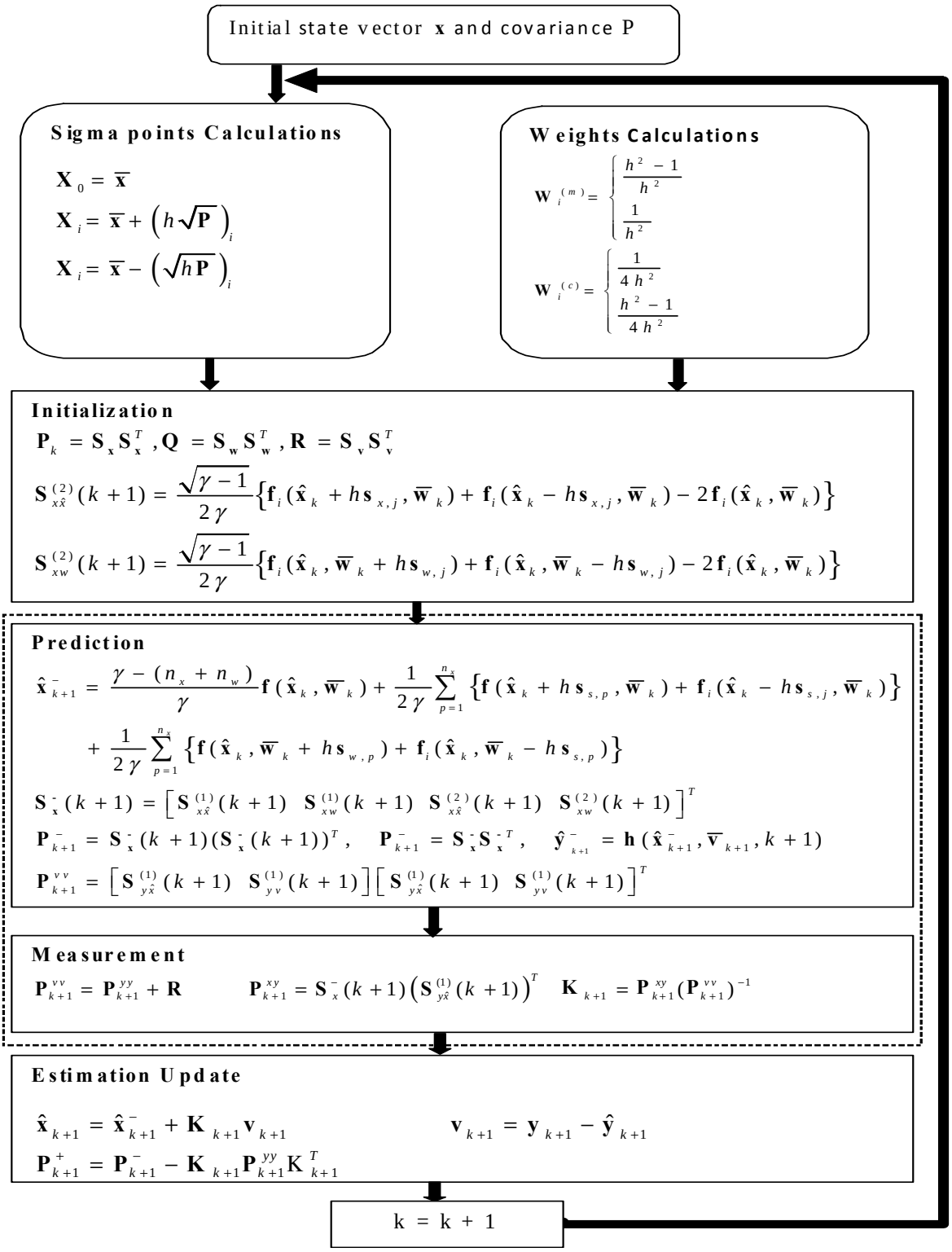

Figure 4.3: Divided difference filter II algorithm

Step I: Initialization:
$\hat{\mathbf{x}}_k = \mathbf{E}[\mathbf{x}_k]$,
$\mathbf{P}_k = E[(\mathbf{x}_k - \hat{\mathbf{x}}_k)(\mathbf{x}_k - \hat{\mathbf{x}}_k)^T]$

Step II: Square Cholesky factorizations:
$\mathbf{P}_k = \mathbf{S}_\mathbf{x}\mathbf{S}_\mathbf{x}^T, \quad \mathbf{Q} = \mathbf{S}_\mathbf{w}\mathbf{S}_\mathbf{w}^T, \quad \mathbf{R} = \mathbf{S}_v\mathbf{S}_v^T$
$\mathbf{S}_{x\hat{x}}^{(1)}(k+1) = \frac{1}{2h}\{\mathbf{f}_i(\hat{\mathbf{x}}_k + h\mathbf{s}_{x,j}, \bar{\mathbf{w}}_k) - \mathbf{f}_i(\hat{\mathbf{x}}_k - h\mathbf{s}_{x,j}, \bar{\mathbf{w}}_k)\}$
$\mathbf{S}_{xw}^{(1)}(k+1) = \frac{1}{2h}\{\mathbf{f}_i(\hat{\mathbf{x}}_k, \bar{\mathbf{w}}_k + h\mathbf{s}_{w,j}) - \mathbf{f}_i(\hat{\mathbf{x}}_k, \bar{\mathbf{w}}_k - h\mathbf{s}_{w,j})\}$
$\mathbf{S}_{x\hat{x}}^{(2)}(k+1) = \frac{\sqrt{\gamma-1}}{2\gamma}\{\mathbf{f}_i(\hat{\mathbf{x}}_k + h\mathbf{s}_{x,j}, \bar{\mathbf{w}}_k) - \mathbf{f}_i(\hat{\mathbf{x}}_k - h\mathbf{s}_{x,j}, \bar{\mathbf{w}}_k) - 2\mathbf{f}_i(\hat{\mathbf{x}}_k, \bar{\mathbf{w}}_k)\}$
$\mathbf{S}_{xw}^{(2)}(k+1) = \frac{\sqrt{\gamma-1}}{2\gamma}\{\mathbf{f}_i(\hat{\mathbf{x}}_k, \bar{\mathbf{w}}_k + h\mathbf{s}_{w,j}) + \mathbf{f}_i(\hat{\mathbf{x}}_k, \bar{\mathbf{w}}_k - h\mathbf{s}_{w,j}) - 2\mathbf{f}_i(\hat{\mathbf{x}}_k, \bar{\mathbf{w}}_k)\}$

Step III*: State and covariance Propagation:*
$\hat{\mathbf{x}}_{k+1}^- = \frac{\gamma-n}{\gamma}\mathbf{f}(\hat{\mathbf{x}}_k, \bar{\mathbf{w}}_k) + \frac{1}{2\gamma}\sum_{p=1}^{n_x}\{\mathbf{f}(\hat{\mathbf{x}}_k + h\mathbf{s}_{x,p}, \bar{\mathbf{w}}_k) + \mathbf{f}(\hat{\mathbf{x}}_k - h\mathbf{s}_{x,p}, \bar{\mathbf{w}}_k)\} +$
$\frac{1}{2\gamma}\sum_{p=1}^{n_w}\{\mathbf{f}(\hat{\mathbf{x}}_k, \bar{\mathbf{w}}_k + h\mathbf{s}_{w,p}) + \mathbf{f}(\hat{\mathbf{x}}_k, \bar{\mathbf{w}}_k - h\mathbf{s}_{w,p})\}$
$\mathbf{S}_\mathbf{x}^-(k+1) = \begin{bmatrix}\mathbf{S}_{x\hat{x}}^{(1)}(k+1) & \mathbf{S}_{xw}^{(1)}(k+1) & \mathbf{S}_{x\hat{x}}^{(2)}(k+1) & \mathbf{S}_{xw}^{(2)}(k+1)\end{bmatrix}$
$\mathbf{P}_{k+1}^- = \mathbf{S}_\mathbf{x}^-(k+1)(\mathbf{S}_\mathbf{x}^-(k+1))^T$
$\mathbf{S}_{y\hat{x}}^{(2)}(k+1) = \frac{\sqrt{\gamma-1}}{2\gamma}\{\mathbf{h}_i(\hat{\mathbf{x}}_{k+1}^- + h\mathbf{s}_{x,j}^-, \bar{\mathbf{v}}_{k+1}) + \mathbf{h}_i(\hat{\mathbf{x}}_{k+1}^- - h\mathbf{s}_{x,j}^-, \bar{\mathbf{v}}_{k+1}) + 2\mathbf{h}_i(\hat{\mathbf{x}}_{k+1}^-, \bar{\mathbf{v}}_{k+1})\}$
$\mathbf{S}_{yv}^{(2)}(k+1) = \frac{\sqrt{\gamma-1}}{2\gamma}\{\mathbf{h}_i(\hat{\mathbf{x}}_{k+1,}^-\bar{\mathbf{v}}_{k+1} + h\mathbf{s}_{x,j}^-) + \mathbf{h}_i(\hat{\mathbf{x}}_{k+1}^-, \bar{\mathbf{v}}_{k+1} - h\mathbf{s}_{x,j}^-) + 2\mathbf{h}_i(\hat{\mathbf{x}}_{k+1}^-, \bar{\mathbf{v}}_{k+1})\}$
$\mathbf{S}_v(k+1) = \begin{bmatrix}\mathbf{S}_{y\hat{x}}^{(1)}(k+1) & \mathbf{S}_{yv}^{(1)}(k+1) & \mathbf{S}_{y\hat{x}}^{(2)}(k+1) & \mathbf{S}_{yv}^{(2)}(k+1)\end{bmatrix}$

Step IV: *Observation and Innovation Covariance Propagation:*
$\hat{\mathbf{y}}_{k+1}^- = \frac{\gamma-n}{\gamma}\mathbf{h}(\hat{\mathbf{x}}_{k+1}, \bar{\mathbf{v}}_{k+1}) + \frac{1}{2\gamma}\sum_{p=1}^{n_x}\{\mathbf{h}(\hat{\mathbf{x}}_{k+1}^- + h\mathbf{s}_{x,p}^-, \bar{\mathbf{v}}_{k+1}) + \mathbf{h}(\hat{\mathbf{x}}_{k+1}^- - h\mathbf{s}_{x,p}^-, \bar{\mathbf{v}}_{k+1})\}$
$+\frac{1}{2\gamma}\sum_{p=1}^{n_w}\left\{\mathbf{h}(\hat{\mathbf{x}}_{k+1}^-, \bar{\mathbf{v}}_{k+1} + h\mathbf{s}_{v,p}) + \mathbf{h}(\hat{\mathbf{x}}_{k+1}^-, \bar{\mathbf{v}}_{k+1} - h\mathbf{s}_{v,p})\right\}$
$\mathbf{P}_{k+1}^{vv} = \mathbf{S}_v(k+1)\mathbf{S}_v^T(k+1)$
$\mathbf{P}_{k+1}^{xy} = \mathbf{S}_x^-(k+1)\left(\mathbf{S}_{y\hat{x}}^{(1)}(k+1)\right)^T$

Step V: *Update*
$K_{k+1} = \mathbf{P}_{k+1}^{xy}\left(\mathbf{P}_{k+1}^{vv}\right)^{-1}$
$\hat{\mathbf{x}}_{k+1} = \hat{\mathbf{x}}_{k+1}^- + K_{k+1}\left(\mathbf{y}_{k+1} - \hat{\mathbf{y}}_{k+1}\right)$
$\mathbf{P}_{k+1}^+ = \mathbf{P}_{k+1}^- - K_{k+1}\mathbf{P}_{k+1}^{vv}K_{k+1}^T$

Table 4.3: DDF2 algorithm

can replace the EKF and its higher-order estimators in practical real-time applications that require accurate estimation, but at less computational cost. In the next section, a new nonlinear transformation for the mean and covariance will be introduced to handle the linearization issue.

4.6 The UKF

4.6.1 Background

For non-linear dynamic system model, the conventional Kalman algorithm can be invoked to obtain the parameter estimates. The most well known application of the Kalman filter framework to non-linear systems is the EKF. Even though the EKF is one of the most widely used approximate solutions for non-linear estimation and filtering, it has some limitations as those discussed by Wan and Merwe [74,77]. The EKF first linearizes the system around the current state estimate using a first-order truncation of the multidimensional Taylor series expansion. However, these approximations are valid if all the higher order derivatives of the non-linear function are effectively zero over the 'uncertainty region' of $\mathbf{x}$. Stated in other words it requires the zeroth and first order terms to dominate the rest of the terms, over the region of the state-space defined by the prior distribution of $\mathbf{x}$. Thus the linearization method employed by the EKF fails to take into account the inherent uncertainty in the prior random variable. This has large implications for the accuracy and consistency of the

resulting EKF algorithm. These approximations often introduce large errors in the EKF calculated posterior mean and covariance of the transformed GRV, which may lead to suboptimal performance and sometimes divergence of the filter. The EKF only achieves first order accuracy in the calculation of both the posterior mean and covariance of the transformed random variables. Since the EKF only uses the first order terms of the Taylor series expansion of the non-linear functions, it often introduces large errors in the estimated statistics of the posterior distributions of the states. It is quite evident when the models are highly non-linear and the local linearity assumption breaks down, i.e., the effects of the higher order terms of the Taylor series expansion becomes significant. And also linearization can be applied only if the Jacobian matrix exists. However, this is not always the case. Some systems contain discontinuities, others have singularities. Calculating Jacobian matrices can be very difficult.

UKF, unlike EKF, does not explicitly approximate the non-linear process and observation models. Rather it utilizes the true non-linear models and approximates the distribution of the state random variable. The UKF is a recursive MMSE estimator based on the optimal Gaussian approximate Kalman filter framework that addresses some of the approximation issues of the EKF [77,78]. The state distribution is still represented by a GRV, but it is specified using a minimal set of deterministically chosen sample points known as 'sigma points'. These sample points completely capture the true mean and covariance of the GRV, and when propagated through the true non-linear system, capture the posterior mean and covariance accurately up to the

2nd order for any non-linearity, with errors only introduced in the 3rd and higher orders. The mean and covariance of the transformed ensemble can then be computed as the estimate of the non-linear transformation of the original distribution. The mathematical description of the UKF based approach is provided in Appendix I where we have adopted the mathematical convention described in [74].

4.6.2 Algorithmic Steps

Given an n-dimensional Gaussian distribution having covariance $\mathbf{P}$, we generate a set of points having the same covariance from the columns (or rows) of the matrices (the positive and negative roots). This set of points is zero mean, but if the original distribution has mean $\bar{\mathbf{x}}$, then simply adding $\bar{\mathbf{x}}$ to each of the points yields a symmetric set of $2n$ points having the desired mean and covariance. Because the set is symmetric its odd central moments are zero, so its first three moments are the same as the original Gaussian distribution. This is the minimal number of points capable of encoding this information. The set of sigma points are given by

$$\begin{aligned} X_0 &= \bar{\mathbf{x}} & i &= 0 \\ X_i &= \bar{\mathbf{x}} + \left(\sqrt{(n+\lambda)\mathbf{P}}\right) & i &= 1, ..., n \\ X_i &= \bar{\mathbf{x}} - \left(\sqrt{(n+\lambda)\mathbf{P}}\right) & i &= n+1, ..., 2n \end{aligned} \tag{4.64}$$

Suppose that we have a vector x with a known mean $\bar{x}$ and covariance P, a

nonlinear function $y = h(x)$, and we want to approximate the mean of y. We transform each individual sigma point using the nonlinear function $h(.)$, and then taking the weighted sum of the transformed sigma points to approximate the mean of y. The transformed sigma points are computed as follows

$$\mathbf{W}_i^m = \begin{cases} \frac{\lambda}{(\lambda+n)} & i = 0 \\ \frac{1}{2(\lambda+n)} & i = 1, ..., 2n \end{cases}$$
$$\mathbf{W}_i^c = \begin{cases} \frac{\lambda}{(\lambda+n)} + (1 - \alpha^2 + \beta) & i = 0 \\ \frac{1}{2(\lambda+n)} & i = 1, ..., 2n \end{cases} \tag{4.65}$$

where α controls the spread of the sigma points and should be a small number ($0 \leq \alpha \leq 1$), $\lambda = \alpha^2(n + \kappa) - n$, where κ is a scaling parameter used to describe the scaling direction of the sigma points and β incorporates the prior knowledge of the distribution of $\mathbf{x}$. These sigma points are propagated through the non-linear transformation. The algorithm is as follows:

Apply unscented transformations to find translated sigma points

$$\mathbf{X}_{i,k+1} = \mathbf{f}(\mathbf{X}_{i,k}, k) \tag{4.66}$$

The predicted state vector $\hat{x}(l + 1)$ and predicted covariance $P(l + 1)$ are computed by

$$\hat{\mathbf{x}}_{k+1}^{-} = \sum_{i=0}^{2n} \mathbf{W}_i^{(m)} \mathbf{X}_{i,k+1} \tag{4.67}$$

$$\mathbf{P}_{k+1}^{-} = \sum_{i=0}^{n} \mathbf{W}_i^{(c)} [\mathbf{X}_{i,k+1} - \hat{\mathbf{x}}_{k+1}^{-}][\mathbf{X}_{i,k+1} - \hat{\mathbf{x}}_{k+1}^{-}]^T \tag{4.68}$$

where n is dimensionality of the state. The predicted observation vector and predicted covariance are calculated as

$$\mathbf{Y}_{i,k+1} = \mathbf{h}(\mathbf{X}_i, k+1) \tag{4.69}$$

$$\hat{\mathbf{y}}_{k+1}^{-} = \sum_{i=0}^{2n} \mathbf{W}_i^{(m)} \mathbf{Y}_{i,k+1} \tag{4.70}$$

$$\mathbf{P}_{k+1}^{yy} = \sum_{i=0}^{2n} W_i^{(c)} [\mathbf{Y}_{i,k+1} - \hat{\mathbf{y}}_{k+1}^{-}] [\mathbf{Y}_{i,k+1} - \hat{\mathbf{y}}_{k+1}^{-}]^T \tag{4.71}$$

The innovation covariance is given by

$$\mathbf{P}_{k+1}^{vv} = \mathbf{P}_{k+1}^{yy} + \mathbf{R}_{k+1} \tag{4.72}$$

The cross covariance matrix of x and y is determined by using

$$\mathbf{P}_{k+1}^{xy} = \sum_{i=0}^{2n} \mathbf{W}_i^{(c)} [\mathbf{X}_{i,k+1} - \hat{\mathbf{x}}_{k+1}^{-})][\mathbf{Y}_{i,k+1} - \hat{\mathbf{y}}_{k+1}^{-}]^T \tag{4.73}$$

The Kalman gain is computed using

$$\mathbf{K}_{k+1} = \mathbf{P}_{k+1}^{xy}(\mathbf{P}_{k+1}^{vv})^{-1} \tag{4.74}$$

The updated mean estimate is

$$\hat{\mathbf{x}}_{k+1} = \hat{\mathbf{x}}_{k+1}^{-} + \mathbf{K}_{k+1}\mathbf{v}_{k+1} \tag{4.75}$$

$\hat{\mathbf{x}}_{k+1}^{+} = \hat{\mathbf{x}}_{k+1}^{-} + \mathbf{K}_{k+1}\mathbf{v}_{k+1}$where $\mathbf{v}_{k+1}$ is the innovation given by

$$\mathbf{v}_{k+1} = \mathbf{y}_{k+1} - \hat{\mathbf{y}}_{k+1} \tag{4.76}$$

The updated covariance is given by

$$\mathbf{P}_{k+1} = \mathbf{P}_{k+1}^{-} - \mathbf{K}_{k+1}\mathbf{P}_{k+1}^{vv}\mathbf{K}_{k+1}^{T} \tag{4.77}$$

After the parameter estimates and the error covariance matrices are updated, the process is repeated for the remaining samples. The block diagram of UKF algorithm is shown in Figure (4.4) and is summarized in table 4.5.

4.7 Numerical Complexities

We need to consider the numerical complexity of estimation techniques that have been presented in this chapter. The complexity of an algorithm usually measured as a function of some measure of the operations to solve any problem. One of the

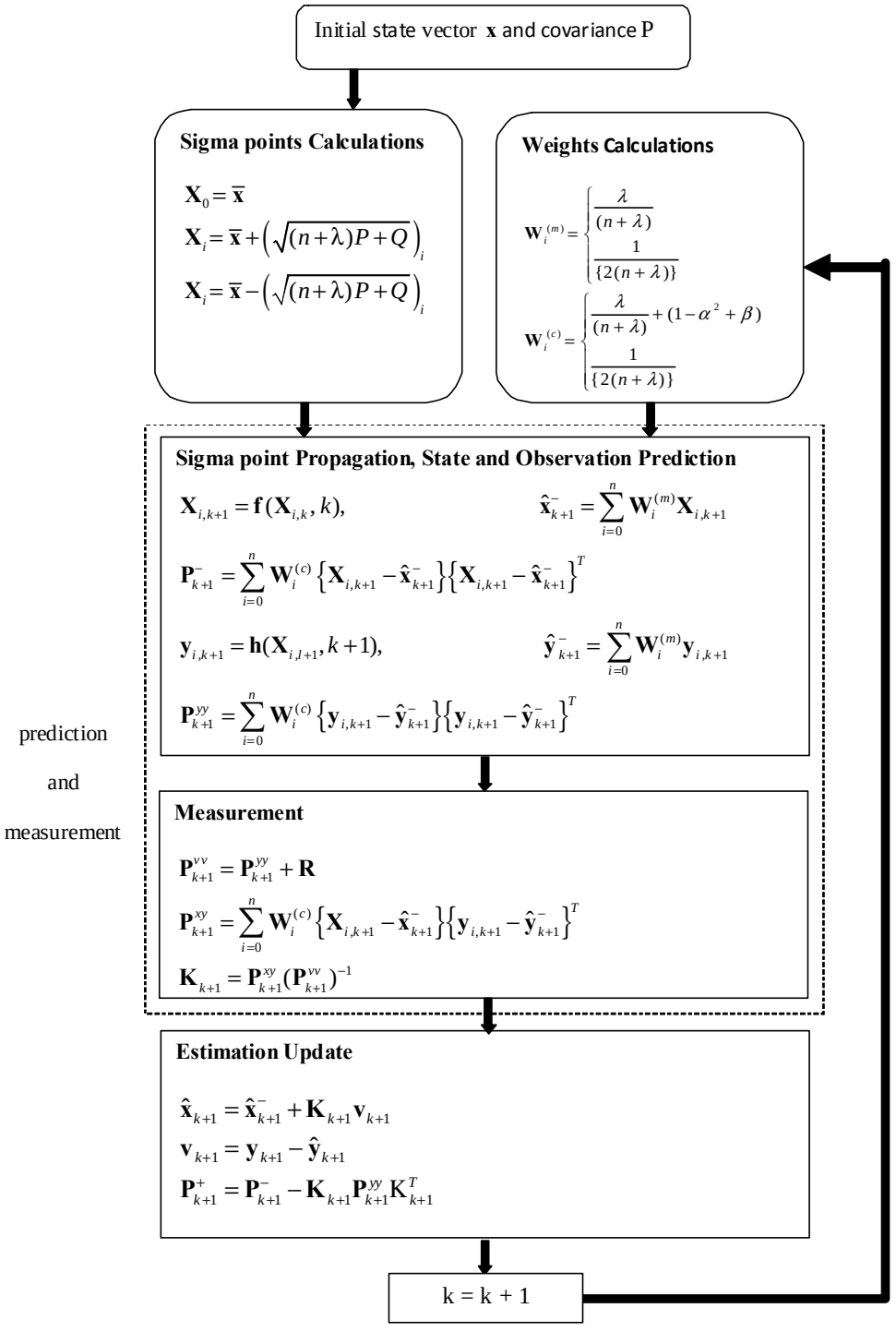

Figure 4.4: Unscented Kalman filter algorithm

Step I: *Sigma Points Calculation*

$$\mathbf{X}_0 = \bar{\mathbf{x}} \qquad i = 0$$

$$\mathbf{X}_i = \bar{\mathbf{x}} + \left(\sqrt{(n+\lambda)\mathbf{P}}\right) \qquad i = 1, ..., n$$

$$\mathbf{X}_i = \bar{\mathbf{x}} - \left(\sqrt{(n+\lambda)\mathbf{P}}\right) \qquad i = n+1, ..., 2n$$

$$\mathbf{W}_i^{(m)} = \begin{cases} \lambda/(n+\lambda) & i = 0 \\ 1/\{2(n+\lambda)\} & i = 1, ..., 2n \end{cases}$$

$$\mathbf{W}_i^{(c)} = \begin{cases} \lambda/(n+\lambda) + (1-\alpha^2+\beta) & i = 0 \\ 1/\{2(n+\lambda)\} & i = 1, ..., 2n \end{cases}$$

Step II: *Prediction*

1. Prediction State

$$\mathbf{X}_{i,k+1} = \mathbf{f}(\mathbf{X}_{i,k}, k)$$

$$\hat{\mathbf{y}}_{k+1}^- = \sum_{i=0}^{2n} \mathbf{W}_i^{(m)} \mathbf{X}_{i,k+1}$$

$$\mathbf{P}_{k+1}^- = \sum_{i=0}^{2n} \mathbf{W}_i^{(c)} [\mathbf{X}_{i,k+1} - \hat{\mathbf{x}}_{k+1}^-][\mathbf{X}_{i,k+1} - \hat{\mathbf{x}}_{k+1}^-]^T$$

2. Observation Prediction

$$\mathbf{Y}_{i,k+1} = \mathbf{h}(\mathbf{X}_i, k+1)$$

$$\hat{\mathbf{y}}_{k+1}^- = \sum_{i=0}^{2n} \mathbf{W}_i^{(m)} \mathbf{Y}_{i,k+1}$$

$$\mathbf{P}_{k+1}^{yy} = \sum_{i=0}^{2n} \mathbf{W}_i^{(c)} [\mathbf{Y}_{i,k+1} - \hat{\mathbf{y}}_{k+1}^-] [\mathbf{Y}_{i,k+1} - \hat{\mathbf{y}}_{k+1}^-]^T$$

Step III: *Measurement Update*

1. Compute the innovation covariance and cross covariance

$$\mathbf{P}_{k+1}^{vv} = \mathbf{P}_{k+1}^{yy} + \mathbf{R}_{k+1}$$

$$\mathbf{P}_{k+1}^{xy} = \sum_{i=0}^{2n} \mathbf{W}_i^{(c)} [\mathbf{X}_{i,k+1} - \hat{\mathbf{x}}_{k+1}^-)][\mathbf{Y}_{i,k+1} - \hat{\mathbf{y}}_{k+1}^-]^T$$

2. Calculate Kalman Gain

$$\mathbf{K}_{k+1} = \mathbf{P}_{k+1}^{xy} (\mathbf{P}_{k+1}^{vv})^{-1}$$

3. Update state estimation

$$\hat{\mathbf{x}}_{k+1} = \hat{\mathbf{x}}_{k+1}^- + \mathbf{K}_{k+1} \mathbf{v}_{k+1}$$

$$\mathbf{v}_{k+1} = \mathbf{y}_{k+1} - \hat{\mathbf{y}}_{k+1}$$

4. Update the covariance

$$\mathbf{P}_{k+1} = \mathbf{P}_{k+1}^- - \mathbf{K}_{k+1} \mathbf{P}_{k+1}^{vv} \mathbf{K}_{k+1}^T$$

Table 4.4: UKF algorithm

measure is to count the number of floating-point arithmetic operations required to be performed to pass from the input to the output of an algorithm. A floating-point operation (FLOP) is any mathematical operation or an assignment involving floating-point numbers. Numerical complexity is represented by counting the number of FLOPs in an algorithm i.e., counting total number of additions, subtractions, multiplication and divisions etc. used in the algorithm. Alternatively the numerical complexity may also be represented by counting number of mathematical operations (NOs). NO is a programme-independent and machine-independent index of numerical complexity. In the next section the complexity of the filtering algorithms presented in this chapter based on NO has been carried out and a comparison has also been made among these algorithms.

Elementary Operations and NOs

(1) Matrix addition/subtraction

Let $A_{n\times m} \in \mathbb{R}^{n\times m}, B_{n\times m} \in \mathbb{R}^{n\times m}$

NOs : $A_{n\times m} \pm B_{n\times m} \ = \sum_{i=1}^{n} m = n.m$

(2) Matrix multiplication

$$\text{NOs} : (A_{n\times m} \times B_{m\times k}) = \sum_{i=1}^{n}\sum_{j=1}^{k}(m \text{ multiplications} + m - 1 \text{ addition})$$
$$= (2m-1).n.k$$

(3) Vector addition/subtraction

Let $\mathbf{x} \in \mathbb{R}^n, \mathbf{y} \in \mathbb{R}^n$

NOs : $(\mathbf{x} \pm \mathbf{y}) = n$

EKF Algorithm	
Operation	NO
Mean Prediction	
$A_k x_k$	$2n^2 - n$
$B_k u_k$	$n(2m-1)$
subtotal	$2n^2 - n + n(2m-1) + n = 2n^2 + 2mn - n$
Covariance Prediction	
$A_k P_k A_k^T$	$2(2n^3 - n^2)$
subtotal	$2(2n^3 - n^2) + n^2 = 4n^3 - n^2$
Covariance Update	
$S_k = H_k P_{k\|k-1} H_k^T + R_k$	$2rn^2 + 2r^2 n - rn$
$\mathbf{S}_r^{-1}$	$2r^3 - 2r^2 + r$
$K_k = P_{k\|k-1} H_k^T \mathbf{S}_r^{-1}$	$2rn(n + r - 1)$
$P_{k\|k} = (1 - K_k H_k^T) P_{k\|k-1}$	$2n^3 + 2(r-1)n^2 + n$
subtotal	$2n^3 + (6r-2)n^2 + (4r^2 - 3k + 1) + 2r^3 - 2r^2 + r$
Update	
$\hat{y}_k = y_k - H_k \hat{x}_{k\|k-1}$	$2rn$
$\hat{x}_k = \hat{x}_{k\|k-1} + K_k \hat{y}_k$	$2rn$
subtotal	$4rn$
Total NO's for EKF	$6n^3 + (6n-1)n^2 + (2m + 4r^2 + r)n + 2r^3 - 2r^2 + r$
$\approx$	$\approx O(6n^3)$

Table 4.5: Computational cost of EKF

(4) Cholesky factorization

Let $A \in \mathbb{R}^{n \times n}$

$$Chol(A) = (n^3 - n)/3 + (n^2 - n)/2$$

$$= \frac{2n^3 + 3n^2 + n}{6}$$

Comparison of Numerical Complexity

The table 4.8 presents a comparison of the numerical complexities of the three algorithms. When we compare the computational complexity of EKF with those of SPKF algorithms we observe that the computational complexity of EKF is less than

UKF Algorithm	
Operation	NO
Sigma Point Calculations	
Cholesky Factorization of $\mathbf{S}_k = \sqrt{\mathbf{P}}$	$\frac{2n^3+3n^2+n}{6}$
$\gamma\sqrt{\mathbf{P}}$	n^2
$\hat{\mathbf{x}}_k + \gamma\mathbf{S}_k$	n^2
$\hat{\mathbf{x}}_k - \gamma\mathbf{S}_k$	n^2
subtotal	$\frac{2n^3+3n^2+n}{6} + 3n^3$
Sigma Point Prediction	
$\mathbf{X}_{i,k+1} = \mathbf{f}(\mathbf{X}_{i,k}, k)$	$4n^3 + 4nm^2 + (2m-1)n$
Mean Prediction	
$\hat{\mathbf{x}}^-_{k+1} = \sum_{i=0}^{2n} W_i^{(mean)} \mathbf{X}_{i,k+1}$	$4n^2 + n$
Covariance Prediction	
$\mathbf{P}^-_{k+1} = \sum_{i=0}^{n} W_i^{(c)} [\mathbf{X}_{i,k+1} - \hat{\mathbf{x}}^-_{k+1}][\mathbf{X}_{i,k+1} - \hat{\mathbf{x}}^-_{k+1}]^T$	$4n^3 + 6n^2 + 2n$
Measurement Prediction	
$\mathbf{Y}_{i,k+1} = \mathbf{h}(\mathbf{X}_i, k+1)$	$r(4n^2-1)$
subtotal	$4nr(n+1)$
Update	
Covariance Update	
$\mathbf{P}^{yy}_{k+1} = \sum_{i=0}^{2n} W_i^{(c)} [\mathbf{Y}_{i,k+1} - \hat{\mathbf{y}}^-_{k+1}] [\mathbf{Y}_{i,k+1} - \hat{\mathbf{y}}^-_{k+1}]^T$	$4(r^2+r)n + 2r^2 + 2r$
$\mathbf{P}^{xy}_{k+1} = \sum_{i=0}^{2n} W_i^{(c)} [\mathbf{X}_{i,k+1} - \hat{\mathbf{x}}^-_{k+1})][\mathbf{Y}_{i,k+1} - \hat{\mathbf{y}}^-_{k+1}]^T$	$nr(4n+1)$
$\mathrm{K}_{k+1} = \mathbf{P}^{xy}_{k+1}(\mathbf{P}^{vv}_{k+1})^{-1}$	$(2r-1)rn + 2r^3 - 2r^2 + r$
$\mathbf{P}_{k+1} = \mathbf{P}^-_{k+1} - \mathrm{K}_{k+1}\mathbf{P}^{vv}_{k+1}\mathrm{K}^T_{k+1}$	$2rn^2 + (2r-1)rn$
subtotal	$6rn^2 + (8r+3)rn + 2r^3 + 3r$
Mean Update	
$\hat{\mathbf{x}}_{k+1} = \hat{\mathbf{x}}^-_{k+1} + \mathrm{K}_{k+1}\mathbf{v}_{k+1}$	$2rn + r$
Total NO's for UKF	$\frac{25}{3}n^3 + (10r + 4m + \frac{27}{2})n^2$
	$+(8r^2 + 9r + 2m + \frac{13}{6})n + 2r^3 + 4r$
	$\approx 1.39 \times O(EKF)$

Table 4.6: Computational cost of UKF

DDF Algorithm	
Operation	NO
Sigma Point Calculations	
Cholesky Factorization of $\sqrt{\mathbf{P}}$	$\frac{2n^3+3n^2+n}{6}$
$\gamma\sqrt{\mathbf{P}}$	n^2
$\hat{\mathbf{x}}_k + \gamma\sqrt{\mathbf{P}}$	n^2
$\hat{\mathbf{x}}_k - \gamma\sqrt{\mathbf{P}}$	n^2
subtotal	$\frac{2n^3+3n^2+n}{6} + 3n^3$
Cholesky Factorization of $\sqrt{\mathbf{Q}}$and $\sqrt{\mathbf{R}}$	$\frac{2n^3+3n^2+n}{3}$
Sigma Point Prediction	
Sigma Point Prediction	$4n^3 + 4nm^2 + (2m-1)n$
Mean Prediction	
mean prediction	$4n^2 + n$
Covariance Prediction	
Covariance Prediction	$8n^3 + 12n^2 + 4n + \frac{2n^3+3n^2+n}{3}$
Measurement Prediction	
Measurement Prediction	$4nr(n+1)$
Update	
Covariance Update	
$\mathbf{P}_{k+1}^{yy}$	$4(r^2+r)n + 2r^2 + 2r$
$\mathbf{P}_{k+1}^{xy}$	$nr(4n+1)$
K_{k+1}	$(2r-1)rn + 2r^3 - 2r^2 + r$
$\mathbf{P}_{k+1}$	$2rn^2 + (2r-1)rn$
subtotal	$6rn^2 + (8r+3)rn + 2r^3 + 3r$
Mean Update	
$\hat{\mathbf{x}}_{k+1} = \hat{\mathbf{x}}_{k+1}^- + \mathrm{K}_{k+1}\mathbf{v}_{k+1}$	$2rn + r$
Total NO's for DDF	$\frac{102}{6}n^3 + (23+18r)n^2$
	$+(\frac{14}{6} + 2m + 4m^2 + 11r + 10r^2)n + 4r^3 + 7r$
	$\approx 2.04 \times O(EKF)$

Table 4.7: Computational cost of DDF

Computational Complexity	
Algorithm	NO
EKF	$O(6n^3)$
UKF	$1.39 \times O(EKF)$
DDF	$2.04 \times O(EKF)$

Table 4.8: Comparison of complexity of three algorithms

these two Kalman filters. However, EKF may cause significant errors for highly non-linear systems because of truncation of higher order terms [74]. The downside of the two sigma point Kalman filters is higher computational complexity which is approximately 1.4 and 2 times higher for UKF and DDF than that of the EKF. However, the superior performance of SPKF algorithms in terms of robustness and estimator accuracy is clearly visible in the parameter estimation process shown through a number of simulations presented in the next section. Moreover, the SPKF algorithms do not require the derivation of any Jacobians when they are compared with the EKF.

4.8 Simulation Results and Discussion

For the purpose of simulation we have considered a multiuser multipath scenario. We have simulated the multipath channel with one,two and three paths with path spacing of 1/2 and 1/10 of a chip. We have shown only the first arriving path as it will be used for multiuser radiolocation. The delays have been assumed to be constant during one measurement. The spreading codes length is 31 with oversampling factor of 2. The UKF requires proper initialization. For the simulation results, we assume such

an initial estimator is used to start the tracking algorithm fairly close to the true values. We note that the data bits, $d_{k,m}$, are not included in the estimation process, but are assumed unknown apriori. Since it has been shown that DDF1 is equivalent in performance to the EKF [78], so we will simulate DDF2 to make a comparison with EKF and UKF. In the simulations, we assume that the data bits are available from decision-directed adaptation, where the symbols $d_{k,m}$ are replaced by the $\hat{d}_{k,m}$ decisions as shown in Figure (4.5). For the state space model we have taken state transition matrix to be $\mathbf{F} = 0.999\mathbf{I}_{n\times n}$ and the process noise covariance matrix as $\mathbf{Q} = 0.001\mathbf{I}_{n\times n}$. The scaling parameter $\gamma = 3$ for the DDF2 algorithm and for the UKF $\alpha = 0.01$, and $\kappa = 0$. The other parameter $\beta = 2$ is set to capture higher order (fourth) terms in the Taylor series expansion.

We start with the simulation of two-user model for the EKF. The power of the strong user is $P_1 = 1$ and that of the weak user is $P1/10$ and exponential power delay profile has been used for the two path model. The true delay of the weak user is $\tau = 14.7$ chips. Figure (4.6) shows the tracking of the 1st path when the initial error is greater than the path spacing. It is seen to diverge from the true delay. However when the initial error is less than the path spacing, the EKF converges and the error is within few samples of a chip. This is shown in Figure (4.7). It shows that the EKF is very sensitive to the initialization . These two results show that when the initial value is not close to the true delay value the steady state error is of the order of a chip or more. This is expected as the EKF introduces error due to the reasons

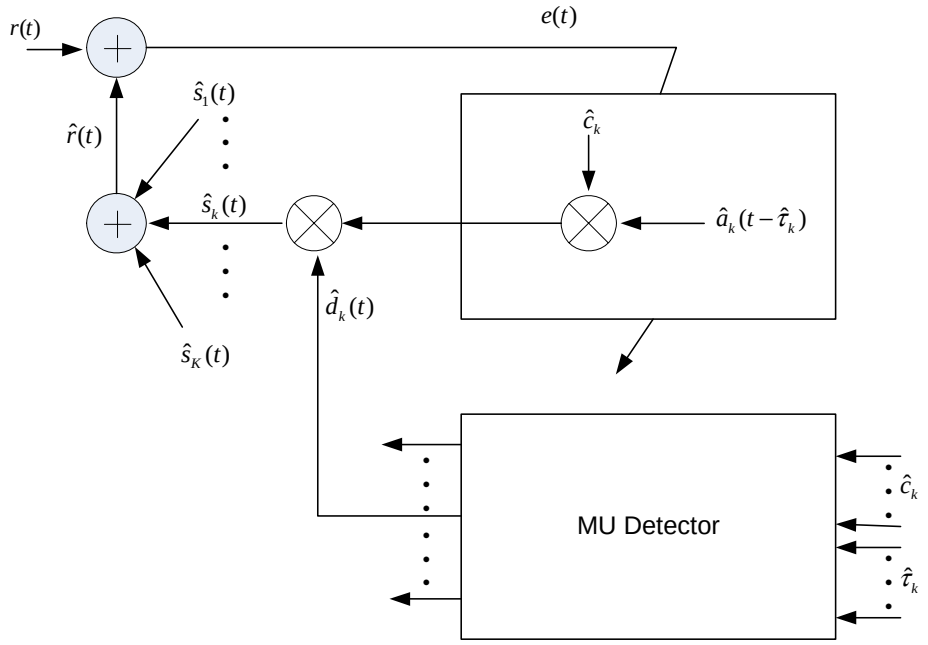

Figure 4.5: Multiuser parameter estimation receiver

discussed earlier. The Figure (4.8) shows the timing epochs for the first arriving path against the number of samples for the weaker and stronger user in a two path scenario with path separation of 1/2 chip for the UKF algorithm in a ten-user environment. Again the power of the strongest user is $P_1 = 1$ and that of the weakest user is $P1/10$. We can see that the estimator converges to the true values for both of the users. This demonstrates the robustness of the proposed estimator in near-far environment. Figure (4.9) shows the delay estimation error against samples for varying number of users.

Near-far resistance in the context of multiuser delay estimation refers to the sensitivity of the mean squared estimation error to changes in the level of MAI - the more the MSE changes for a given change in MAI, the poorer the detector's near-far resis-

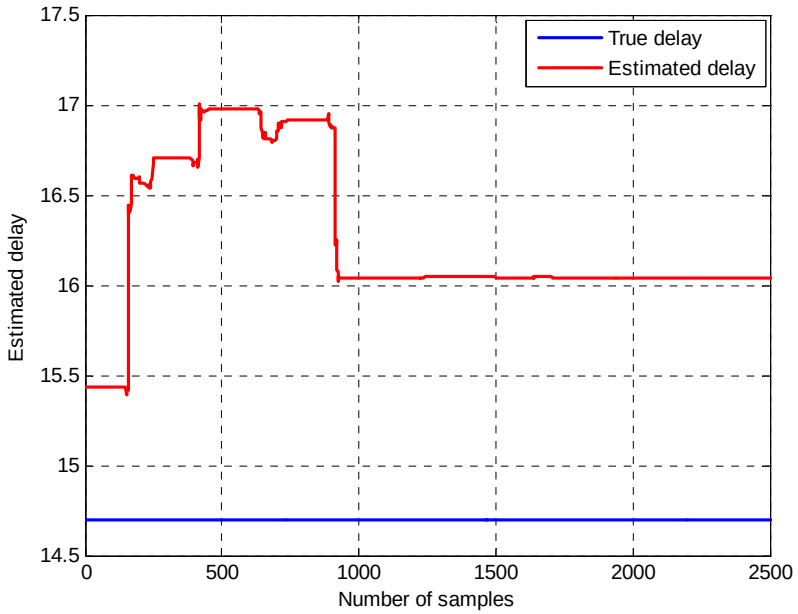

Figure 4.6: EKF based timing epoch estimation for first arriving path of two users two path channel model (path spacing=Tc/2) - the estimator diverges when the initial error is greater than the path spacing

tance [81]. A comparison of MSE for the EKF with UKF has been shown in Figure (4.10). It is quite evident from the MSE results that the proposed multiuser UKF detector is approximately near-far resistant, whereas the multiuser EKF detector is severely affected by MAI.

Figures (4.11) and (4.12) show the delay estimation in a perfectly power control and a near-far scenario for DDF2 in ten-user two-path channel model with path spacing of 1/2 chip. The true delay of the weakest user is $\tau = 13.7$ chips and that strongest user is $\tau = 20$ chips. These figures show that DDF2 is near-far resistant in both the environments.

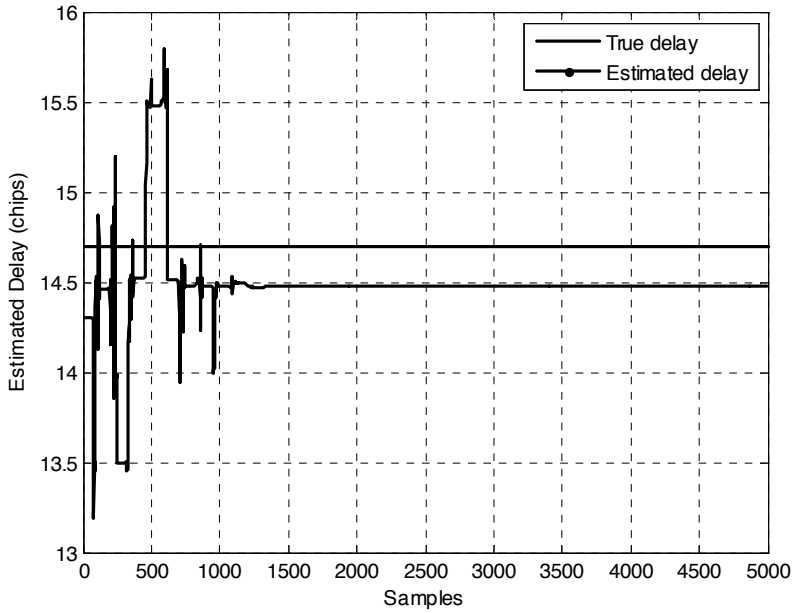

Figure 4.7: EKF based timing epoch estimation for first arriving path

We observe that the estimator under perfect power control and in a near-far scenario is able to converge. It can be seen that both UKF and DDF2 are robust i.e. that these estimators are not sensitive to the starting point.

Figure (4.13) shows the histogram of the first arriving path for the weaker user for a Monte Carlo simulation of 100 runs with true delay $\tau = 14.7$ chips for the UKF in a three path 1/2 chips spaced channel model has been considered. It can be observed that the estimator converges to the true value and is normally distributed around the true value. Similar observation is made for the DDF2 algorithm as can be seen in Figure (4.14). The tracking performance of UKF for a twelve-user three-path model with path spacing of 1/5 of a chip has been shown in Figure (4.15). The true delay of

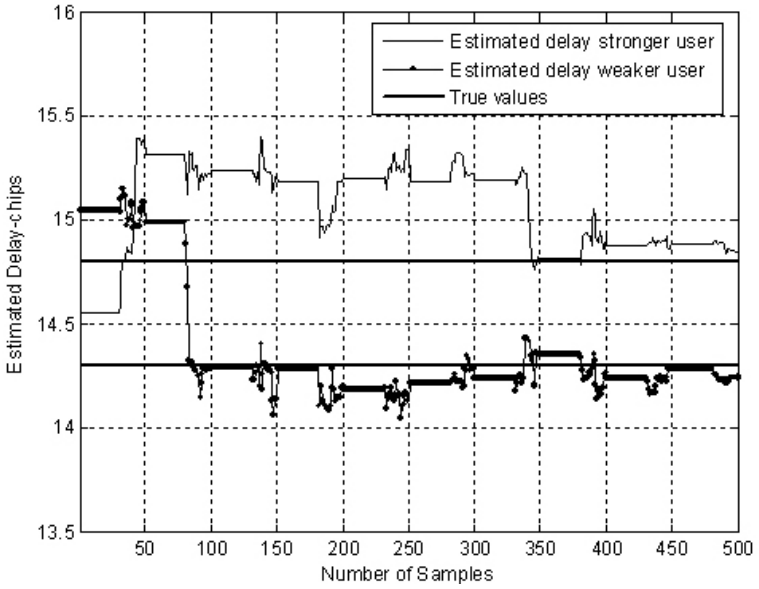

Figure 4.8: Timing epoch for the first arriving path of the weaker user in a ten users-two path channel model (UKF) (2nd path within 1/2 chip)

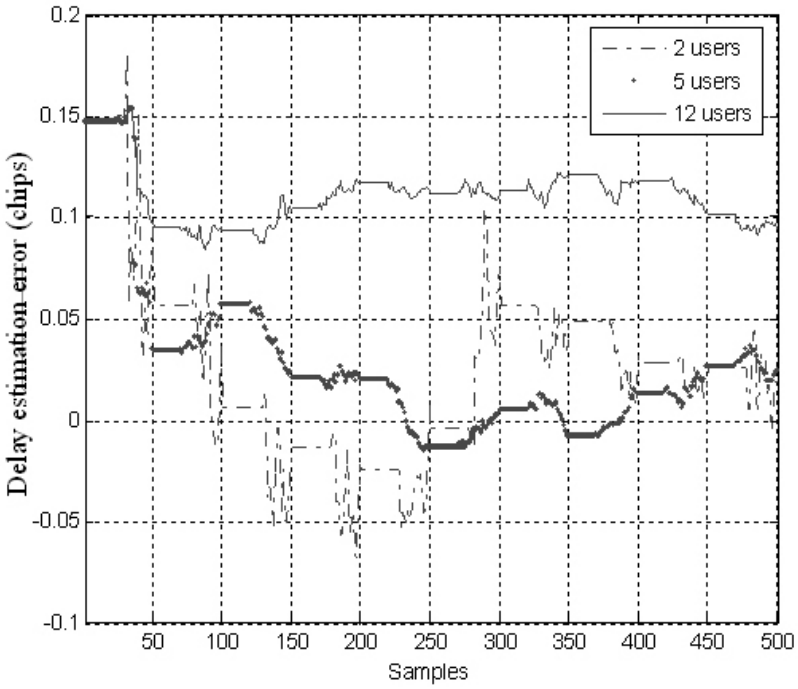

Figure 4.9: Delay estimation error for first arriving path of the weaker user with varying number of users in a three path channel model (UKF)

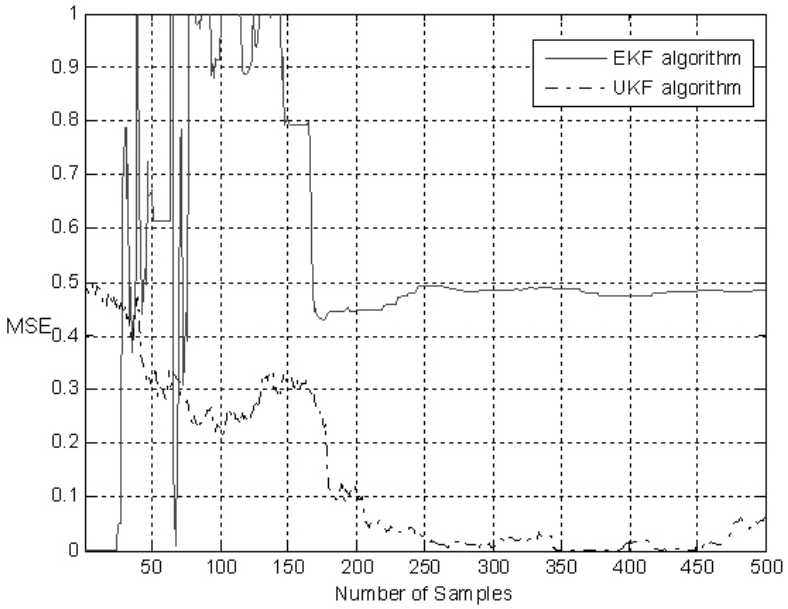

Figure 4.10: Comparison of the MSE of timing epoch estimation for first arriving path for UKF and EKF

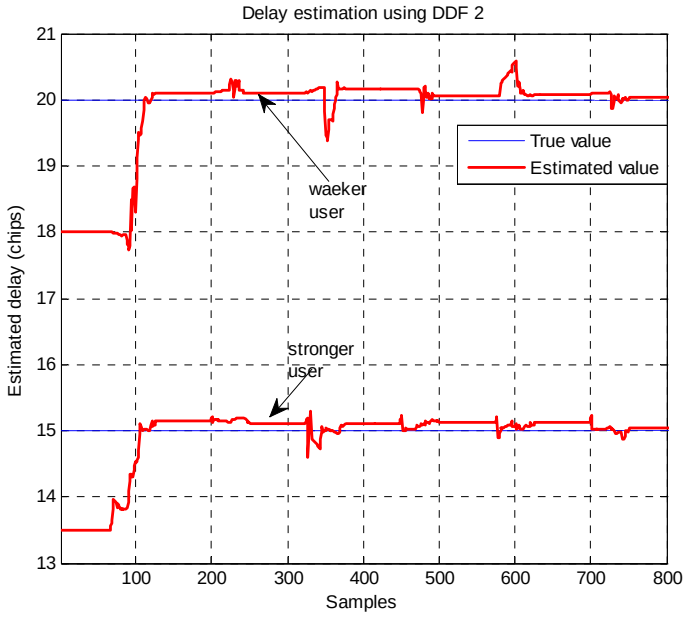

Figure 4.11: Timing epoch of the first arriving path of the weaker and stronger user (near far ratio=20dB)(DDF2)

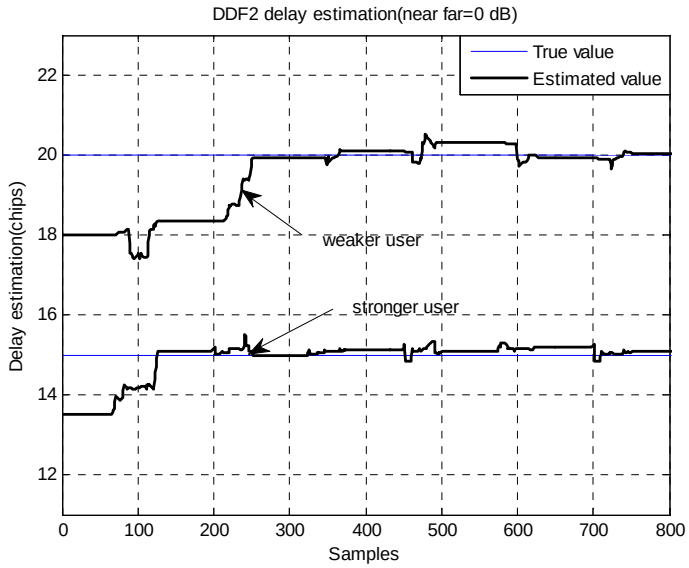

Figure 4.12: Timing epoch of the first arriving path of the weaker and stronger user (near far ratio=0dB)(DDF2)

the weakest user is $\tau = 15$ chips and that strongest user is $\tau = 20$ chips. We observe that the UKF-based detector is capable of accurately converging to the correct delays. The effect of process noise on the performance of the filter is evaluated in Figure (4.16), where we see higher MSE as the process noise rises for the delay estimate in a five-user three-path model. This result matches our intuition that an increase in process noise increases uncertainty.

MSE from simulation of the estimator is compared to that predicted by the CRLB. The CRLB was evaluated where the first user was assumed to be the desired user in near–far situation. From Figure (4.17), we find that the computed MSE for UKF and DDF2 is slightly greater than the CRLB indicating that the estimators is nearly efficient. We also note that the EKF estimator is rapidly increasing in the MSE above

near-far ratio of 20 dB, and it shows that a larger error happened showing it is not a near-far resistant whereas UKF and DDF2 are near-far resistant. Thus we find that the UKF and DDF2 estimator with fourth order and 2nd order accuracy respectively, are more near-far resistant and have strong noise power immunity than the EKF estimator with 1st order accuracy. The DDF2 performance, in terms of MSE, is lower than UKF. It indicates that the neglected higher-order terms in the series expansion are not ignorable and could affect the prediction accuracy of the filter as evident from Figure (4.18) where the MSE for the first arriving path delay estimates in five user two path model with 1/2 chip path spacing has been plotted. We can see that the MSE for UKF is lower than that of DDF showing that it is more near-far resistant than DDF2.

Chapter Summary

This chapter presented three different filtering approaches for the multiuser parameter estimation. The simulation results demonstrated that SPKFs are near-far resistant and accurately track time delays when compared to the EKF. A comparison was also presented with the CRLB on the basis of MSE. It was shown the SPKFs nearly achieve the lower bound. We also observed that the UKF has smaller MSE than the DDF2. In the next chapter we will present two new receiver structures employing interference cancellation approach combined with DLL to estimate time delays.

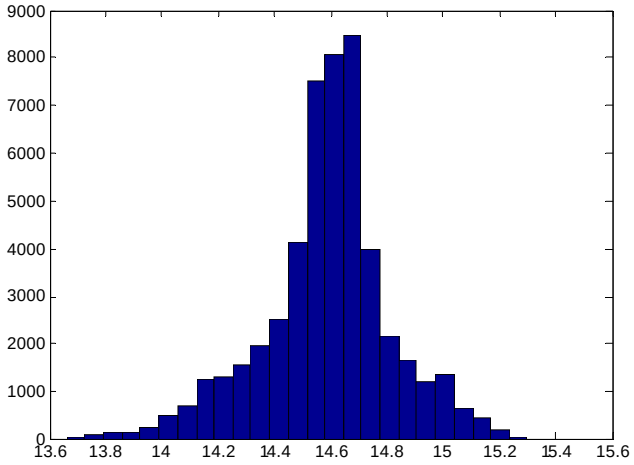

Figure 4.13: Histogram of the delay estimation error of the first arriving path in a twelve users and three-path channel model for the weaker user (2nd path within $\frac{1}{2}$ -chip delay)

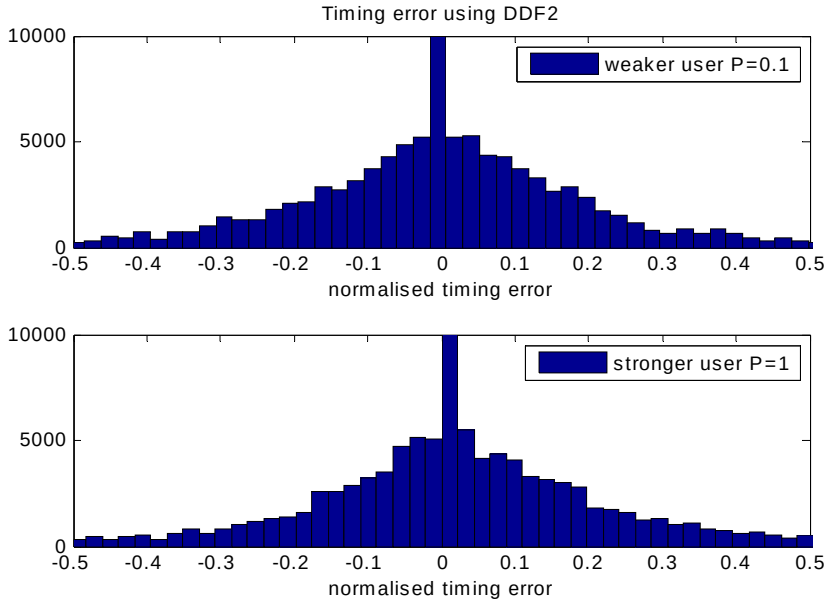

Figure 4.14: Histogram of the delay estimation error of the first arriving path of the weaker and stronger user (near far ratio=20dB)(DDF2)

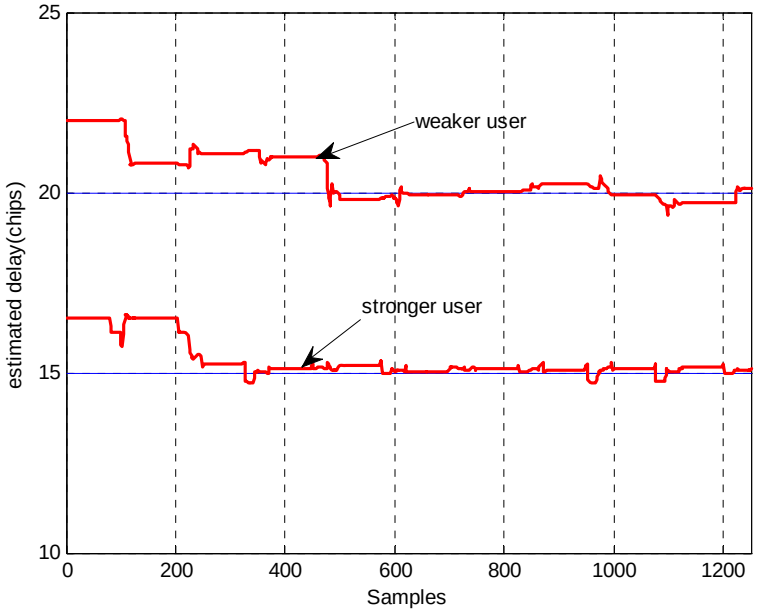

Figure 4.15: Timing epoch of the first arriving path of the weaker and stronger user in a twelve-user three paths (paths 1/5 chip apart)

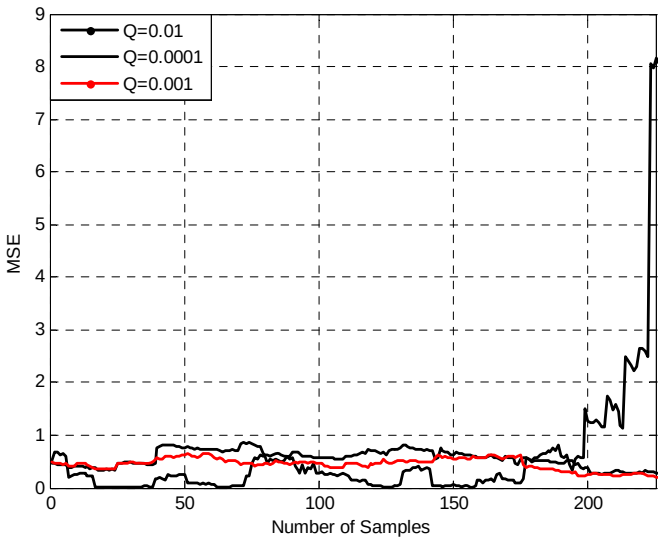

Figure 4.16: The effect of process noise on the performance of UKF

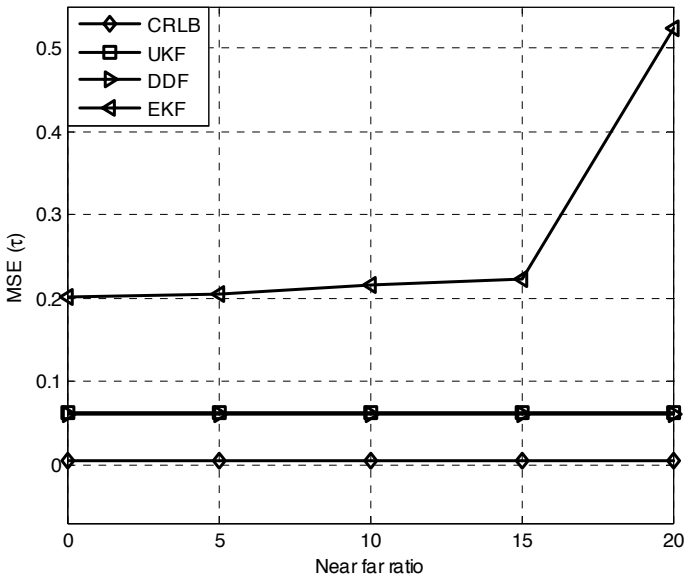

Figure 4.17: The MSE of the time delay estimates versus near-far ratio for three estimators and the CRLB.

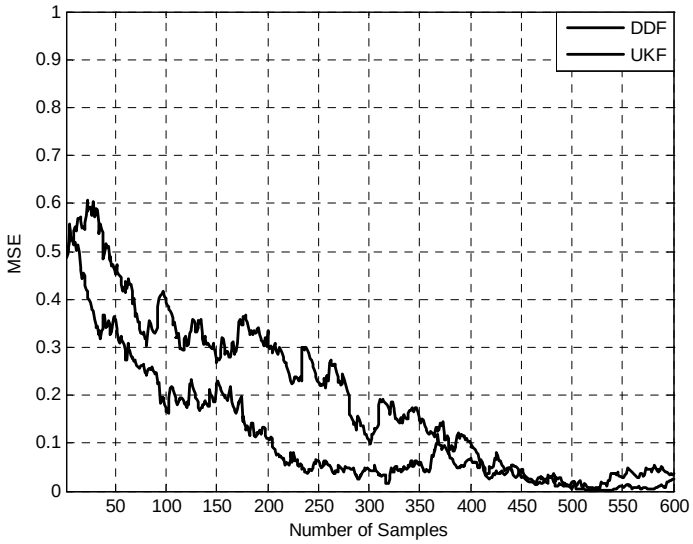

Figure 4.18: Comparison of MSE for delay - UKF vs DDF

Chapter 5

Modified Delay Locked Loop Based Approaches

In this chapter we will present a multiuser delay tracking receiver that integrates successive interference cancellation (SIC) technique with DLL. This approach tracks the delay of the weak users by estimating and then cancelling the interference caused by strong users in a successive manner.

In the reverse link, time synchronization of the receiver to the received signal can be achieved in two stages: initially, the two code signals are aligned in phase to uncertainty less than one chip duration through a process called code acquisition or coarse synchronization. In other words, the acquisition is aligning the unknown phase of the received code with the known phase of the local code generated at the receiver within one chip (or a fraction of a chip). Once the incoming code is acquired, tracking

or fine synchronization takes place which is maintained by a closed loop tracking system. However, if for some reason the tracking system has gone out of lock, the acquisition system will be re-activated in order to acquire the incoming code and the tracking system takes over again to maintain code synchronization. In this thesis we are concerned with the code synchronization.

The tracking loop for CDMA systems is delay locked loop (DLL) discussed in chapter 3. Tracking the acquired code phase is usually confronted with the effects of multipath interference and the multiuser interference driving it out of lock. The effects of multipath fading on tracking loop performance have been discussed in [26,65] and presents a modified tracking loop that outperforms the traditional DLL in a multipath fading channel. As previously discussed in chapter 3, the DLL performance is severely affected by MAI [68,69], where it has been shown that increasing the number of interferers increases the rms tracking error. Even in the case when a single user is received with significantly more power than the desired user in a two-user scenario, the effects are worse than when there are many users with equal received strength. Different delay trackers have been proposed including those that employ interference cancellation approach combined with DLL [40,41,65] to alleviate the effects of MAI.

This chapter describes the application of a signal processing technique, known as successive interference cancellation (SIC), to the tracking of weak signals in the other users signals. Significant near-far resistance can theoretically be achieved if a user can negate or cancel the effect of the other users on his signal. A more fundamental

view of this is to treat it as a multiuser detection problem, in which all transmissions are considered as signals for all users. In this way, signals intended for other users are specifically modeled and/or accounted for. The proposed structure employs a multistage SIC to estimate and cancel the strongest user signal from the composite received signal in an iterative manner to track the weak user.

5.1 Proposed Structure

Our proposed structure is based on SIC that takes a serial approach to cancel interference. Each stage of the detector identifies the parameters of the strongest remaining signal component; then it regenerates and cancels out this component from the received signal. As a result, when the next stage attempts to acquire and track the remaining signals, it sees less MAI. The first stage implements the following steps.

1) Detect the strongest signal, $s_1$using a conventional detector. The conventional detection starts with the acquisition stage where sequential search in Doppler and code offset to find the approximate signal parameters. It is followed by tracking loops which provide more accurate measurements of the code offset and Doppler. The code tracking is performed by a delay lock loop consisting of an "early" and "late" correlator, spaced symmetrically about the desired "prompt" signal. The carrier tracking loop may be a frequency lock loop, or a Costas loop for phase tracking and data recovery.

2) Regenerate an estimate of the strong signal, $\hat{s}_1$, using knowledge of its PN

sequence and estimates of its timing, amplitude and phase. These parameters are derived from the tracking loops in the conventional detector.

3) Subtract $\hat{s}_1$, from the total received signal $r(t)$, yielding a partially cleaned version of the remainder of the received signal with little influence on other users code tracking loops. If the estimates of the strong signal parameters are accurate, the output of the first stage is a correct data decision on the strongest signal and a modified received signal without the MAI caused by the strongest signal. The process of tracking, demodulating, estimating and canceling with the resulting waveform which contains no trace of the signal due to the strongest user is repeated in a multistage structure until all the users are demodulated. A block diagram of the detector is shown in Figure (5.1).

The reasons for canceling the signals in the descending order of signal strength are straightforward. First, it is easiest to achieve acquisition and demodulation on the strongest signal. Second, the removal of strongest signal gives the most benefit for the remaining weak signals. The result of this algorithm is that the acquisition and tracking of the strongest signal may not benefit from any MAI reduction in the first iteration, whereas the weakest signals will potentially see a significant reduction in their MAI. The stronger the interferer signal, the better will be its parameter estimates obtained in the tracking loop. Accurate signal parameter estimates result in proper cancellation. However, if the interferer signal becomes weaker due to an increasing distance from the receiver, then the estimates of the signal parameters will

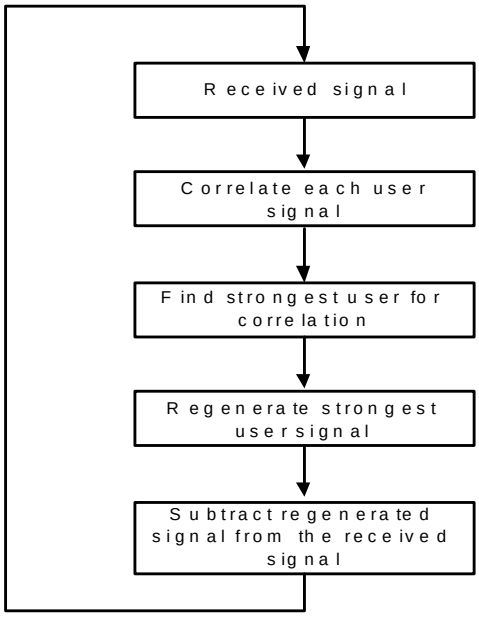

Figure 5.1: Successive interference cancellation approach

deteriorate. This results in an inaccurate cancellation and actually has a harmful effect on the subsequent signal acquisition efforts.

5.2 System Model

We consider here an asynchronous DS/CDMA system with BPSK modulation [82-84]. The binary data signal transmitted by a user k is denoted by $b_k(t)$, which is defined as follows:

$$b_k(t) = \sum_l A_{k,l} \;\; p_T(t - lT)$$

where $A_{k,l} \in \{1, -1\}$ is the information-bearing signal amplitude for the kth user's lth symbol element, and $p_T(t)$ is the rectangular pulse of duration T. Let the kth user's signature sequence to be denoted as follows:

$$a_k(t) = \sum_l C_{k,l} \;\; p_{T_c}(t - lT_c)$$

where $C_{k,l}$ denotes the kth user's lth chip of duration T_c. Then the transmitted signal for the kth user is given by

$$s_k(t) = \sqrt{2P_k} a_k(t) b_k(t) \cos(\omega_c t + \theta_k)$$

with P_k being the signal power and θ_k, being a phase for user k. For the DS/CDMA system with K multiple access users, the received signal $r(t)$ is given as [81],

$$r(t) = \sum_{k=1}^{K} \sqrt{2P_k} a_k(t - \tau_k) b_k(t - \tau_k) \cos(\omega_c t + \phi_k) + n(t) \tag{5.1}$$

where τ_k is the total delay, ϕ_k is the changed phase given as $\phi_k = (\theta_k - \omega_c \tau_k)$ for the kth user, ω_c is the carrier frequency, and n(t) is the additive white Gaussian noise (AWGN) process with a two-sided spectral density $N_o/2$. The τ_k and ϕ_k can be modeled to be the i.i.d. random variables with the uniform distributions over $[0, T]$ and $[0, 2\pi]$, respectively. We also assume that the spread sequences of all users are known.

In the successive IC (SIC) scheme the basic idea of detecting a particular user is

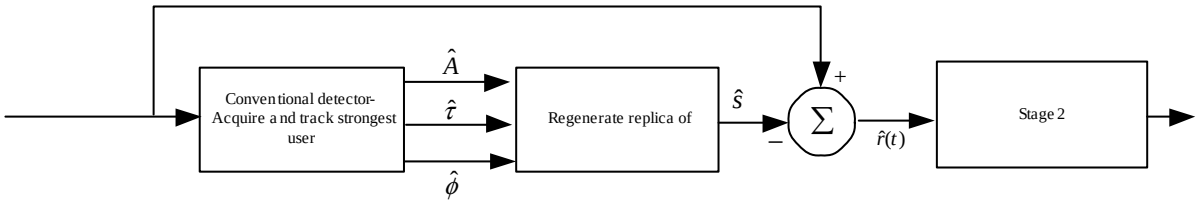

Figure 5.2: Successive interference cancellation architecture

to cancel the estimated interference of the stronger user signals than itself from the total received signal. At each iteration of the SIC, a user of the strongest correlation value is selected among those obtained from the conventional bank correlators, and its estimated signal is regenerated by estimating its power and re-spreading its detected bit with the corresponding PN chip sequence. This process is iterated until the weakest user is decoded. Figure (5.2) shows such a structure.

Denoting the total received signal by $r^1(t) = r(t)$. The initial decision for the lth bit of kth user is given as [81]

$$Y_{k,l}^{(1)} = \frac{1}{T}\int_{lT+\tau_k}^{(l+1)T+\tau_k} r^{(1)}(t)a_k(t-\tau_k)\cos(\omega_c t+\phi_k)dt \tag{5.2}$$

If we denote the remaining signal at the start of *(s-l)st* cancellation stage by $r^{(s-1)}(t)$, the corresponding decision variable is given as

$$Y_{k,l}^{(s-1)} = \frac{1}{T}\int_{lT+\tau_k}^{(l+1)T+\tau_k} r^{(s-1)}(t)a_k(t-\tau_k)\cos(\omega_c t+\phi_k)dt \tag{5.3}$$

which is to be used for estimating the signal to be canceled at this stage. For the simplicity of presentation in the following analysis, we further denote the user of strongest decision variable by the index k in each cancellation stage. The estimated signal to be canceled in the $(s-l)st$ stage is given as follows:

$$\hat{s}_k^{(s-1)}(t-\tau_k) = \sum_l \sqrt{2\hat{P}_{k,l}^{(s-1)}} a_k(t-\tau_k)\hat{b}_{k,l}(t-\tau_k)\cos(\omega_c t + \hat{\phi}_k) \tag{5.4}$$

where $\hat{P}_{k,l}^{(s-1)}$ unbiased estimate for the power of lth bit for the kth user, $\hat{b}_{k,l}(t) = \hat{A}_{k,l}P_T(t-lT)$ with $\hat{A}_{k,l}$ determined by a hard decision given by $\hat{A}_{k,l} = sgn(Y_{k,l}^{(s-1)})$. Therefore, the remaining signal at the sth cancellation stage is given as

$$r^{(s)}(t) = r(t) - \sum_{j=1}^{s-1} \hat{s}_k^{(j)}(t-\tau_k) \tag{5.5}$$

For the further simplicity of presentation, without loss of generality, we assume that the users are ordered in a descending manner in terms of received signal, i.e., the strongest and the weakest users are denoted in their indices by $k=1$ and $k=K$ respectively and thus,

$$\begin{aligned} r^{(s)}(t) &= r(t) - \textstyle\sum_{j=1}^{s-1} \hat{s}_k^{(j)}(t-\tau_k) \\ &= \textstyle\sum_{j=s}^{K} s_j(t-\tau_k) + \sum_{j=1}^{s-1}\{s_j(t-\tau_k) - \hat{s}_j^{(j)}(t-\tau_k)\} + n(t) \end{aligned} \tag{5.6}$$

In the current sth stage, the decision variable for kth user is determined as in (1) using the remaining signal $r^{(s)}(t)$ and furthermore, can be expressed in terms of MAI

components as follows:

$$\begin{aligned} Y_{k,l}^{(s)} &= \tfrac{1}{T}\int_{lT+\tau_k}^{(l+1)T+\tau_k} r^{(s)}(t)a_k(t-\tau_k)\cos(\omega_c t+\phi_k)dt \\ &= \sqrt{\tfrac{P_{k,l}}{2}} + \textstyle\sum_{j=k+1}^{K} I_{j,k}(\tau_{j,k},\phi_{j,k}) + \sum_{j=1}^{K-1}\left\{I_{j,k}(\tau_{j,k},\phi_{j,k}) - \hat{I}_{j,k}(\tau_{j,k},\phi_{j,k})\right\} + \xi \end{aligned} \tag{5.7}$$

The second term $I_{j,k}(\tau_{j,k},\phi_{j,k})$ constitutes the MAI due to cross-correlation between the jth and kth users given by

$$I_{j,k}(\tau_{j,k},\phi_{j,k}) = \left(\sqrt{\frac{P_{j,l}}{2}}\cos(\hat{\phi}_j-\phi_k)\right)\left(\frac{1}{T}\int_{lT+\tau_k}^{(l+1)T+\tau_k} r^{(s)}(t)a_k(t-\tau_k)\cos(\omega_c t+\phi_k)dt\right)\Bigg\} \tag{5.8}$$

and the third term $\hat{I}_{j,k}(\tau_{j,k},\phi_{j,k})$ is the MAI from cross-correlation between the kth user signal and the estimated signal of jth user and ξ is a Gaussian random variable defined as

$$\xi = \frac{1}{T}\int_0^T n(t)a_k(t-\tau_k)dt \tag{5.9}$$

The structure of the proposed SIC based approach for delay estimation is shown in Figure (5.3). The idea is to identify and then remove multipath in order to produce a cleaner version of the received signal. The proposed implementation acquires, tracks, and removes the direct as well as the multiple estimates of the strongest signal(s). These multipath signals are summed and cancelled from the incoming signal $r(t)$ to

give a partially cleaned-up version of the signal. Acquisition and tracking is then performed on $r_c(t)$ to get improved phase and timing estimates.

5.3 Early Late Delay Tracking Algorithm

The code synchronization process is performed in two stages: acquisition and tracking. Acquisition is used to coarsely align the received signal with the locally generated PN code to within one chip duration and then tracking is initiated to minimize the delay offset to maintain synchronization between the signals. Code tracking techniques proposed in the literature include closed loop structures, such as the delay-locked loop (DLL) and the tau-dither loop (TDL), have extensively been used to perform tracking of delays to minimize the timing error. These loops correlate the incoming signal either simultaneously (in DLL) or alternatively (in TDL) with advanced and delayed versions of the locally generated code (usually one chip or less apart), and the correlators outputs are subtracted to generate an error signal. This error signal is used to adjust a voltage controlled clock (VCC) that derives the local PN code generator to minimize the time delay offset. Other variations of the basic DLL and TDL have also been proposed.

In this section we present a modified DLL that employs an early and late channel with LMS-type algorithm which is used for the update of the delay estimate.

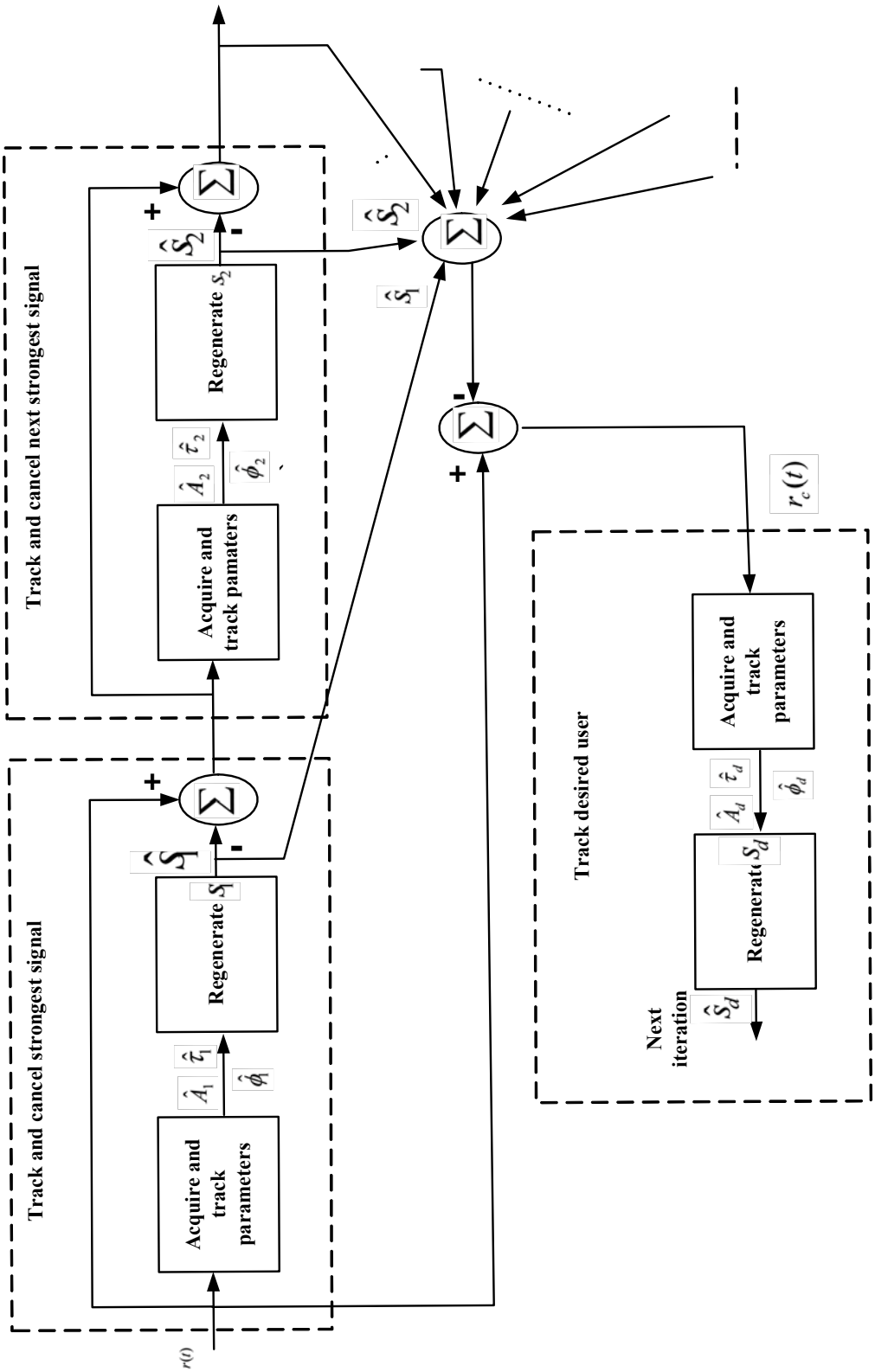

Figure 5.3: SIC based structure employing DLL

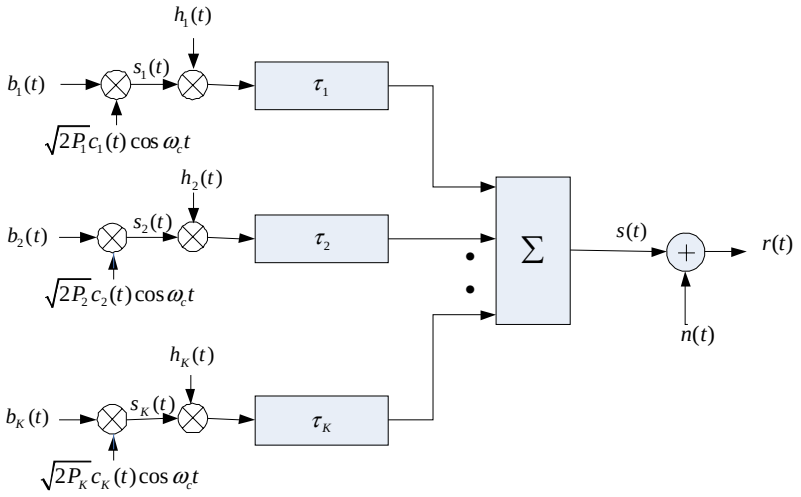

Figure 5.4: System model

5.3.1 The System Model

The signal model of a DS/CDMA system is shown in the Figure (5.4), in which the received signal consists of a sum of K users' signal plus additive white Gaussian noise. The transmitter for the kth user is also shown

The received kth user's data signal in a DS/CDMA channel can be modeled by an equivalent complex baseband representation as

$$s_k(t) = \sqrt{2P_k}\, b_k(i) c_k(t - iT_b)\cos\omega_c t \tag{5.10}$$

where is b_k the ith information bit transmitted by the kth user given by

$$b_k(t) = \sum_{i=-\infty}^{\infty} b_k(i) p_{T_b}(t - iT_c) \tag{5.11}$$

$c_k(t)$ is the spreading waveform of the kth user,

$$c_k(t) = \sum_{m=0}^{N_c} c_k(m)\, p_{T_c}(t - mT_c) \tag{5.12}$$

where p_T is a pulse waveform of length , T_c and is the number of chips in one spreading code period given as $N_c = \frac{T_b}{T_c}$. The spreading sequence is binary, i.e. $c_k(m) \in \{-1, 1\}$,

τ_k is the transmission delay of the kth user. It is assumed that τ_k is independent and uniformly distributed over $[0, T_b]$. The combined transmitted signal due to all K users in the channel is thus given by

$$s(t) = \sum_{k=0}^{K} s_k(t - \tau_k) h_k(t - \tau_k) \tag{5.13}$$

where $h_k(t)$ is the channel response associated with the kth user and is given by

$$h_k(t) = a_k(t) e^{j\phi_k(t)} \delta(t) \tag{5.14}$$

where $a_k(t)$ is the amplitude response of the channel and $\phi_k(t)$ is the phase response associated with it. The received signal is given by

$$
\begin{aligned}
r(t) &= s(t) + n(t) \\
&= \sum_{k=0}^{K} s_k(t-\tau_k) h_k(t-\tau_k) + n(t) \\
&= \sum_{k=0}^{K} \sqrt{2P_k} b_k(i_k) h_k(t-\tau_k) c_k(t-iT_b-\tau_k) \cos(\omega_c t(t-\tau_k)) + n(t)
\end{aligned}
\tag{5.15}
$$

where $i_k = \left\lfloor \frac{(t-\tau k}{Tb}) \right\rfloor$ and $n(t)$ is complex base band additive white Gaussian noise with zero mean and pass band two-sided power spectral density $N_0/2$.

5.3.2 Proposed Structure

In this work, we have introduced a block for non-linear LMS for update of the delay as shown in Figure (5.5). The two channels, an early and a late channel, are used for the purpose of delay adjustment. Each channel has a bank of matched filter (MF) and a multiuser interference estimation block shown in Figure (5.6). The top channel is called the early channel as the relative delay to the MF bank is "earlier than" the estimated delay $\hat{\tau}$. Similarly, the other channel is called the late channel as the relative delay to the MF bank is "delayed than" the estimated delay $\hat{\tau}$.

Figure (5.5) shows how estimated delay $\hat{\tau}$ can be used to generate the early $\hat{M}^e(i)$ and the late $\hat{M}^l(i)$estimated interference from K-1 users, respectively.

Let $Z_k^e(i)$ and $Z_k^l(i)$, respectively, represent the output of early and late matched filters as shown in Figure (5.5). Thus, for the kth user can be obtained by taking real part of the matched filter operation using kth user's spreading waveform as follows:

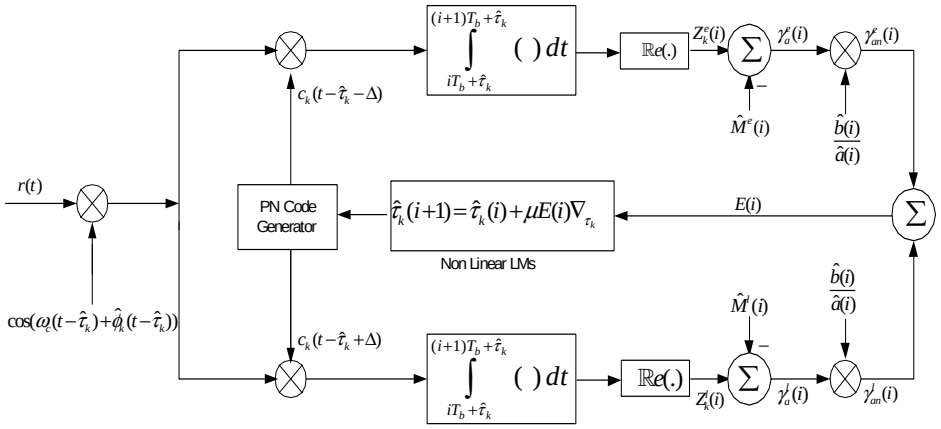

Figure 5.5: proposed early late delay tracking structure

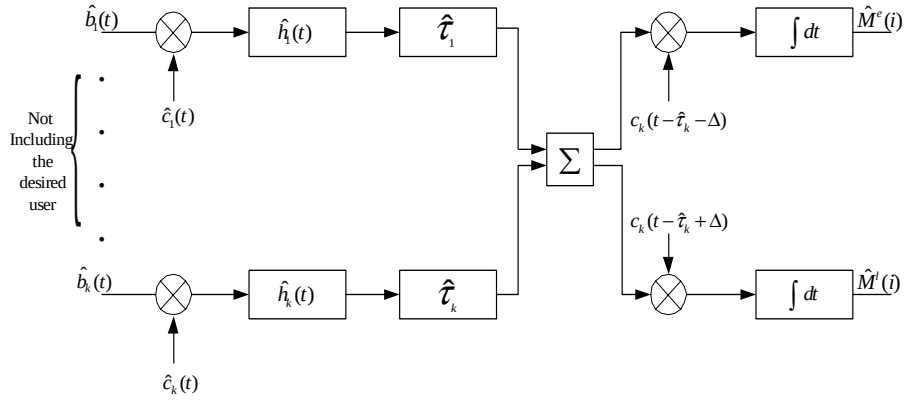

Figure 5.6: $\hat{M}^e(l)$ and $\hat{M}^l(l)$ estimation block

$$Z_k^e(i) = \mathbb{R}e\left\{\frac{1}{T_b}\int_{iT_b+\hat{\tau}_k}^{(i+1)T_b+\hat{\tau}_k} r(t)c_k(t-\hat{\tau}_k-\Delta)\cos(\omega_c(t-\hat{\tau}_k)+\phi_k(t-\hat{\tau}_k))\,dt\right\}$$
$$= \sqrt{\frac{P_k}{2}}b_k(i_k)a_k(i_k)R_{kk}^e(i) + \sum_{\substack{m=0\\m\neq k}}^{k}\sqrt{\frac{P_m}{2}}b_m(i_m)a_m(i_m)R_{mk}^e(i) + n^e(i) \tag{5.16}$$

for the early channel where $i_k = \left\lfloor \frac{t-T_b}{\tau_k} \right\rfloor$. Here $R_{kk}^e(i)$ and $R_{km}^e(i)$, respectively, represent the early auto correlation of the kth user and early cross-correlation of the kth and mth user, that is,

$$R_{kk}^e(i) = \frac{1}{T_b}\int_{iT_b+\hat{\tau}_k}^{(i+1)T_b+\hat{\tau}_k} c_k(t-\tau_1)c_k(t-\hat{\tau}_k-\Delta)\cos(\omega_c(t-\tau_k)+\phi_k(t-\tau_k))$$
$$\times\cos(\omega_c(t-\hat{\tau}_k)+\phi_k(t-\hat{\tau}_k))dt \tag{5.17}$$

$$R_{km}^e(i) = \frac{1}{T_b}\int_{iT_b+\hat{\tau}_k}^{(i+1)T_b+\hat{\tau}_k} c_k(t-\tau_m)c_k(t-\hat{\tau}_k-\Delta)\cos(\omega_c(t-\tau_m)+\phi_m(t-\tau_m))$$
$$\times\cos(\omega_c(t-\hat{\tau}_k)+\phi_k(t-\hat{\tau}_k))dt \tag{5.18}$$

Similarly, for the late channel, $Z_k^l(i)$, $R_{kk}^l(i)$ and $R_{km}^l(i)$ can be obtained as follows:

$$Z_k^l(i) = \mathbb{R}e\left\{\frac{1}{T_b}\int_{iT_b+\hat{\tau}_k}^{(i+1)T_b+\hat{\tau}_k} r(t)c_k(t-\hat{\tau}_k-\Delta)\cos(\omega_c(t-\hat{\tau}_k)+\phi_k(t-\hat{\tau}_k))\,dt\right\}$$
$$= \sqrt{\frac{P_k}{2}}b_k(i_k)a_k(i_k)R_{kk}^l(i) + \sum_{\substack{m=0\\m\neq k}}^{k}\sqrt{\frac{P_m}{2}}b_m(i_m)a_m(i_m)R_{mk}^l(i) + n^l(i) \tag{5.19}$$

for the early channel where $i_k = \left\lfloor \frac{t-T_b}{\tau_k} \right\rfloor$, where

$$Z_k^l(i) = \mathbb{R}e\left\{\frac{1}{T_b}\int_{iT_b+\hat{\tau}_k}^{(i+1)T_b+\hat{\tau}_k} r(t)c_k(t-\hat{\tau}_k+\Delta)\cos(\omega_c(t-\hat{\tau}_k)+\phi_k(t-\hat{\tau}_k))\,dt\right\}$$
$$= \sqrt{\frac{P_k}{2}}b_k(i_k)a_k(i_k)R_{kk}^l(i) + \sum_{\substack{m=0\\m\neq k}}^{k}\sqrt{\frac{P_m}{2}}b_m(i_m)a_m(i_m)R_{mk}^l(i) + n^l(i) \tag{5.20}$$

$$R_{kk}^l(i) = \frac{1}{T_b}\int_{iT_b+\hat{\tau}_k}^{(i+1)T_b+\hat{\tau}_k} c_k(t-\tau_1)c_k(t-\hat{\tau}_k+\Delta)\cos(\omega_c(t-\tau_k)+\phi_k(t-\tau_k))$$
$$\times\cos(\omega_c(t-\hat{\tau}_k)+\phi_k(t-\hat{\tau}_k))dt \tag{5.21}$$

$$R_{mk}^l(i) = \frac{1}{T_b}\int_{iT_b+\hat{\tau}_k}^{(i+1)T_b+\hat{\tau}_k} c_k(t-\tau_m)c_k(t-\hat{\tau}_k+\Delta)\cos(\omega_c(t-\tau_m)+\phi_m(t-\tau_m))$$
$$\times\cos(\omega_c(t-\hat{\tau}_k)+\phi_k(t-\hat{\tau}_k))dt \tag{5.22}$$

The adjusted matched filter output for the early channel may be expressed as

$$\begin{aligned}\gamma_a^e(i) &= Z_k^e(i) - \hat{M}^e(i) \\ &\approx z^e(i) + \sqrt{\frac{P_k}{2}} b_k(i_k) a_k(i_k) R_{kk}^e(i)\end{aligned} \tag{5.23}$$

Similarly, for the late channel, we have

$$\begin{aligned}\gamma_a^l(i) &= Z_k^l(i) - \hat{M}^l(i) \\ &\approx z^l(i) + \sqrt{\frac{P_k}{2}} b_k(i_k) a_k(i_k) R_{kk}^l(i)\end{aligned} \tag{5.24}$$

Let $\hat{a}^e(i)$ and $\hat{a}^l(i)$ be the estimated complex amplitudes for the early and late channels, with $\hat{b}^e(i)$ and $\hat{b}^l(i)$ be the estimated symbols, then normalized adjusted output is

$$\gamma_{na}^e(i) = \frac{\gamma_a^e(i)}{\hat{a}^e(i)} \tag{5.25}$$

and

$$\gamma_{na}^l(i) = \frac{\gamma_a^l(i)}{\hat{a}^l(i)} \tag{5.26}$$

The error signal between early and late estimate of the desired symbol is given by

$$
\begin{aligned}
E(i) &= \gamma_{na}^{e}(i)\hat{b}^{e}(i) - \gamma_{na}^{l}(i)\hat{b}^{i}(i) \\
&= \sqrt{\frac{P_k}{2}} b_k(i)\hat{b}^{e}(i)\frac{a_k(i)}{\hat{a}_k(i)} R_{kk}^{e}(i) - \sqrt{\frac{P_k}{2}} b_k(i)\hat{b}^{l}(i)\frac{a_k(i)}{\hat{a}_k(i)} R_{kk}^{l}(i) + \tilde{n}(i)
\end{aligned}
\tag{5.27}
$$

with

$$
\tilde{n}(i) = n^{e}(i) - n^{l}(i)
$$

if the amplitude and data bits are estimated close enough for each channel, then

$$
\begin{aligned}
\frac{a^{e}(i)}{\hat{a}^{e}(i)} &\approx 1, \\
\frac{a^{l}(i)}{\hat{a}^{l}(i)} &\approx 1
\end{aligned}
$$

and

$$
\begin{aligned}
b^{e}(i)\hat{b}^{e}(i) &\approx 1, \\
b^{l}(i)\hat{b}^{l}(i) &\approx 1
\end{aligned}
$$

so that

$$
\begin{aligned}
E(i) &= \gamma_{na}^{e}(i) - \gamma_{na}^{l}(i) \\
&\approx \sqrt{\frac{P}{2}} R_{kk}^{e}(i) - \sqrt{\frac{P}{2}} R_{kk}^{l}(i) + \tilde{n}(i)
\end{aligned}
\tag{5.28}
$$

which represents the error signal between early and late channels.

Derivation of Blind Non Linear LMS

This algorithm is termed as blind non-linear LMS algorithm as it does not have desired output available to calculate the update error and it has non-linearity because the delay is inside the cosine function. According to well known steepest descent approach, the LMS-type algorithm for the update of the delay estimate can be set up as follows

$$\hat{\tau}_k(i+1) = \hat{\tau}_k(i) + \mu \nabla_{\hat{\tau}_k}(J) \tag{5.29}$$

where μ is defined as the step size and J represents the cost function to be minimized which is chosen as the square of the error signal $E(i)$ and is given by

$$\begin{aligned} \mathrm{J} &= \mathrm{E}[E^2(i)] \\ \nabla_{\hat{\tau}_k} \mathrm{J} &= \frac{\partial}{\partial \hat{\tau}_k} \mathrm{J} \\ &= 2E(i) \frac{\partial}{\partial \hat{\tau}_k} E(i) \\ &= 2E(i) \left[R_{kk}^{e\,'}(i) - R_{kk}^{l\,'}(i) \right] \end{aligned} \tag{5.30}$$

The above equation involves the differentiation of early and late auto correlation of the kth user. For the purpose of differentiation, we use [85],

$$\frac{d}{da} \int_{\psi(a)}^{\varphi(a)} f(x,a)dx = f(\varphi(a),a)\frac{d\varphi(a)}{da} - f(\psi(a)\frac{d\psi(a)}{da} + \int_{\psi(a)}^{\varphi(a)} f(x,a)dx \tag{5.31}$$

we may write the above formula as the sum of three terms given by

$$I = I_1 + I_2 + I_3$$

where

$I_1 = f(\varphi(a), a)\frac{d\varphi(a)}{da}$, $I_2 = -f(\psi(a)\frac{d\psi(a)}{da}$, $I_3 = \int_{\psi(a)}^{\varphi(a)} f(x, a)dx$

and for the differentiation of cosine terms we have used the approach of [81]. For the early channel

$$\begin{aligned} R_{kk}^{e\,'}(i) &= \frac{\partial}{\partial \hat{\tau}_k} R_{kk}^{e}(i) \\ &= \frac{\partial}{\partial \hat{\tau}_k}\left\{\frac{1}{T_b}\int_{iT_b+\hat{\tau}_k}^{(i+1)T_b+\hat{\tau}_k} c_k(t-\tau_1)c_k(t-\hat{\tau}_k-\Delta)\cos(\omega_c(t-\tau_k)+\phi_k(t-\tau_k))\times\cos(\omega_c(t-\hat{\tau}_k)+\phi_k(t-\hat{\tau}_k))dt\right\} \end{aligned} \tag{5.32}$$

After applying the (5.31) we get I_1^e,I_2^e and I_3^e given by the following expressions

$$I_1^e = \left\{c_k(iT_b+\hat{\tau}_k-\tau_k)c_k(iT_b-\Delta)\cos(\omega_c(iT_b+\hat{\tau}_k-\tau_k)+\phi_k(iT_b+\hat{\tau}_k-\tau_k))\times\cos(\omega_c(iT_b)+\phi_k(iT_b))\right\}$$

$$I_2^e = -\begin{Bmatrix} c_k((i+1)T_b+\hat{\tau}_k-\tau_k)c_k((i+1)T_b-\Delta)\times\cos(\omega_c((i+1)T_b+\hat{\tau}_k-\tau_k)+\phi_k((i+1)T_b+\hat{\tau}_k-\tau_k))\times \\ \cos(\omega_c(i+1)T_b+\phi_k(i+1)T_b) \end{Bmatrix}$$

and

$$I_3^e = \int_{iT_b+\hat{\tau}_k}^{(i+1)T_b+\hat{\tau}_k} c_k(t-\tau_k)Sign\left\{c_k(t-\lceil \hat{\tau}_k \rceil-\Delta)-c_k(t-\lfloor \hat{\tau}_k \rfloor-\Delta)\right\}dt$$

Hence for the early channel

$$I^e = I_1^e + I_2^e + I_3^e$$

Similarly for the late channel

$$\begin{aligned} R_{kk}^{l\,'}(i) &= \frac{\partial}{\partial \hat{\tau}_k} R_{kk}^l(i) \\ &= \frac{\partial}{\partial \hat{\tau}_k}\left\{\frac{1}{T_b}\int_{iT_b+\hat{\tau}_k}^{(i+1)T_b+\hat{\tau}_k} c_k(t-\tau_m)c_k(t-\hat{\tau}_k+\Delta)\cos(\omega_c(t-\tau_m)+\phi_m(t-\tau_m))\times\cos(\omega_c(t-\hat{\tau}_k)+\phi_k(t-\hat{\tau}_k))dt\right\} \end{aligned} \tag{5.33}$$

After applying the (5.31) we get I_1^l,I_2^l and I_3^l given by the following expressions

$$I_1^l = \left\{c_k(iT_b+\hat{\tau}_k-\tau_k)c_k(iT_b+\Delta)\cos(\omega_c(iT_b+\hat{\tau}_k-\tau_k)+\phi_k(iT_b+\hat{\tau}_k-\tau_k))\times\cos(\omega_c(iT_b)+\phi_k(iT_b))\right\}$$

$$I_l^2 = -\left\{\begin{matrix} c_k((i+1)T_b+\hat{\tau}_k-\tau_k)c_k((i+1)T_b+\Delta)\times\cos(\omega_c((i+1)T_b+\hat{\tau}_k-\tau_k)+\phi_k((i+1)T_b+\hat{\tau}_k-\tau_k))\times \\ \cos(\omega_c(i+1)T_b+\phi_k(i+1)T_b) \end{matrix}\right\}$$

and

$$I_l^3 = \int_{iT_b+\hat{\tau}_k}^{(i+1)T_b+\hat{\tau}_k} c_k(t-\tau_k) Sign\left\{c_k(t-\lceil \hat{\tau}_k \rceil + \Delta) - c_k(t-\lfloor \hat{\tau}_k \rfloor + \Delta)\right\} dt$$

Hence for the early channel

$$I^l = I_1^l + I_2^l + I_3^l$$

So (5.30) can be written as

$$\nabla_{\hat{\tau}_k} \mathrm{J} = 2E(i)\left[I^e - I^l\right] \tag{5.34}$$

so the delay update is adjusted by an amount that is proportional to the error $E(i)$.

5.4 Simulation Results

The following parameters have been used for the simulation of the proposed receiver. PN code synchronization follows a procedure of combined tracking/reacquisition/tracking, etc., after an initial acquisition. That is, during tracking whenever $|\varepsilon_l| > \varepsilon_{\max} > 0$, a new acquisition will be initiated and a new tracking follows. This value is set to $\varepsilon_{\max} = 0.5$. The spreading code is 128. We have simulated signals in a Rayleigh fading channel with two path channel from MS to BS. We have assumed that the initial time

estimates are available from the acquisition stage within half of Tc. Since the proposed structure is to be employed in the multiuser radiolocation, we have simulated system with 10 users in a cellular network. Due to power control in CDMA systems, all mobiles are received with nearly the same power. But the same is not true for the neighboring base stations. An MS served by the first base station can be received at much lower power compared than the MS's belonging to that neighboring cell. In fact, only when the mobile to be located is in a soft handover with one or more neighbor cells, its received power is relatively close to the serving cell. The TOA measurements strongly depend on the received MAI level.

First we consider the accuracy of DLL-based TOA estimation for two different cases as shown in Figure (5.7). The histogram of the residual timing error at the mobile serving base station shown in (a) is compared with that of non serving BS. It can be seen that the DLL timing error remains unaffected with timing error distributed over $\pm T_c/2$ which is the same as initially assumed after the acquisition stage

When we compare the timing error for the SIC based DLL structure we immediately see improved results. This has been shown in the following Figures (5.8). The timing error for the serving BS is almost the same as in the previous case. But there is significant improvement with the timing error converging to zero for the non serving mobiles. Similarly, the normalized timing error for the early-late delay tracker integrated with the receiver structure in Figure (5.3) has been shown in Figure (5.9). Here the system model consists of five users of equal power and we display the timing

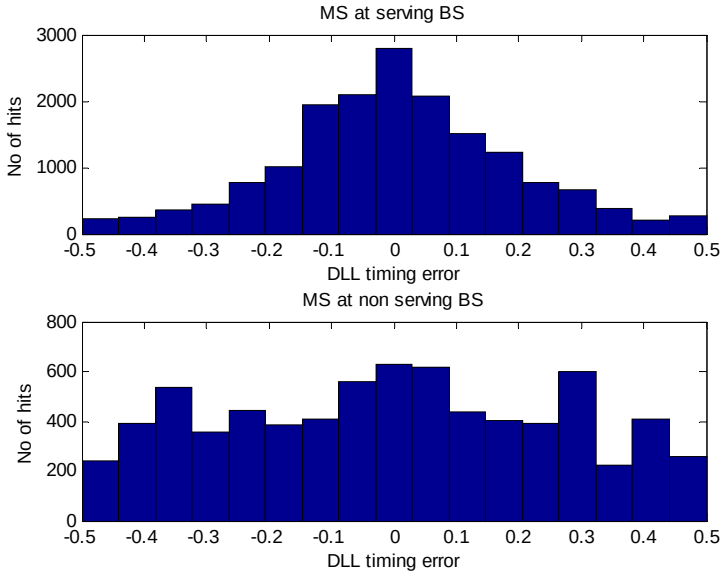

Figure 5.7: Histograms for PDF's of DLL timing error (normalized by Tc) for two cases: a) mobile received at serving BS, and b) at non-serving BS

error for an MS in the serving BS. The timing estimate is seen to have improved when compared with Figure (5.7). These timing estimates will improve the TOA based mobile location as we will discuss it in the next chapter.

Chapter Summary

In this chapter we looked into the performance of the new proposed DLL employing SIC structure to cancel the users progressively to enhance the timing estimate of the weak user. A comparison with the classical DLL was made to show that the proposed SIC based DLL is able to track the weaker users in a multiuser environment. In the next chapter we will use the time estimates obtained from the methods described in the previous two chapters to estimate the MS in a cellular network.

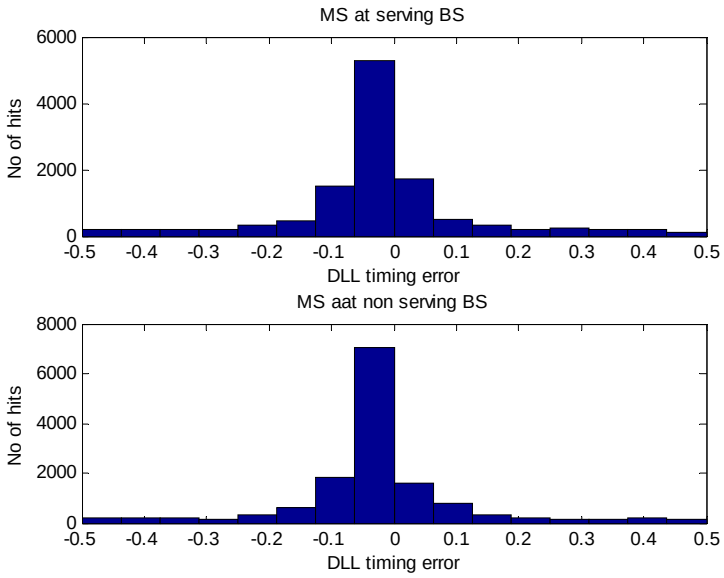

Figure 5.8: Histograms for PDF's of SIC based DLL timing error (normalized by Tc) for two cases: a) mobile received at serving BS, and b) at non-serving BS

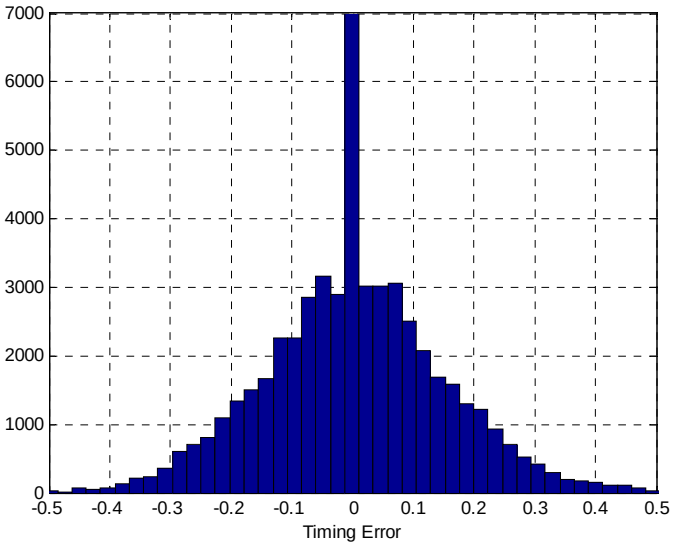

Figure 5.9: Histogram of the timing error for MS in serving BS in five user two path model for early late tracking algorithm

Chapter 6

Radiolocation based on Time of Arrival Techniques

For network-based wireless location systems, different data fusion techniques are used that combine data from multiple sources and gather that information in order to achieve inferences, which will be more efficient and potentially more accurate when compared if they were achieved by means of a single source. The time of arrival (TOA) and time difference of arrival (TDOA) are two time-based measures usually used in calculating the location of a mobile station. In this chapter we present and evaluate a method for accurate TOA estimation in a multiuser multipath fading channels for positioning purposes.

6.1 Approximate Maximum Likelihood Algorithm

The focus of our research is based on TOA using the first arriving path delay estimate. Radiolocation involves measuring the distance between an MS and a BS finding the one-way propagation time between an MS and BS. This distance is given by the time multiplied by the speed of light ($c = 3 \times 10^8$m/s). Geometrically, it results in a circle, centered at the BS. Localization in two-dimensions (2-D) requires at least three BS's and the MS is located at the intersection of these circles as shown in Figure (2.5). However,due to noise, interference and synchronization problems, the three circles may not intersect at a single point making it necessary to find an estimate of the emitter location that minimizes the inconsistencies. For TOA , the localization equations are nonlinear. The standard solution is linearization followed by gradient searches. They suffer from initial condition sensitivity and convergence problems. This lead some researchers to develop closed-form linear techniques which can give optimum location estimates only at high signal-to-noise (SNR) ratio Finding the maximum likelihood (ML) estimates source location corresponds to solving a nonlinear maximization problem. This procedure can be computationally expensive. A suboptimal solution known as Approximate Maximum Likelihood (AML) algorithm has shown to be computationally cheaper and easier to implement [87]. It begins with the ML equations,changing them into two linear equations in the unknown (x,y), whose coefficients are also dependent on (x,y). Then, with some initial values of (x, y), it solves the linear equations for new (x, y) and updates their coefficients. It has been shown

in [87] that minimum solution is obtained after five updates. AML will constitute our TOA based radiolocation in this chapter.

The initial estimate is obtained by using the least squares solution as given by (2.13) is

$$\hat{\mathbf{x}} = (\mathbf{H}^T\mathbf{H})^{-1}\mathbf{H}^T\mathbf{b} \tag{6.1}$$

Hence the estimated mobile location is given by $\hat{\mathbf{x}}$ in the above equation.

The MS position estimate can further be refined by using approximate likelihood algorithm (AML) and the subsequent mathematical derivation for AML has been taken from [86]. We start with the estimate obtained from LS method as an initial measured distance given by

$$\begin{aligned} d_i &= \sqrt{(x-x_i)^2+(y-y_i)^2} + \epsilon_i \qquad i = 1, 2, .., N \\ &= R_i + \epsilon_i \end{aligned}$$

where R_i is the true distance between BS_i and MS, and ϵ_i is the measurement noise in the ith estimation. The vector form of the measured distance can be written as

$$\mathbf{D} = \mathbf{R} + \boldsymbol{\epsilon} \tag{6.2}$$

The TOA measurements can be obtained by dividing $\mathbf{D}$ by the speed of light c

$$\mathbf{T} = \frac{\mathbf{D}}{c} + \frac{\boldsymbol{\epsilon}}{c} \tag{6.3}$$

where $\boldsymbol{\epsilon}$ is a vector of additive measurement errors. The elements of $\boldsymbol{\epsilon}$ are independent, zero mean Gaussian random variables with covariance matrix

$$\mathbf{Q} = E\{\boldsymbol{\epsilon}\boldsymbol{\epsilon}^T\} = diag\{\sigma^2....\sigma^2\}$$

and

$$\mathbf{D} = [d_1 \ ... \ d_N]^T = \mathbf{D}(\boldsymbol{\theta})$$

The probability density function (pdf) [87] of $\mathbf{T}$ given θ is given by

$$f(\mathbf{T}/\boldsymbol{\theta}) = (\boldsymbol{2\pi})^{\frac{N}{2}} (\det \mathbf{Q})^{\frac{1}{2}} \exp\{-\frac{J}{2}\} \tag{6.4}$$

where

$$J = \left[\mathbf{T} - \frac{\mathbf{D}(\boldsymbol{\theta})}{c}\right]^T \mathbf{Q}^{-1} \left[\mathbf{T} - \frac{\mathbf{D}(\boldsymbol{\theta})}{c}\right] \tag{6.5}$$

The ML estimate is the $\boldsymbol{\theta}$ that minimizes J. Minimizing J is done by setting the gradient of J with respect to $\boldsymbol{\theta}$ to zero, gives the two ML equations,

$$\begin{aligned} \sum_{i=1}^{N} \frac{(R_i - d_i)(x - x_i)}{R_i} &= 0 \\ \sum_{i=1}^{N} \frac{(R_i - d_i)(y - y_i)}{R_i} &= 0 \end{aligned} \tag{6.6}$$

an ordinary LS solution would suffice if (6.6) were is linear. But if they are non-linear, AML provides the solution. Substituting

$$(R_i - d_i) = \frac{(R_i - d_i)^2}{(R_i + d_i)^2}$$

into (6.6)

$$\begin{aligned} \sum_{i=1}^{N} \frac{(R_i^2 - d_i^2)(x - x_i)}{R_i(R_i + d_i)} &= 0 \\ \sum_{i=1}^{N} \frac{(R_i^2 - d_i^2)(y - y_i)}{R_i(R_i + d_i)} &= 0 \end{aligned} \tag{6.7}$$

Expanding (6.7) into matrix form, we get

$$2 \begin{bmatrix} \sum g_i x_i & \sum g_i y_i \\ \sum h_i x_i & \sum h_i y_i \end{bmatrix} \begin{bmatrix} x_m \\ y_m \end{bmatrix} = \begin{bmatrix} \sum g_i (s + k_i - d_i^2) \\ \sum h_i (s + k_i - d_i^2) \end{bmatrix} \tag{6.8}$$

$$g_i = \frac{x_m - x_i}{R_i(R_i + d_i)}, \qquad h_i = \frac{y_m - y_i}{R_i(R_i + d_i)}, \qquad s = x_m^2 + y_m^2, \qquad k_i = x_i^2 + y_i^2$$

We can write (6.8) as

$$\mathbf{A}\boldsymbol{\theta} = \mathbf{b} \tag{6.9}$$

Using the LS estimate gives values of $\mathbf{A}$ and $\mathbf{b}$ produces a new value of θ to update $\mathbf{A}$ and $\mathbf{b}$ and then $\boldsymbol{\theta}$. This procedure, called the approximate ML (AML) estimator [85], stops after five updates and takes the $\boldsymbol{\theta}$ that gives the smallest J as the solution. This ensures that AML will not diverge, and will, at worst, have the errors of the linear estimator. Simulation results in [87] show that the AML actually attains the Cramer–Rao lower bound (CRLB).

6.2 Cellular RF Network Modeling & Analysis

For the purpose of evaluating the effects of MAI on radiolocation, we consider a cellular network consisting of a central cell with three tiers of surrounding cells as illustrated in Figure (6.1). Each of the BS has an omni-directional antenna in the center with mobile users assumed to be uniformly distributed across the network coverage area [86].

The signal propagating from the MS to each of the BS$_i$ ($i = 1, 2, ..., N$) undergoes

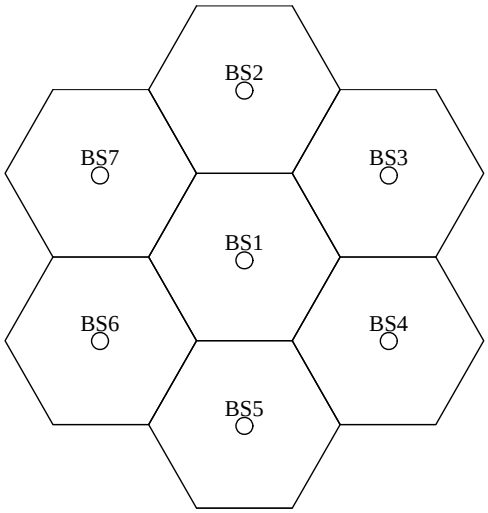

Figure 6.1: Cellular network

attenuation including distance path loss and lognormal shadowing. The radio channel is modelled as [86],

$$\alpha(d_{BS_i}, \xi_{BS_i}) = p(d_{BS_i}) 10^{\xi_{BS_i}/10} \tag{6.10}$$

where $p(d)$ is the distance path loss, and $\xi_{BS_i}$is the shadowing variable. The path loss part follows a two-segment model with breakpoint at d_o [86],

$$p(d) = 10n \log_{10}(d) \tag{6.11}$$

where n is the path loss slope assumed to take two different values, depending on whether the mobile is within or beyond the given breakpoint. In simulations, we have used the slopes $n = 2$, and a breakpoint at 200m, with a cell radius of 2km.

Since CDMA systems employ power control mechanisms, at a given base station of interest termed as the "serving" base station, all mobiles are received with nearly the same power (we later assume it to be same, i.e., perfect power control). However, at neighboring base stations, a given mobile served by the first base station can be received at much lower power compared to the mobiles belonging to that neighboring cell. In fact, only when the mobile to be located is in a soft-handover with one or more neighbor cells, its received power is relatively close to the original cell.

Since time-of-arrival estimation accuracy strongly depends on the received MAI levels, this issue can be a limiting factor in mobile radiolocation which typically requires TOA data from at least three base stations. For example, if we assume that the mobile is served by the center base station BS_1 and will be radiolocated by the strongest seven base stations BS_1, BS_2,..., BS_7 (sorted in a descending order from the base station that receives the highest average received power), then we define the ratio of its average received power at BS_i compared to BS_1as [86],

$$\beta_i = \mathbf{P}_i/\mathbf{P}_1 \tag{6.12}$$

where P_i is the received power in BS_i and $\beta_1 = 1 \geq \beta_2 \geq \beta_3 \geq \cdots \geq \beta_7$

It is found that this ratio can fluctuate widely depending on the mobile position relative to the base stations of interest. As an illustration, we present examples for four scenarios that will be used in the subsequent numerical results [86,88].

Case-1 refers to a mobile located anywhere in the central cell BS1 (the mobile

	β_1	β_2	β_3	β_4	β_5	β_6	β_7
Case 1	1	0.1412	0.0629	0.0343	0.0212	0.0140	0.0095
Case 2	1	0.0216	0.0113	0.0069	0.0045	0.0031	0.0021
Case 3	1	0.6982	0.2215	0.1202	0.0735	0.0485	0.0331
Case 4	1	0.7922	0.6353	0.2993	0.1701	0.1065	0.0706
the averages of the β - factors for various soft-handover link conditions when the shadowing standard deviation $\sigma_{sh} = 8$ dB and the cell radius is 2km [86]							

Table 6.1: Averages of the beta factors[86]

serving base station).

Case-2 refers to a mobile in close proximity to its "serving" BS1, with a signal at least 10dB above that at the other two base stations.

Case-3 represents a two-way soft handover scenario, with the mobile power at base station 2 within 3dB (as an example) from that at BS1, and

Case-4 denotes the 3-way soft handover situation where the mobile signal is within 3dB at both BS2 and BS3 compared to BS1

6.3 Simulation Results

For the purpose of radiolocation we consider the cellular network shown in Figure (6.1) and TOA algorithm described earlier with TOA estimates from UKF, DDF2 and SIC based DLL approach. We assume a uniformly loaded network, with 10 users per cell assuming a LOS path exists between an MS and the BS. We will show the cumulative distribution function (cdf) of the MS positioning error for the 4 cases when using the delay estimates for UKF, DDF, SIC based DLL and early late tracking loop integrated

with SIC.

Comparison between UKF and DDF

Figure (6.2) shows the cdf of positioning error when UKF-based delay estimates are used for positioning. It can be seen that positioning error is minimum for the case-4 where a 3-way soft handover condition exists followed by the positioning errors for the case 3 where a two-way handover scenario is considered. The positioning error is the highest for the case 2 when there is no handover. This is because when the MS is close to its serving BS (case-2), the weak MS signal at non serving BS results in poor timing estimates at those BSs which in turn translate into higher positioning errors. Similar observations can be made for the positioning error cdf for the case of DDF-based delay estimates are used for positioning as shown in Figure (6.3). The comparison of positioning error for the UKF and the DDF is shown for the 4-cases in Figures (6.4)-(6.7). These figures show that the performance of these two filters are comparable with UKF showing slightly better performance than the DDF. However, for the case 2, we see a deviation from this behavior when initially DDF performs slightly better than the UKF and after the crossover point the reversal in performance occurs for the two filters. This is the case when two non serving base stations are receiving relatively weak signals compared to the serving base station. Such a deviation is not observed for other cases and needs further investigation. In general the relative inferior performance of DDF compared to UKF may be attributed to the fact some of the higher order cross product terms (to avoid excessive computational cost) in

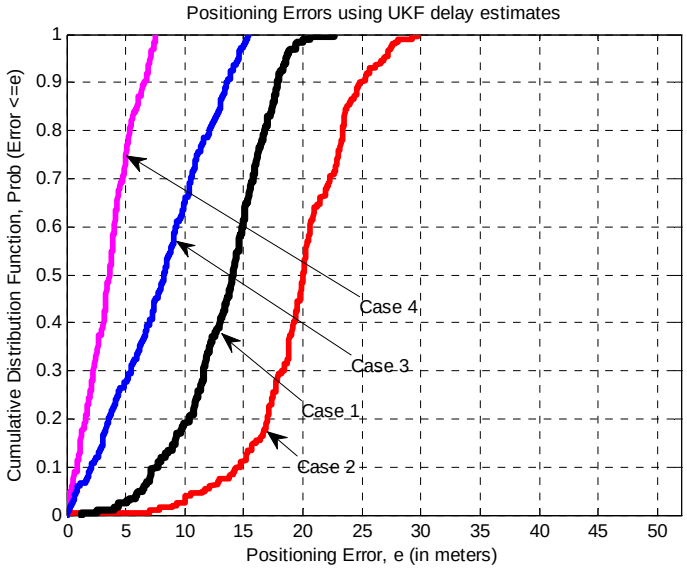

Figure 6.2: Cumulative distribution function (CDF) for the residual mobile positioning error for 4 cases using UKF

the derivation of the Sterling approximation estimate of the covariance are discarded [74,77].

Figure (6.8) shows the cdf of the MS positioning error for the SIC based DLL. It is clearly seen that the case for 3-way soft handover (case 4) gives the best performance, followed by 2-way soft handover one (case 3), followed by the case when the mobile is located anywhere is the serving BS (case 1). The positioning error is again the highest for case 2 when the MS is closest to its own base station. Figure (6.9) shows the positioning error cdf for the SIC based early late tracking loop. The error performance for the 4-cases is similar to the SIC based DLL with least positioning errors in 3-way soft handover (case 4) and worst when the MS is closest to its serving BS (case 2).

If we make a comparison of the positioning errors obtained from SIC-based DLL

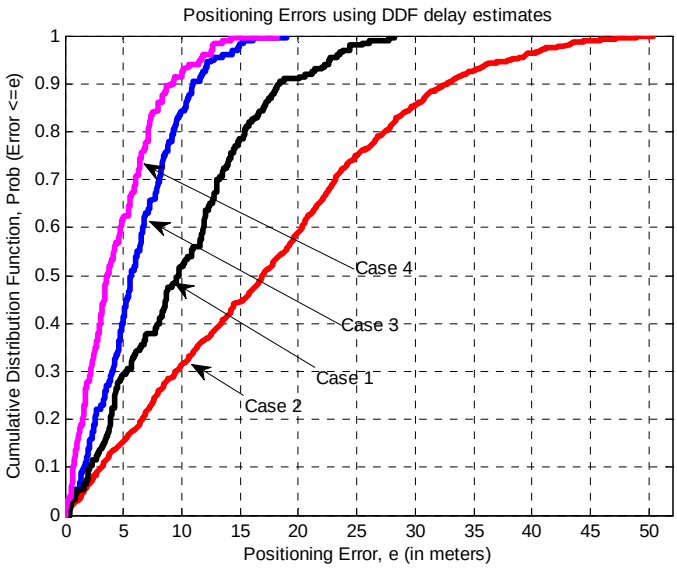

Figure 6.3: Cumulative distribution function (CDF) for the residual mobile positioning error for 4 cases using DDF

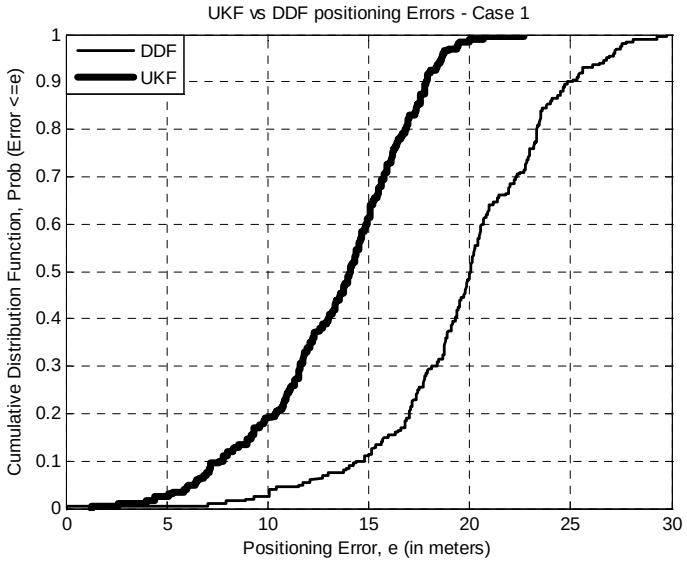

Figure 6.4: Comparison of cumulative distribution function (CDF) for the residual mobile positioning error for UKF and DDF - case 1

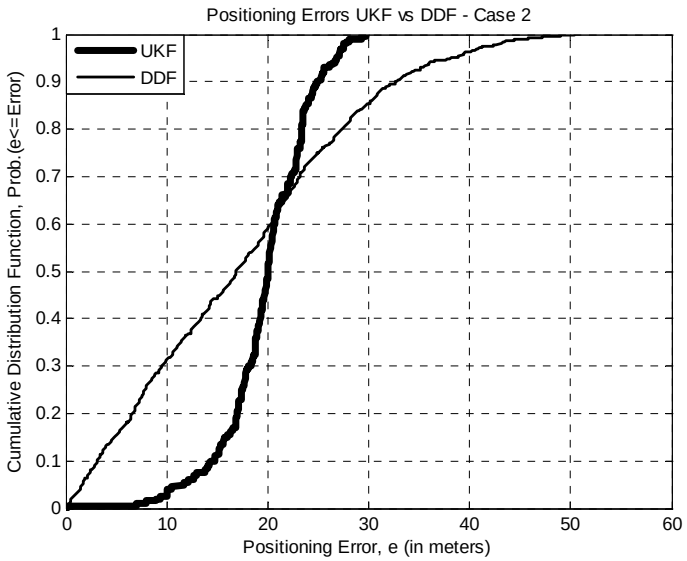

Figure 6.5: Comparison of cumulative distribution function (CDF) for the residual mobile positioning error for UKF and DDF - case 2

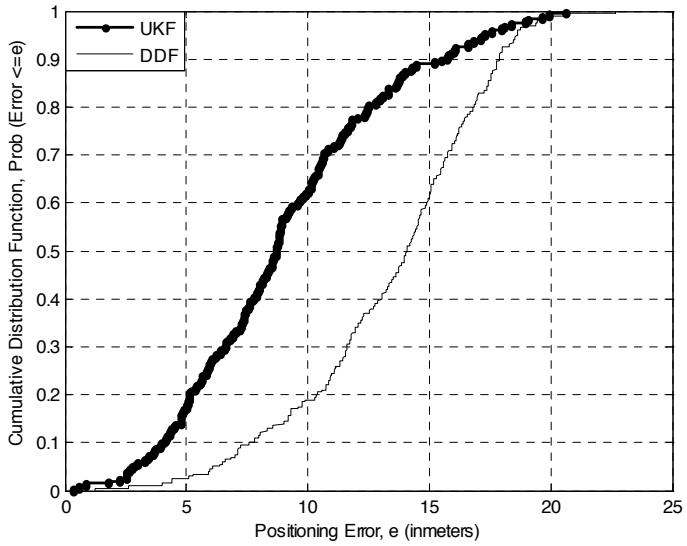

Figure 6.6: Comparison of cumulative distribution function (CDF) for the residual mobile positioning error for UKF and DDF - case 3

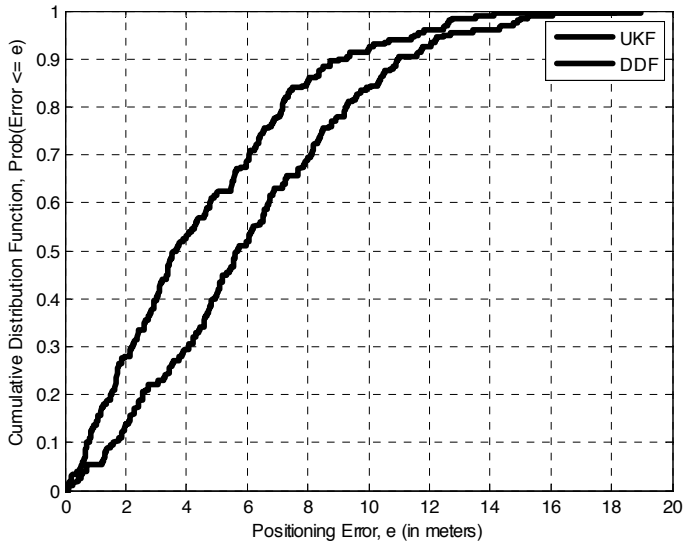

Figure 6.7: Comparison of cumulative distribution function (CDF) for the residual mobile positioning error for UKF and DDF - case 4

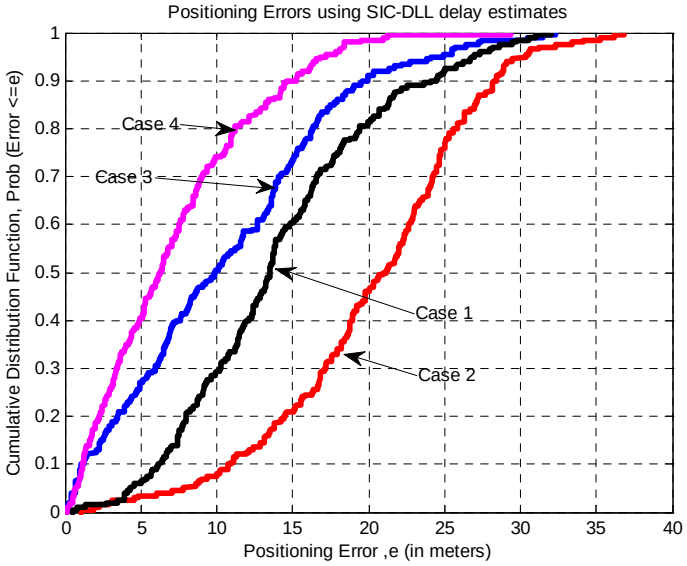

Figure 6.8: Cumulative distribution function (CDF) for the residual mobile positioning error using SIC-based DLL delay estimates

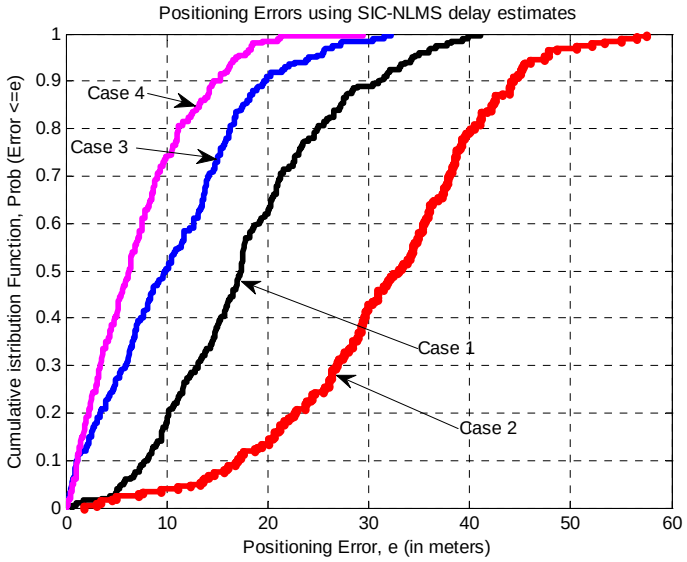

Figure 6.9: Cumulative distribution function (CDF) for the residual mobile positioning error using SIC-based early late delay tracking loop estimates

with early late tracking algorithm integrated with SIC shown in Figure (6.10), we see that the former performs better than the later.

Comparison between SIC based tracking loops

A comparison of the SIC based DLL with DLL without SIC is shown in Figure (6.10). It is seen that for the proposed receiver location error is below 36m 90% of time and it is 60m 60% of time for DLL with no interference cancellation. We see from all the figures the position location error increases as the MS approaches its serving BS (case-2). This is because the MS, closer to the serving BS, needs to transmit at lower power levels to maintain the fixed received power at the serving BS. We may also observe that as the distance to the neighboring BSs increases, the signal experiences greater path loss. So the received signal power at the neighboring

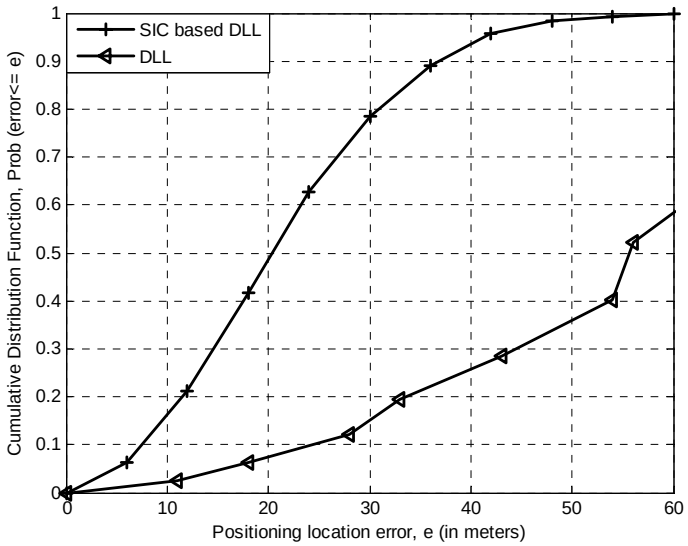

Figure 6.10: Comparison of cumulative distribution function (CDF) for the residual mobile positioning error for SIC-DLL and DLL without SIC

BSs reaches lower levels, making position location error to sharply rise. This in turn decreases the position location accuracy.

A comparison of the filtering based approaches with the SIC-based tracking approaches shows that the cdf of the positioning error for all 4 cases is the least when using UKF based delay estimates for positioning in a multiuser multipath environment. It verifies what has been stated in chapter 4 that UKF is near far resistant and accurately tracks multiuser parameters providing higher position accuracy when compared with other techniques considered in this thesis.

Effect of number of users per cell on the Radiolocation error

For the shadowing standard deviation $\sigma_s = 8dB$, we vary the number of users to investigate its effects on the radiolocation. The final results have been averaged over

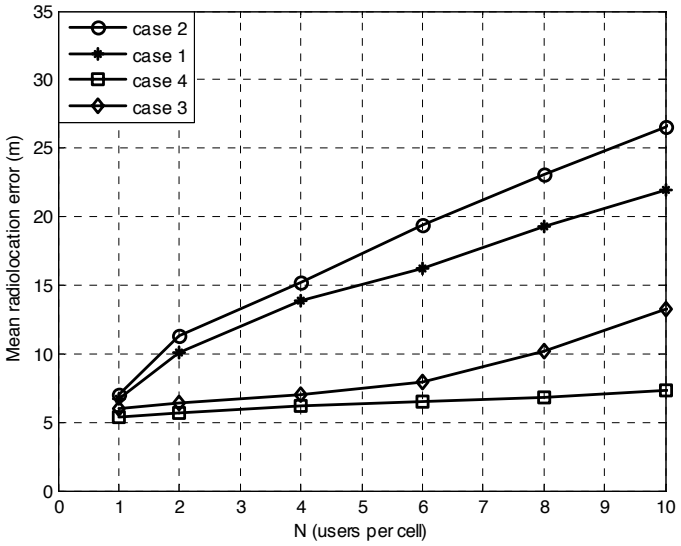

Figure 6.11: Mean positioning error vs number of users (UKF)

50 runs. It can be seen from Figures (6.11-6.14) that the positioning error increases with increasing number of users. This is because of the degradation of SNR with increasing number of users per cell. Again we observe that the positioning error is the lowest for the case of UKF and highest for the LMS-based tracking loop. The positioning error for the DDF and SIC based DLL lies between these two extremes.

Chapter Summary:

In this chapter we presented the performance of time of arrival based techniques for mobile positioning in CDMA cellular networks using approximate maximum likelihood. Firstly, we showed that delay estimates based on near far resistant SPKF

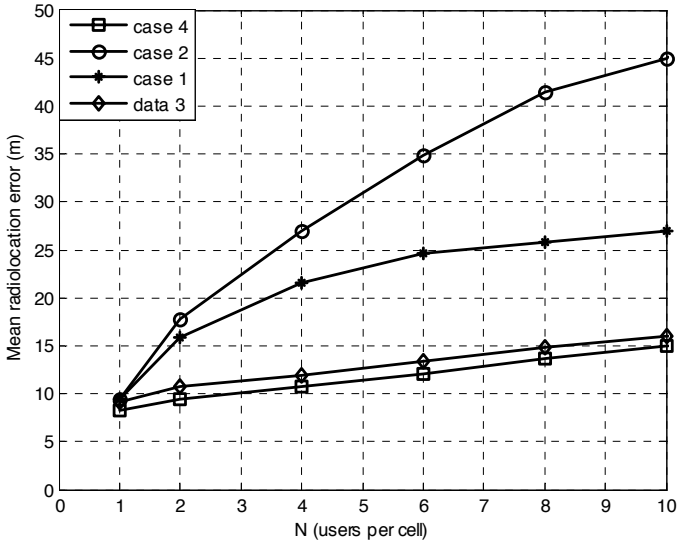

Figure 6.12: Mean radiolocation error vs number of users (DDF)

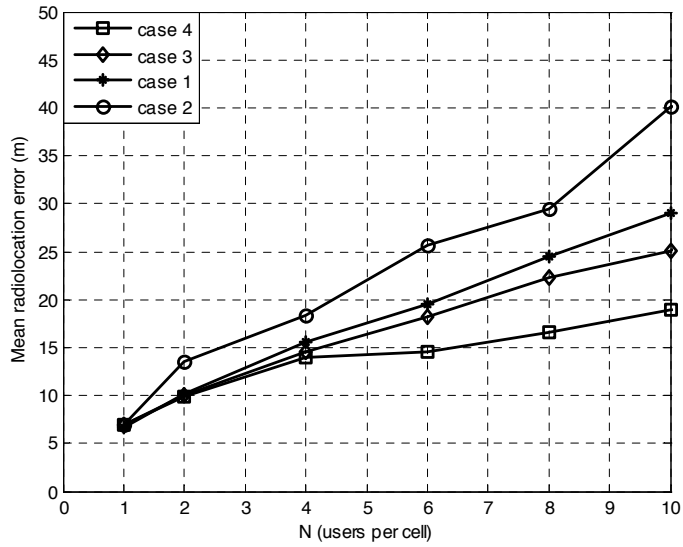

Figure 6.13: Mean positioning error vs number of users (SIC-based DLL)

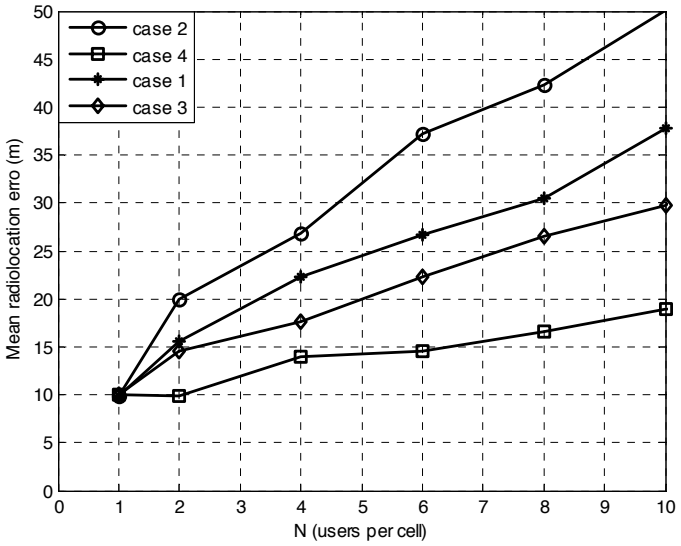

Figure 6.14: Mean positioning error vs number of users (ealry late tracking loop)

algorithms can be used to provide accurate positioning in a multiuser scenario. Secondly, the DLL and early late tracking loop combined with interference cancellation were used for TOA estimation. It was shown that MAI cancellation has a clear impact on the precision of mobile radiolocation, owing to the fact that, with interference cancellation the delay estimates will be improved which in turn lowers the positioning error. We showed through simulations that the proposed methods provide better location estimates than those obtained by using the classical DLL.

Chapter 7

Thesis Contributions and Recommendations for Future Work

7.1 Dissertation Contributions and Conclusions

In this work, we have developed delay estimators for the position location of mobile terminal in CDMA network using TOA. The focus has been on the parameter estimation in a multipath propagation channel with particular emphasis on the estimation of the first timing epoch. We assumed a LOS path exists between the MS and the BS. The major contributions of this dissertation are following:

The first part of this dissertation aims at estimating the multiuser parameter of the arriving signal. In this context we developed estimators based on the linear, linearized and the nonlinear filtering approaches. We obtained the multiuser parameters i.e.

channel coefficients and delays using EKF, DDF and UKF filtering methods. The algorithms have been evaluated through computer simulations. The Cramer Rao lower bound on the variance of the parameters error is also derived and compared with the simulation results. The analysis of the proposed parameters estimation is also provided.

The second part of this dissertation describes two new approaches for the delay estimation.

- The first approach is based on the DLL employing SIC. It estimates the stronger signal and cancels it successively from the received signal which in turn reduces the residual timing error of the weaker users.

- The second approach is based on an early late tracking loop. It employs a bank of matched filters where the loop time update is obtained using nonlinear LMS. Computer simulations have been performed and a relative comparison with the standard DLL has also been presented.

The third part deals with the multiuser radiolocation. In this context we have considered approximate maximum likelihood algorithm for the radiolocation. Different scenarios have been considered for the MS in the cellular network. A comprehensive comparison is provided to analyze these scenarios in terms of positioning errors. A comparison between filtering approach based radiolocation with the SIC-based tracking approaches has also been presented.

7.2 Recommendations for Future Work

There are few suggestions regarding the future works. In our work, we have assumed that LOS path is available from the MS to each of the BS involved in positioning. However this condition is not always true. All wireless communication systems suffer from NLOS problem and the measurements are biased in such an environment. Unless this bias is mitigated in some way, the location estimates will be far from the true values regardless of the accuracy of TOA estimates. This work can be extended by developing techniques to mitigate NLOS bias in location estimation.

Similarly, other grid based filtering approaches such as particle filters and its variant may be used for parameter estimation purposes and a comparison can be made with the filtering approaches considered in this thesis.

In this thesis we considered the impact of TOA estimation errors on the user location that was mainly characterized by extensive simulations. In future work, one could attempt to quantify analytically the relation between estimation by incorporating both TOA/AOA data and the cumulative distribution function of the location error.

The estimation techniques presented in thesis for user location estimation can be applied to wideband CDMA standards. In future work, one could study the effect of the enhancements they offer on the wireless location process and its accuracy.

A useful modification is to incorporate some scheme that adapts parameters depending on whether the MS being tracked represents a pedestrian, a vehicle on a

urban/suburban street or on a highway, etc. In this case the range measurements at each BS will vary with time. Thus we can have more than one independent range measurement at each BS, which in turn can used for better location estimation.

Appendix I.

Divided Difference Filter

Consider a nonlinear function, $y = \mathbf{h}(x)$ with a random variable x with mean $\bar{x}$ and covariance P_{xx}. The second order divided difference approximation of the function is formulated by using the vector form of Stirling's interpolation formula, which is similar to the extension of the Taylor series approximation [78-80]

$$y \simeq \mathbf{h}(\bar{x}) + \tilde{D}_{\Delta x}\mathbf{h} + \frac{1}{2!}\tilde{D}^2_{\Delta x}\mathbf{h} \tag{7.1}$$

Where the operators $\tilde{D}_{\Delta x}$ and $\tilde{D}^2_{\Delta x}$ are given by

Where the operators $\tilde{D}_{\Delta x}$ and $\tilde{D}^2_{\Delta x}$ are given by

$$\tilde{D}_{\Delta x}\mathbf{h} = \frac{1}{h}\left(\sum_{p=1}^{n} \Delta x_p \mu_p \delta_p\right)\mathbf{h}(\bar{x}) \tag{7.2}$$

$$\tilde{D}^2_{\Delta x}\mathbf{h} = \frac{1}{h^2}\left(\sum_{p=1}^{n} \Delta x_p^2 \delta_p^2 + \sum_{p=1}^{n}\sum_{q=1,p\neq q}^{n} \Delta x_p \Delta x_q (\mu_p \delta_p)(\mu_q \delta_q)\right)\mathbf{h}(\bar{x}) \tag{7.3}$$

where $\Delta x_p = (x - \bar{x})_p$ is the pth component of $x - \bar{x}$ and h is an interval of length, taken as $h = \sqrt{3}$ for a Gaussian distribution and δ_p and $\mu_p$denote the partial difference operator and the partial average operator respectively

$$\delta_p \mathbf{h}(\bar{x}) = \mathbf{h}\left(\bar{x} + \frac{h}{2}\mathbf{e}_p\right) - \mathbf{h}\left(\bar{x} - \frac{h}{2}\mathbf{e}_p\right) \tag{7.4}$$

$$\mu_p \mathbf{h}(\bar{x}) = \frac{1}{2}\left\{\mathbf{h}\left(\bar{x} + \frac{h}{2}\mathbf{e}_p\right) + \mathbf{h}\left(\bar{x} - \frac{h}{2}\mathbf{e}_p\right)\right\} \tag{7.5}$$

The following linear transformation of $\mathbf{x}$ is introduced to illustrate how others can be derived.

$$\mathbf{z} = \mathbf{S}_x^{-1}\mathbf{x}$$

where $\mathbf{S_x}$ is the Cholesky factor of the covariance matrix $\mathbf{P_{xx}}$. A new function $\tilde{h}$ is defined by

$$\tilde{\mathbf{h}}(z) \equiv \mathbf{h}(\mathbf{S}_x z) = \mathbf{h}(x)$$

The Taylor series approximation of $\tilde{\mathbf{h}}$ is identical to that of $\mathbf{h}$, while the interpolation formula does not yield the same results for $\tilde{\mathbf{h}}$ and $\mathbf{h}$ due to the following

$$2\mu_p\delta_p\tilde{\mathbf{h}}(\bar{z}) = \tilde{\mathbf{h}}(\bar{z}+h) - \tilde{h}(\bar{\mathbf{z}} - h\mathbf{e}_p) = h(\bar{\mathbf{x}} + \mathbf{s}_p) - h(\bar{\mathbf{x}} - h\mathbf{s}_p) \tag{7.6}$$

where $\mathbf{s}_p$ denotes the pth column of $\mathbf{S}_x$. Thus, $\tilde{D}_{\Delta x}\mathbf{h}$ and $\tilde{D}^2_{\Delta x}\mathbf{h}$ will be different from $\tilde{D}_{\Delta z}\tilde{\mathbf{h}}$ and $\tilde{D}^2_{\Delta z}\tilde{\mathbf{h}}$.

Unscented Kalman Filter (UKF)

Consider a nonlinear function

$$\mathbf{y} = \mathbf{h}(\mathbf{x}) \tag{7.7}$$

We expand $\mathbf{h}(x)$ in a Taylor series around some nominal operating point $x = \bar{x}$, defining deviation from mean as $\tilde{x} = x - \bar{x}$,

$$\mathbf{h}(x) = \mathbf{h}(\bar{x}) + \left.\frac{\partial \mathbf{h}}{\partial x}\right|_{\bar{x}} \tilde{x} + \frac{1}{2!}\left.\frac{\partial^2 \mathbf{h}}{\partial x^2}\right|_{\bar{x}} \tilde{x}^2 + \frac{1}{3!}\left.\frac{\partial^3 \mathbf{h}}{\partial x^3}\right|_{\bar{x}} \tilde{x}^3 + \cdots \tag{7.8}$$

Now we define the operation

$$D^k_{\tilde{x}}\mathbf{h} = \left.\left(\sum_{i=1}^{n} \tilde{x}_i \frac{\partial}{\partial x_i}\right)^k \mathbf{h}(\mathbf{x})\right|_{\bar{x}} \tag{7.9}$$

using this definition we write the Taylor series expansion of $\mathbf{h}(x)$ as

$$\mathbf{h}(\mathbf{x}) = \mathbf{h}(\bar{\mathbf{x}}) + D_{\tilde{x}}\mathbf{h} + \frac{1}{2!}D^2_{\tilde{x}}\mathbf{h} + \frac{1}{3!}D^3_{\tilde{x}}\mathbf{h} + \cdots \tag{7.10}$$

The mean of y can therefore be expanded as

$$\begin{aligned}\bar{\mathbf{y}} &= E\left[\mathbf{h}(\bar{x}) + D_{\tilde{x}}\mathbf{h} + \frac{1}{2!}D_{\tilde{x}}^2\mathbf{h} + \frac{1}{3!}D_{\tilde{x}}^3 h + \cdots\right] \\ &= h(\bar{x}) + E\left[D_{\tilde{x}}h + \frac{1}{2!}D_{\tilde{x}}^2 h + \frac{1}{3!}D_{\tilde{x}}^3 h + \cdots\right]\end{aligned} \tag{7.11}$$

Now

$$\begin{aligned}E[D_{\bar{x}}h] &= E\left[\sum_{i=1}^{n}\tilde{x}_i\frac{\partial}{\partial x_i}h(x)\bigg|_{x=\bar{x}}\right] \\ &= \sum_{i=1}^{n}E(\tilde{x}_i)\,\frac{\partial}{\partial x_i}h(x)\bigg|_{x=\bar{x}} \\ &= 0\end{aligned} \tag{7.12}$$

because $E(\tilde{x}_i) = 0$. Similarly

$$\begin{aligned}E[D_{\tilde{x}}^3 h] &= E\left[\left(\sum_{i=1}^{n}\tilde{x}_i\frac{\partial}{\partial x_i}\right)^3 h(x)\bigg|_{x=\bar{x}}\right] \\ &= 0\end{aligned} \tag{7.13}$$

This is because all of the odd moments of a zero-mean random variable with a symmetric pdf are equal to 0. So

$$\bar{y} = h(\bar{x}) + \frac{1}{2!}E[D_{\tilde{x}}^2 h] + \frac{1}{4!}E[D_{\tilde{x}}^4 h] + \cdots \tag{7.14}$$

The covariance of the nonlinear transformation

$$P_y = E[(y - \bar{y})(y - \bar{y})^T] \tag{7.15}$$

we can write

$$y - \bar{y} = \left[D_{\tilde{x}} h + \frac{1}{2!} D_{\tilde{x}}^2 h + \cdots \right] - \left[\frac{1}{2!} E(D_{\tilde{x}}^2 h) + \frac{1}{4!} E(D_{\tilde{x}}^4 h) + \cdots \right]$$

We substitute this expression into the previous equation ,we see that all of the odd-powered terms in the expected value evaluate to zero (assuming that $\tilde{x}$ is zero-mean with a symmetric pdf). This results in

$$\begin{aligned} P_y &= E\left[D_{\tilde{x}} h (D_{\tilde{x}} h)^T \right] + \\ &\quad E\left[\frac{D_{\tilde{x}} h (D_{\tilde{x}}^3 h)^T}{3!} + \frac{D_{\tilde{x}}^2 h (D_{\tilde{x}}^2 h)^T}{2!2!} + \frac{D_{\tilde{x}}^3 h (D_{\tilde{x}} h)^T}{3!} \right] + \\ &\quad E\left(\frac{D_{\tilde{x}}^2 h}{2!} \right) E\left(\frac{D_{\tilde{x}}^2 h}{2!} \right)^T + \cdots \end{aligned} \tag{7.16}$$

The first term on the right side of the above equation can be written as

$$
\begin{aligned}
E\left[D_{\tilde{x}}h(D_{\tilde{x}}h)^T\right] &= E\left[\sum_{i=1}^{n}\tilde{x}_i\frac{\partial h}{\partial x_i}\bigg|_{x=\bar{x}}(\cdots)^T\right] \\
&= E\left[\sum_{i,j}^{n}\tilde{x}_i\frac{\partial h}{\partial x_i}\bigg|_{x=\bar{x}}\frac{\partial h^T}{\partial x_j}\bigg|_{x=\bar{x}}\tilde{x}_j\right] \\
&= \sum_{i,j}H_iE(\tilde{x}_i\tilde{x}_j)H_j^T \\
&= HPH^T
\end{aligned}
\tag{7.17}
$$

$$
\begin{aligned}
P_y &= HPH^T + E\left[\frac{D_{\tilde{x}}h(D_{\tilde{x}}^3h)^T}{3!} + \frac{D_{\tilde{x}}^2h(D_{\tilde{x}}^2h)^T}{2!2!} + \frac{D_{\tilde{x}}^3h(D_{\tilde{x}}h)^T}{3!}\right] + \\
&\quad E\left(\frac{D_{\tilde{x}}^2h}{2!}\right)E\left(\frac{D_{\tilde{x}}^2h}{2!}\right)^T + \cdots
\end{aligned}
\tag{7.18}
$$

This is the complete Taylor series expansion for the covariance of a nonlinear transformation. In the EKF, we use only the first term of this expansion to approximate the covariance of the estimation error. An unscented transformation is based on two fundamental principles. First, it is easy to perform a nonlinear transformation on a single point (rather than an entire pdf). Second, it is not too hard to find a set of individual points in state space whose sample pdf approximates the true pdf of a state vector.

Taking these two ideas together, suppose that we know the mean $\bar{x}$ and covariance P of a vector x. We then find a set of deterministic vectors called sigma points

whose ensemble mean and covariance are equal to $\bar{x}$ and P. We next apply our known nonlinear function $y = h(x)$ to each deterministic vector to obtain transformed vectors. The ensemble mean and covariance of the transformed vectors will give a good estimate of the true mean and covariance of y. This is the key to the unscented transformation.

We choose 2n sigma points such that

$$\begin{aligned} x^{(i)} &= \bar{x} + \tilde{x} & i &= 1, ..., 2n \\ \tilde{x}^{(i)} &= \left(\sqrt{nP}\right)_i^T & i &= 1, ..., n \\ \tilde{x}^{(n+i)} &= -\left(\sqrt{nP}\right)_i^T & i &= 1, ..., n \end{aligned} \tag{7.19}$$

where $\sqrt{nP}$ is the matrix square root of nP such that $\left(\sqrt{nP}\right)^T \sqrt{nP} = nP$, and $\left(\sqrt{nP}\right)_i$ is the ith row of $\sqrt{nP}$.

Mean approximation

Suppose that we have a vector x with a known mean $\bar{x}$ and covariance P, a nonlinear function $y = h(x)$, and we want to approximate the mean of y. We transform each individual sigma point using the nonlinear function $h(.)$, and then taking the weighted sum of the transformed sigma points to approximate the mean of y. The transformed sigma points are computed as follows

$$y^{(i)} = h(x^{(i)}) \qquad i = 1, ..., 2n \tag{7.20}$$

The true mean of y is denoted as $\bar{y}$. The approximated mean of y is denoted as $\bar{y}_u$and is computed as follows:

$$\bar{y}_u = \sum_{i=1}^{2n} W^{(i)} y^{(i)} \tag{7.21}$$

We can write the weighting coefficient as

$$W^{(i)} = \frac{1}{2n} \qquad i = 1, ..., 2n \tag{7.22}$$

$\bar{y}_u$ can be written

$$\bar{y}_u = \frac{1}{2n} \sum_{i=1}^{2n} y^{(i)} \tag{7.23}$$

Now let's compute the value of $\bar{y}_u$ to see how well it matches the true mean of y. Expanding $y^{(i)}$ using Taylor series around $\bar{x}$

$$\begin{aligned} \bar{y}_u &= \frac{1}{2n} \sum_{i=1}^{2n} \left(h(\bar{x}) + D_{\tilde{x}} h + \frac{1}{2!} D_{\tilde{x}}^2 h + \cdots \right) \\ &= h(\bar{x}) + \sum_{i=1}^{2n} \left(D_{\tilde{x}} h + \frac{1}{2!} D_{\tilde{x}}^2 h + \cdots \right) \end{aligned} \tag{7.24}$$

for any integer $k \geq 0$,we have

$$\begin{aligned}
\sum_{j=1}^{2n} D_{\tilde{x}^{(j)}}^{2k+1} h &= \sum_{j=1}^{2n} \left[\left(\sum_{i=1}^{n} \tilde{x}_i^{(j)} \frac{\partial}{\partial x_i} \right)^{2k+1} h(x)|_{x=\bar{x}} \right] \\
&= \sum_{j=1}^{2n} \left[\sum_{i=1}^{n} \left(\tilde{x}_i^{(j)} \right)^{2k+1} \frac{\partial^{2k+1}}{\partial x_i^{2k+1}} h(x)|_{x=\bar{x}} \right] \\
&= \sum_{i=1}^{n} \left[\sum_{j=1}^{2n} \left(\tilde{x}_i^{(j)} \right)^{2k+1} \frac{\partial^{2k+1}}{\partial x_i^{2k+1}} h(x)|_{x=\bar{x}} \right] \\
&= 0
\end{aligned} \tag{7.25}$$

Therefore, all of the odd terms evaluate to zero and we have

$$\begin{aligned}
\bar{y}_u &= h(\bar{x}) + \frac{1}{2n} \sum_{i=1}^{2n} \left(\frac{1}{2!} D_{\tilde{x}^{(i)}}^2 h + \frac{1}{4!} D_{\tilde{x}^{(i)}}^4 h + \cdots \right) \\
&= h(\bar{x}) + \frac{1}{2n} \sum_{i=1}^{2n} \frac{1}{2!} D_{\tilde{x}^{(i)}}^2 h + \\
&\quad \frac{1}{2n} \sum_{i=1}^{2n} \left(\frac{1}{4!} D_{\tilde{x}^{(i)}}^4 h + \frac{1}{6!} D_{\tilde{x}^{(i)}}^6 h + \right)
\end{aligned} \tag{7.26}$$

the second term on the right side of the above equation

$$\begin{aligned}
\frac{1}{2n}\sum_{i=1}^{2n}\frac{1}{2!}D^2_{\tilde{x}^{(i)}}h &= \frac{1}{2n}\sum_{k=1}^{2n}\frac{1}{2!}\left(\sum_{j=1}^{2n}\tilde{x}_i^{(k)}\frac{\partial}{\partial x_i}\right)^2 h(x)|_{x=\bar{x}} \\
&= \frac{1}{4n}\sum_{k=1}^{2n}\sum_{i,j=1}^{n}\tilde{x}_i^{(k)}\tilde{x}_j^{(k)}\frac{\partial^2}{\partial x_i\partial x_j}\,h(x)|_{x=\bar{x}} \\
&= \frac{1}{4n}\sum_{i,j=1}^{n}\sum_{k=1}^{2n}\tilde{x}_i^{(k)}\tilde{x}_j^{(k)}\frac{\partial^2}{\partial x_i\partial x_j}\,h(x)|_{x=\bar{x}} \\
&= \frac{1}{2n}\sum_{i,j=1}^{n}\sum_{k=1}^{n}\tilde{x}_i^{(k)}\tilde{x}_j^{(k)}\frac{\partial^2}{\partial x_i\partial x_j}\,h(x)|_{x=\bar{x}}
\end{aligned} \tag{7.27}$$

so

$$\begin{aligned}
\frac{1}{2n}\sum_{i,j=1}^{n}\sum_{k=1}^{n}\tilde{x}_i^{(k)}\tilde{x}_j^{(k)}\left.\frac{\partial^2 h(x)}{\partial x_i\partial x_j}\right|_{x=\bar{x}} &= \frac{1}{2n}\sum_{i,j=1}^{n}\sum_{k=1}^{n}\left(\sqrt{nP}\right)_{ki}\left(\sqrt{nP}\right)_{kj}\left.\frac{\partial^2 h(x)}{\partial x_i\partial x_j}\right|_{x=\bar{x}} \\
&= \frac{1}{2n}\sum_{i,j=1}^{n}nP_{ij}\left.\frac{\partial^2 h(x)}{\partial x_i\partial x_j}\right|_{x=\bar{x}} \\
&= \frac{1}{2n}\sum_{i,j=1}^{n}P_{ij}\left.\frac{\partial^2 h(x)}{\partial x_i\partial x_j}\right|_{x=\bar{x}}
\end{aligned} \tag{7.28}$$

so that

$$\begin{aligned}
\bar{y}_u &= h(\bar{x}) + \frac{1}{2}\sum_{i,j=1}^{2n}P_{ij}\left.\frac{\partial^2 h(x)}{\partial x_i\partial x_j}\right|_{x=\bar{x}} + \\
&\quad \frac{1}{2n}\sum_{i=1}^{2n}\left(\frac{1}{4!}D^4_{\tilde{x}^{(i)}}h + \frac{1}{6!}D^6_{\tilde{x}^{(i)}}h + \right)
\end{aligned} \tag{7.29}$$

We know that the true mean of y is given by

$$\bar{y} = h(\bar{x}) + \frac{1}{2!}E[D_{\tilde{x}}^2 h] + \frac{1}{4!}E[D_{\tilde{x}}^4 h] + \cdots \tag{7.30}$$

The second term of the above equation can be written as

$$\begin{aligned}
\frac{1}{2!}E[D_{\tilde{x}}^2 h] &= \frac{1}{2!}E\left[\left(\sum_{i=1}^{n}\tilde{x}_i\frac{\partial}{\partial x_i}\right)^2 h(x)\bigg|_{x=\bar{x}}\right] \\
&= \frac{1}{2!}E\left[\sum_{i,j=1}^{n}\tilde{x}_i\tilde{x}_j\frac{\partial^2 h}{\partial x_i \partial x_j}\bigg|_{x=\bar{x}}\right] \\
&= \frac{1}{2!}\sum_{i,j=1}^{n}E\left(\tilde{x}_i\tilde{x}_j\right)\frac{\partial^2 h}{\partial x_i \partial x_j}\bigg|_{x=\bar{x}} \\
&= \frac{1}{2!}\sum_{i,j=1}^{n}P_{ij}\frac{\partial^2 h}{\partial x_i \partial x_j}\bigg|_{x=\bar{x}}
\end{aligned} \tag{7.31}$$

so that

$$\bar{y} = h(\bar{x}) + \frac{1}{2!}\sum_{i,j=1}^{n}P_{ij}\frac{\partial^2 h}{\partial x_i \partial x_j}\bigg|_{x=\bar{x}} + +\frac{1}{4!}E[D_{\tilde{x}}^4 h] + \frac{1}{6!}E[D_{\tilde{x}}^6 h] + \cdots \tag{7.32}$$

Comparing this with Equation (7.20) we see that $\bar{y}_u$, (the approximated mean of y) matches the true mean of y correctly up to the third order, whereas linearization only matches the true mean of y up to the first order.

Covariance approximation

Now the approximated covariance

$$\begin{aligned} P_u &= \sum_{i=1}^{2n} W^{(i)}(y^{(i)} - y_u)(y^{(i)} - y_u)^T \\ &= \frac{1}{2n}\sum_{i=1}^{2n}(y^{(i)} - y_u)(y^{(i)} - y_u)^T \end{aligned} \tag{7.33}$$

as $y = h(x)$,so

$$\begin{aligned} P_u &= \frac{1}{2n}\sum_{i=1}^{2n}\left[h(x^{(i)}) - y_u\right]\left[h(x^{(i)}) - y_u\right]^T \\ &= \frac{1}{2n}\sum_{i=1}^{2n}\Bigg[h(\bar{x}) + D_{\tilde{x}_{(i)}}h + \frac{1}{2!}D^2_{\tilde{x}_{(i)}}h + \frac{1}{3!}D^3_{\tilde{x}_{(i)}}h + \cdots \\ &\quad -h(\bar{x}) - \frac{1}{2n}\sum_{j=1}^{2n}\frac{1}{2!}D^2_{\tilde{x}_{(j)}}h + \frac{1}{4!}D^4_{\tilde{x}_{(j)}}h\Bigg][\cdots] \end{aligned} \tag{7.34}$$

which simplifies to

$$P_u = \frac{1}{2n}\sum_{i=1}^{2n}\Bigg\{\left(D_{\tilde{x}_{(i)}}h\right)(\cdots)^T + \underbrace{\left[\frac{1}{2}\left(D_{\tilde{x}_{(i)}}h\right)\left(D^2_{\tilde{x}_{(i)}}h\right)^T\right]} + \underbrace{\left[\ .\ .\ .\ \right]^T} + \tag{7.35}$$
$$\frac{1}{4!}\left(D^2_{\tilde{x}_{(i)}}h\right)\left(\ .\ .\ .\ \right)^T - \underbrace{\left[D_{\tilde{x}_{(i)}}h\left(\frac{1}{2n}\sum_j \frac{1}{2}D^2_{\tilde{x}_{(i)}}h\right)^T\right]} - \underbrace{\left[\ .\ .\ .\ \right]^T} +$$
$$\frac{1}{4n^2}\left(\sum_j D^2_{\tilde{x}_{(j)}}h\right)\left(\ .\ .\ .\ \right)^T - \left[\frac{1}{4n}D^2_{\tilde{x}_{(i)}}h\left(\sum_j D^2_{\tilde{x}_{(j)}}h\right)^T\right] - \left[\ .\ .\ .\ \right]^T +$$
$$\left[D_{\tilde{x}_{(i)}}h\left(\frac{1}{3!}D^3_{\tilde{x}_{(J)}}h\right)^T\right] + \left[\ .\ .\ .\ \right]^T + \cdots\Bigg\}$$

The marked terms in the equation are zero as noted before because $\tilde{x}^{(i)} = -\tilde{x}^{(i+n)}$ for $i = 1, ..., n$.

So the covariance approximation can be written as

$$P_u = \frac{1}{2n}\sum_{i=1}^{2n}\left(D_{\tilde{x}_{(i)}}h\right)(\cdots)^T + HOT \tag{7.36}$$

where HOT means higher-order terms (i.e., terms to the fourth power and higher). Expanding this equation for P_u while neglecting the higher order terms gives

$$P_u = \frac{1}{2n}\sum_{i=1}^{2n}\sum_{j,k=1}^{n}\left(\tilde{x}^{(i)}_j\frac{\partial h(\bar{x})}{\partial x_j}\right)\left(\tilde{x}^{(i)}_k\frac{\partial h(\bar{x})}{\partial x_k}\right)^T \tag{7.37}$$

as $\tilde{x}^{(i)}_j = -\tilde{x}^{(i+n)}_j$ and $\tilde{x}^{(i)}_j = -\tilde{x}^{(i+n)}_j$ for $i = 1, ..., n$.Therefore, the covariance approximation becomes

$$
\begin{aligned}
P_u &= \frac{1}{2}\sum_{i=1}^{n}\sum_{j,k=1}^{n}\left(\tilde{x}_j^{(i)}\frac{\partial h(\bar{x})}{\partial x_j}\right)\left(\tilde{x}_k^{(i)}\frac{\partial h(\bar{x})}{\partial x_k}\right)^T \\
&= \sum_{j,k=1}^{n} P_{ik}\frac{\partial h(\bar{x})}{\partial x_j}\left(\frac{\partial h(\bar{x})}{\partial x_k}\right)^T \\
&= HPH^T
\end{aligned}
\tag{7.38}
$$

Comparing this equation for P_u with the true covariance of y, we see that it approximates the true covariance of y up to the third order (i.e., only terms to the fourth and higher powers are incorrect). This is the same approximation order as the linearization method, as seen by Equation (4.66). However, we would intuitively expect the magnitude of the error of the unscented approximation in Equation (4.81) to be smaller than the linear approximation HPH^T, because the unscented approximation at least contains correctly signed terms to the fourth power and higher, whereas the linear approximation does not contain any terms other than HPH^T

Bibliography

[1] J.J. Caffery Jr. Wireless location in CDMA cellular radio systems. Kluwer Academic Publishers, 1999

[2] A. H. Sayed, A. Tarighat, and N. Khajehnouri,"Network-based wireless location", IEEE signal processing magazine, pp.24-40, July 2005.

[3] J. J. Caffery Jr. and G.L. Stuber, "Vehicle location and tracking for IVHS in CDMA microcells", 5th IEEE International Symposium on Personal, Indoor and Mobile Radio Communications, pp. 1227 - 1231, vol.4, September 1994.

[4] J. J. Caffery Jr. and S. Venkatraman, "Geolocation techniques for mobile radio systems," Signal Processing for Mobile Communications Handbook (M. Ibnkahla, ed.), CRC Press, 2004.

[5] J. J. Caffery Jr and G.L. Stuber, "Effects of multiple-access interference on the noncoherent delay lock loop", IEEE Transactions On Communications, vol. 48, no. 12, December 2000

[6] W. Zhaocheng, W. Jing, Y. Zhixing and Y. Yan ," Synchronization consideration in multiuser CDMA environment", International Conference on Communication Technology Proceedings, pp.103-106,vol.1,May 1996.

[7] L. A. Stilp, "Carrier and end-user applications for wireless location systems", in Wireless Technologies and Services for Cellular and Personal Communication Services, vol. 2602 of Proceedings of the SPIE, pp. 119-126, October 1995.

[8] Y. Zhao, "Standardization of mobile phone positioning for 3G systems," IEEE Communication Magazine, vol. 40, pp. 108 – 114, July 2002.

[9] M. H. Chiu and M. Bassiouni, "Predictive schemes for handoff prioritization in cellular networks based on mobile positioning", IEEE Journal on Selected Areas in Communications, vol. 18, pp. 510 - 522, March 2000.

[10] S. Wang, S. Sridhar and M. Green, "Adaptive soft handoff method using mobile location information" , IEEE 55th Vehicular Technology Conference, vol. 4, pp. 1936 – 1940, 2002.

[11] R. Jain, A. Puri, and R. Sengupta, "Geographical routing using partial information for wireless ad hoc networks", IEEE Personal Communications, vol. 8, pp. 48 – 57, February 2001.

[12] S. Basagni, I. Chlamtac and V. Syrotiuk, "Dynamic source routing for ad hoc networks using the global positioning system", in IEEE Wireless Communications and Networking Conference, pp. 301 - 305, vol. 1, 1999.

[13] Y. B. Ko and N. H. Vaidya, "Location aided routing (LAR) in mobile ad hoc networks", in Mobile Computing and Networking, pp. 66-75, 1998.

[14] Ivy Yvonne Kelly, "The multipath fingerprint method for wireless E911 location finding", PhD Thesis, University of Texas at Austin, 2000

[15] J. J. Caffery Jr. and G. Stuber, "Overview of radiolocation in CDMA cellular systems", IEEE Communications Magazine, pp. 38 -45, April 1998.

[16] L. Cong and W. Zhuang, "Hybrid TDOA/AOA mobile user location for wideband CDMA cellular systems", IEEE Transactions on Wireless Communications, pp. 439 - 447, vol. 1, July 2002.

[17] P. Deng and P. Fan, "An AOA assisted TOA positioning system", International Conference on Communication Technology Proceedings, pp. 1501 - 1504, vol. 2, 2000.

[18] M. Spirito, "Mobile station location with heterogeneous data," in IEEE VTS Fall VTC 2000, pp. 1583-1589, vol. 4, 2000

[19] Polaris Wireless, Mar 2004. Wireless Location Signatures Technology Whitepaper

[20] G. Wolfle, R. Hoppe, D. Zimmermann and F. Landstorfer, "Enhanced localization technique within urban and indoor environments based on accurate and fast propagation models", European Wireless, Next Generation Wireless Networks: Technologies, Protocols, Services and Applications, no.179, 2002.

[21] P. C. Chen, "A non-line-of-sight error mitigation algorithm in location estimation", IEEE Wireless Communications and Networking Conference, pp. 316-320, vol. 1, 1999.

[22] G. L. Stuber. Principles of Mobile Communication. Kluwer Academic Publishers, 1996.

[23] N. Yousef and S. Sayed, "Detection of fading overlapping multipath components for mobile positioning systems", IEEE International Conference on Communications, pp. 3102 - 3106, vol.10, 2001.

[24] B. Ibrahim and A. Aghvami, "Direct sequence spread spectrum matched filter acquisition in frequency selective Rayleigh fading channels", IEEE Journal on Selected Areas in Communications, pp. 885-890, vol. 12, June 1994.

[25] E. Sourour and S. Gupta, "Direct-sequence spread-spectrum parallel acquisition in a fading mobile channel", IEEE Transactions on Communications, pp. 992-998, vol. 38, July 1990.

[26] W. H. Sheen and G. Stuber, "Effects of multipath fading on delay-locked loops for spread spectrum systems", IEEE Transactions on Communications, pp. 1947-1956, vol. 42, 1994.

[27] E. G. Strom, S. Parkvall and B. E. Ottersten, "Propagation delay estimation of DS-CDMA signals in a fading environment", Global Telecommunications Conference, pp. 85-89, December 1994.

[28] S. Parkvall, E. Strom, L. Milstein, and B. Ottersten, "Asynchronous near-far resistant DS-CDMA receivers without apriori synchronization", IEEE Transactions on Communications, pp. 78-88, vol. 47, January 1999.

[29] R. A. N. Dharamdial and R. Farha, "Multipath delay estimations using matrix pencil," Wireless Communications and Networking Conference , pp. 632 - 635, vol. 1, March 2003.

[30] M. Yi, P. Wei, X. C. Xiao and H. M. Tai, "Delay and Doppler estimation using cyclostationarity based cross correlation in a multipath environment", Midwest Symposium on Circuits and Systems , pp. 426-428, vol. 2, August 2002.

[31] A. S. G. Fock, P. S. Rittich, A.Schenke and H. Meyr, "Low complexity high resolution subspace based delay estimation for DS-CDMA", IEEE International Conference on Communications , pp. 31- 35, vol. 1, April 2002.

[32] N. Yousef and A. H. Sayed, "Detection of fading overlapping multipath components for mobile positioning systems", IEEE International Conference on Communications ,pp. 3102-3106, vol. 10, June 2001.

[33] N. Yousef, L. Jalloul, and A. H. Sayed, "Robust time-delay and amplitude estimation for CDMA location finding", IEEE VTS 50th Vehicular Technology Conference , pp. 2163-2167, vol. 4, September 1999.

[34] E. Strom and F. Malmsten, "A maximum likelihood approach for estimating DS/CDMA multipath fading channels", IEEE Journal on Selected Areas in Communications, pp. 132-140, vol. 18, January 2000.

[35] M. El-Tarhuni and A. Ghrayeb, "A multipath resistant PN code tracking algorithm", IEEE International Symposium on Personal, Indoor and Mobile Radio communications, pp.1834-1838, vol. 4, September 2002.

[36] U. A. D'Amico, U. Mengali and M. Morelli, "Channel estimation for the uplink of a DS-CDMA system", IEEE International Conference on Communications , pp.16-20, vol. 1, April 2002.

[37] L. Xiong, "A selective model to suppress NLOS signals in angle-of-arrival (AOA) location estimation", IEEE PIMRC, pp.461-465, vol. 1, 1998.

[38] L. Cong and W. Zhuang, "Non-Line-of-Sight Error Mitigation in TDOA Mobile Location" ,Globecom, pp. 680-684, vol.4, no.2, 2001.

[39] X. Wang, Z. Wang, and B. O'Dea, "A TOA-based location algorithm reducing the errors due to non-line-of-sight (NLOS) propagation" ,Vehicular Technology Conference , pp.97-100, vol. 1,October 2001.

[40] M. Latva-aho, J. Lilleberg, "Delay trackers for multiuser CDMA receivers", 5th IEEE International Conference on Universal Personal Communications, pp. 326-330, vol.1,1996

[41] M. El-Tarhuni, "A modified non-coherent delay-locked loop for CDMA systems", IEEE 59th Vehicular Technology Conference, pp.1124-1128, vol.2, 2004.

[42] R. Iltis, "A DS-CDMA tracking mode receiver with joint channel/delay estimation and MMSE detection" ,IEEE Transactions on Communications, pp.502-506, vol. 49, October 2001.

[43] Y. Qi and H. Kobayashi, "On geolocation. accuracy with prior information in non line-of-sight environment", Vehicular Technology Conference ,pp. 285-288,vol. 1, September 2002.

[44] M. Silventoinen and T. Rantalainen, "Mobile station emergency locating in GSM", IEEE International Conference on Personal Wireless Communications, pp. 232-238, February 1996.

[45] Vanderveen, M.C. Papadias and C.B. Paulraj, "Joint angle and delay estimation JADE for multipath signals arriving at an antenna array", IEEE Communications Letters, pp.12-14, vol. 1, no.1, January 1997.

[46] R. Schmidt, "Multiple emitter location and signal parameter estimation", IEEE Transactions on Antennas and Propagation, pp. 276-280, vol. 34, March 1986.

[47] M. Wax and A. Leshem, "Joint estimation of time delays and directions of arrival of multiple reflections of a known signal", IEEE Communications Letters, pp.2477-2484, vol. 45, October 1997.

[48] L. Krasny and H. Koorapty, "Enhanced time of arrival estimation with successive cancellation", IEEE Vehicular Technology Conference, pp. 851 - 855, vol.2, 2002.

[49] M. Aatique, "Evaluation of TDOA techniques for position location in CDMA systems", Masters thesis, Virginia Polytechnic Institute and State University,1997

[50] J. Capon, "High resolution frequency-wave number spectrum analysis", Proceedings of IEEE,pp. 1408-1419, vol.57, no. 8, June 2005.

[51] J. Burg, "Maximum entropy spectral analysis," 37th Meeting of the Society of Exploration Geophysicists, 1967.

[52] I. Ziskind and M. Wax, "Maximum likelihood localization of multiple sources by alternating projection," IEEE Transactions on Acoustics, Speech and Signal Processing, pp. 1553 -1560, October 1988.

[53] R. Schmidt, "A signal subspace approach to multiple emitter location and spectral estimation", IEEE Transactions On Antennas and Propagation, vol. Ap-34, no. 3, March 1986

[54] A. Barabell, "Improving the resolution performance of eigenstructure-based direction finding algorithms", International Conference on Acoustics Speech and Signal Processing, pp. 336-339, 1983.

[55] A. Paulraj, R. Roy, and T. Kailath, "Estimation of signal parameters via rotational invariance techniques – ESPRIT", IEEE Transactions on Acoustics, Speech and Signal Processing, pp.984-995,vol.37, no.7, July 1989.

[56] E. Tuncer, B. Freidlander. Classical and Modern Direction of Arrival Estimation, Elsivier Inc. 2009.

[57] Y. Okumura, E. Ohmori, T. Kawano, and K. Fukuda, "Field strength and its variability in VHF and UHF land mobile service", Rev. Electr. Communications Lab No.9-10, pp. 825-873, vol. 16, 1968.

[58] T. Kurt,Y. Le Helloco, B. Breton, "Performance comparison of small scale fading elimination methods", 8th ACM international symposium on Modeling, analysis and simulation of wireless and mobile systems, pp.219-222, 2005.

[59] M. Vanderveen, C. Papadias, and A. Paulraj, "Joint angle and delay estimation (JADE) for multipath signals arriving at an antenna array," IEEE Communication Letters, pp. 12-14, vol. 1, January 1997.

[60] Y. Chan and K. Ho, "A simple and efficient estimator for hyperbolic location," IEEE Transactions on Signal Processing, pp. 1905-1915, vol. 42, August 1994.

[61] C. Ma, R. Klukas, and G. Lachapelle," An enhanced two-step least squared approach for TDOA/AOA wireless location", IEEE International Conference on Communications, pp.987-991,vol. 2, 2003.

[62] R. Lupas and S. Verdu, "near-far resistance of multiuser detectors in asynchronous channels," IEEE Transactions on Communications, pp. 496-508, vol.38, April 1990.

[63] T. S. Rappaport. Wireless Communications: Principles and Practice. Prentice Hall, 2002.

[64] S. G. Glisic. Adaptive WCDMA Theory and Practice. John Wiley & Sons, 2003.

[65] M.A.Abu-Ragheff. Introduction to CDMA Wireless Communications. Elsevier Ltd.,2007

[66] J. J. Caffery Jr. and G.L. Stuber, "Subscriber location in CDMA cellular networks", IEEE Transactions on Vehicular Technology, pp.406-416,vol.47, no.2, May 1998.

[67] J.J. Caffery and G.L. Stuber, "Radio location in urban CDMA microcells," IEEE International Symposium on Personal, Indoor and Mobile Radio Communications, pp. 858-862, vol. 2, September 1995.

[68] S. Hong, S. Yoon, H. Lee, and J. Ahn, "Performance analysis of non-coherent delay-locked loop in multiple access interference", IEICE Trans. on Communications, , pp. 935–941, vol. E78 June 1995.

[69] J. J. Caffery and G. Stuber, "Performance of the non-coherent DLL in multiple access interference", IEEE International Symposium on Spread Spectrum Techniques and Applications, pp. 823-827, vol. 3, September 1998.

[70] J. Holtzmann, S. Nanda, and D. Goodman, "CDMA power control for wireless networks", 3rd Generation of Wireless Information Networks, pp. 299–311, Kluwer Academic Publishers,1992.

[71] U. Madhow and M. PursIey, "Acquisition in direct-sequence spread-spectrum communication networks: an asymptotic analysis," IEEE Transactions on Information Theory, pp. 903-912,vol.39, no. 3, May 1993

[72] G. Corazza and V. Esposti, "Code acquisition in DS-SSMA systems in the presence of multiple access interference and data modulation," European Trans. on Telecomm. and Related Technology , pp. 27–37, vol. 5, February 1994.

[73] A. Lakhzouri, E.S.Lohan, R.Hamila and M.Renfors,"Solving closely-spaced multipath via extended Kalman filter in WCDMA downlink receivers", 5th European Personal Mobile Communications Conference, pp.271-275, 2003.

[74] Dan Simon. Optimal State Estimation Kalman, H∞, and Nonlinear Approaches.Wiley Interscience, 2006.

[75] S. J. Julier and J. K. Uhlmann. "A new extension of the Kalman filter to nonlinear systems", 11th Int. Symposium On Aerospace/Defence Sensing, Simulation and Controls, SPIE, April 1997.

[76] S. J. Julier,"The scaled unscented transformation", American Control Conference, pp. 4555-4559, vol.6, November, 2002.

[77] R. Van der Merwe, E.A.Wan," The square-root unscented Kalman filter for state and parameter estimation", IEEE International Conference on Acoustics,Speech and Signal Processing, pp.3461-3464, vol.6, May 2001.

[78] M. Norgaard, N.K. Poulsen, and O. Ravn, "Advances in derivative-free state estimation for nonlinear systems", Tech. Rep. IMM-REP-1998-15, Tech. Univ. of Denmark, 2000.

[79] Lee, D.-J., and Alfriend, K. T., "Sigma point Kalman filters for efficient orbit estimation," AAS/AIAA Astrodynamics Specialist Conference, pp.1-20,August 3-7, 2003.

[80] Norgaard, M., Poulsen, N. K., and Ravn, O., “New developments in state estimation for nonlinear systems,” Automatica, Vol. 36, No. 11, November 2000, pp.1627–1638.

[81] T. J. Lim and L. K. Rasmussen, "Adaptive symbol and parameter estimation in asynchronous multiuser CDMA detectors," IEEE Transactions on Communications, pp. 213-220, vol. 45, January 1997.

[82] P. Patel and J. Holtzman, "Analysis of a simple successive cancellation scheme in a DS/CDMA system", IEEE journal on Selected Areas in Communications, pp.796-807, vol. 12, no. 5, June 1994.

[83] P. Patel and J. Holtzman, "Performance comparison of a DS/CDMA system using successive interference cancellation (IC) scheme and a parallel IC scheme under fading", IEEE International Conference on Communications, pp. 510-514, 1994.

[84] S.H. Hwang, C.G. Kang, S.W. Kim, "Performance analysis of interference cancellation schemes for a DS/CDMA system under delay constraint", Seventh IEEE International Symposium, pp. 569 -573, vol. 2 , 15-18 October 1996.

[85] I. S. Grandshteyn and I. M. Ryzhik, “Table of integral, series, and products” 7th edition, Academic Press, Elsevier, 2007

[86] M. Landolsi, A. Muqaibel, A. Al-Ahmari,"Near-far problem impact on mobile radiolocation accuracy in CDMA wireless cellular networks", IEEE International Conference on Telecommunications and Malaysia International Conference on Communications, pp.14-17, May 2007.

[87] Y. T. Chan, C. H. Yau, and P. C. Ching, "Exact and approximate maximum likelihood localization algorithms," IEEE Trans. Veh. Technol, vol. 55, no1, January 2006

[88] M. Landolsi, A. Al-Ahmari, A. Muqaibel,"Development of robust techniques to aid mobile phone location in wireless CDMA networks", KACST project report # 24-87, 2008.

[89] Azzedine Zerguine, et al., "Convergence and tracking analysis of a variable normalised LMF (XE-NLMF) algorithm," Journal of Signal Processing Volume 89, Issue 5, May 2009, pp. 778-790

Vitae

- Zahid Ali
- Born in Rawalpindi, Pakistan.
- Worked at PAEC, IBA, Hamdard University,Karachi, Pakistan.
- Joined King Fahd University of Petroleum and Minerals (KFUPM) in September 2004 and currently working in Research Institute, KFUPM.
- Email: {*zalikhan_2000@hotmail.com*}